THE LUMINOSITIES AND THE SPATIAL DISTRIBUTION OF STARS DETECTED ON A TWO MICRON SKY SURVEY

Thesis by

Evan Eugene Hughes Jr.

In Partial Fulfillment of the Requirements

For the Degree of

Doctor of Philosophy

California Institute of Technology

Pasadena, California

1969

ACKNOWLEDGMENTS

The catalog of infrared stars, which contains the data on which this thesis is based, is the product of the efforts of many people working at the California Institute of Technology over a period of six years. I am grateful for their assistance.

The person most responsible for the completion of the catalog is my research advisor, Dr. G. Neugebauer, who directed both the data gathering and data reduction processes and did a great deal of work on the project. Dr. R. B. Leighton designed and supervised the construction of both the survey telescope and the table used for digitizing the data. The interpretation of the survey data presented in this thesis has developed from a suggestion made by him. Both Dr. Neugebauer and Dr. Leighton have provided discussion and criticism during the preparation of this thesis. I thank them for their help.

Dr. B. T. Ulrich initiated the data reduction procedure, and J. D. Kinkade, T. Hilgeman, G. Neugebauer, and E. J. Groth did much of the subsequent work on computer programming. I am especially indebted to Mr. Groth who was largely responsible for the final stages in the production of the catalog and who wrote the program for plotting stars on a galactic coordinate grid.

R. G. Walker and A. P. D'Agati of Air Force Cambridge Research Laboratories provided a catalog of selected stars which was used in obtaining the positions and spectral types of stars detected on the infrared survey.

For discussion and suggestions concerning topics covered in this thesis I thank E. E. Becklin, S. C. Crow, J. H. Oort, and M. Schmidt.

My graduate studies during the period 1962 to 1966 were supported by a National Science Foundation Graduate Fellowship. The California Institute of Technology has provided additional support. Funds for the infrared sky survey were provided by the National Aeronautics and Space Administration through grant NGL-05-002-007.

ABSTRACT

An infrared sky survey, carried out at the California Institute of Technology, has resulted in a catalog of the 5612 sources whose flux at 2.2μ was measured to be greater than 2.5×10^{-15} watts $cm^{-2}\mu^{-1}$. (Neugebauer, G., and Leighton, R. B., *Two Micron Sky Survey, A Preliminary Catalog*, National Aeronautics and Space Administration, Washington, D.C., 1969.) The positions and the fluxes at 2.2μ and 0.8μ of the stars in the catalog are taken here as the input data for a determination of the luminosities and the distribution in space of these stars. The 0.8μ measurements are used only for the purpose of dividing the catalog stars into four groups on the basis of the ratio of 2.2μ flux to 0.8μ flux.

For each of the four groups data are presented which show the distribution of the stars in spectral type and in galactic longitude and latitude. Also presented is the distribution n(t) of an observed quantity t. This quantity is defined as the logarithm of the square of the ratio r_{max}/z, where r_{max} is the maximum distance at which a star can be detected and z is its distance from the galactic plane. An integral equation, which relates n(t) to the space density D(z) and the luminosity distribution, is used to derive luminosity distributions for the stars. The method makes use of the decrease in D(z) at some characteristic distance $z = \sigma$ to determine the distribution of r_{max}/σ.

The results indicate that the least red (i.e., smallest ratio of fluxes) 35 percent of the stars are generally giant stars of type

M0 or earlier and are not luminous enough to be detected beyond the characteristic half-width σ of their z distribution, where $200 < \sigma < 300$ parsecs (pc). The next 20 percent in order of redness are giant stars of spectral type M0 - M3 and can be detected to an average distance about twice their characteristic half-width σ, where $150 < \sigma < 300$ parsecs.

The reddest 45 percent of the stars are generally giants of spectral type later than M3 and can be detected to distances about five times σ, on the average. The luminosity function derived from these reddest stars may be written in terms of absolute K (i.e., 2.2μ) magnitudes M_K as $(D_o/\Delta\sqrt{2\pi})\ \exp\left[-(M_K - M_o)^2/2\Delta^2\right]$ per unit volume per unit magnitude, where $D_o = 29/\sigma^3$, $M_o = -4.3 - 5\ \log_{10}(\sigma/100\ \text{pc})$, and $\Delta = 1.2$. The σ for these stars is probably in the range 200 to 400 parsecs. This luminosity function does not account for about 200 of the stars in the reddest group which form an excess concentration of stars within 1 or 2 degrees of the galactic equator. These excess stars are interpreted as being supergiants with $\sigma \sim 50$ parsecs and $r_{max} \sim 5$ kiloparsecs.

An estimate of the gradient of the space density in the galactic plane is made for the reddest 45 percent of the stars. The estimate is that the space density decreases by a factor of $10^{-0.15}$ in a distance of 5σ.

TABLE OF CONTENTS

TABLE OF CONTENTS (cont.)

TABLE OF CONTENTS (cont.)

LIST OF TABLES

LIST OF FIGURES

LIST OF FIGURES (cont.)

LIST OF FIGURES (cont.)

CHAPTER I

INTRODUCTION

An infrared sky survey was carried out at the California Institute of Technology during the years 1965-1968. This survey was designed to obtain an unbiased sample of celestial objects which are bright enough in the infrared at wavelength 2.2 microns (μ) to be detected by the survey instrumentation. The threshold for detection was a flux density at 2.2μ of about 1×10^{-15} watts $cm^{-2}\mu^{-1}$. (This corresponds to 1.6×10^{-25} watts m^{-2} hz^{-1} at 2.2μ.) In order to obtain some idea of the temperature of the objects detected at 2.2μ, a measurement of the flux at about 0.8μ was made for each object detected. One result of this survey has been the discovery of some sources of infrared radiation which have a ratio of flux at 2.2μ to flux at 0.8μ which is unusually large compared to most known stars. The coordinates and the infrared brightnesses of 17 such objects were published while the survey was still being carried out (1,2).

Another result of the survey is a catalog of infrared stars which was ready for publication by the end of 1968 (3). This catalog does not list all of the approximately 2×10^{4} objects (stars) which were detected on the survey, but includes only those whose flux density at 2.2μ was measured to be greater than 2.5×10^{-5} watts $cm^{-2}\mu^{-1}$, about 2.5 times the minimum detectable flux density. (The flux density values given here and in the preceding paragraph are based on the absolute calibration given by Johnson (4) for the K magnitudes. The

operational criterion for an observed star to be included in the infrared catalog was that its K magnitude be less than 3.01.) The catalog includes 5612 stars. For 5562 of these the average of the measurements of the flux at 2.2μ was above the threshold of 2.5×10^{-15} watts $cm^{-2}\mu^{-1}$. An additional 50 stars were included despite the fact that their average flux was below the threshold, because their flux was measured above the threshold on one or more nights and the change in their flux from one observation to another suggested that they were variable stars. The analysis to be presented in this thesis takes as its input data the observed positions (galactic longitude and latitude) and brightnesses (at 2.2μ and at 0.8μ) of the stars in the infrared catalog. The infrared catalog lists spectral types for over 60 percent of the stars in it, and these are also taken as input data for the analysis. The spectral types were obtained by identifying the infrared stars with those listed in various star catalogs based on visual observations, and are therefore not data obtained from the survey itself.

The previous survey which is most like the present one, in terms of the similarity of the kind of star observed, is an infrared photographic survey of the Milky Way which was carried out at the Warner and Swasey Observatory of the Case Institute of Technology during the early 1950's. Results of that survey have been presented by Nassau and Blanco (5), Nassau, Blanco, and Cameron (6), and Blanco (7). The Case survey made use of Kodak 1-N emulsion plates behind a No. 89 Wratten filter and a 2° objective prism. The resulting infrared spectra covered the wavelengths from about 0.68μ to 0.88μ with a dispersion of

0.34μ/mm near the middle of the wavelength range. The spectra were used to identify stars of spectral type M5-M10, N, R, and S as well as highly reddened stars of spectral type M0-M4. The workers at Case estimated that this survey could identify these late type stars to a limiting infrared magnitude of 10.2. (The infrared magnitude scale used at Case is about the same as the I magnitude, 0.8μ, scale used in the Caltech infrared survey. Both are in agreement with the I magnitude of Kron, White, and Gascoigne (8) according to Chapter III of this thesis and Blanco (9). Comparisons of the I magnitudes of some stars common to both the Case survey and the Caltech survey showed agreement on the average, though with a broad standard deviation.) Roughly speaking, the area of the sky covered by the Case survey was that within 6 degrees of the galactic equator between galactic longitude $\ell^{II} = 5°$ and $\ell^{II} = 233°$; i.e., the Milky way north of declination -23°. The claim that the Case survey detects stars similar to those detected on the Caltech survey is based upon the arguments given in Chapter IV of this thesis to the effect that the reddest half of the stars in the infrared catalog are nearly all of late M spectral type. Additional evidence of similarity has been obtained by identifying over half of the otherwise unidentified infrared catalog stars (in the area common to both surveys) with those on lists of the brightest stars (I < 8.2 mag.) found on the Case survey. Such lists have been published by Nassau and Blanco (10,11) and Nassau, Blanco, and Morgan (12). Some results from the Case survey will be presented in Chapter VI in order to make a comparison with the results derived from the

Caltech infrared catalog.

Two other photographic infrared surveys have been carried out in limited areas of the sky primarily for the purpose of finding stars which appear much brighter in the infrared than in the visible. One of these surveys was the pioneering work carried out in the 1930s by Hetzler (13), who took infrared (effective wavelength 0.85μ) plates covering about 3000 square degrees and searched for "infrared stars" by blinking between a panchromatic plate and an infrared plate. Hetzler published his findings for 8 star fields each covering about 60 square degrees. In these 8 fields he found a total of 96 stars whose color indices blue minus infrared were greater than 5 magnitudes, his definition of "infrared star." Haro and Chavira have done some similar work using comparisons between red and infrared photographic plates. Their work has been reported by Johnson, Mendoza, and Wisniewski (14). In a 40 square degree area near the infrared source NML Cygnus discovered on the Caltech infrared survey (1) Haro and Chavira found 7 other very red stars. A more recent report by Johnson (15) on the survey by Haro and Chavira says that they have found several thousand stars whose color indices red minus infrared are greater than 4 magnitudes. No attempt will be made in this thesis to compare the results of either the Hetzler or the Haro-Chavira surveys with the 2.2μ survey.

CHAPTER II

THE INFRARED SURVEY: INSTRUMENTATION AND DATA REDUCTION

The data included in the infrared catalog were taken between January 1965 and April 1968. During this period the entire sky from declination -33° to declination +81° was surveyed at least twice. This chapter will contain brief descriptions of the instrumentation used for the infrared survey and the procedure by which the data were reduced to the form presented in the catalog.

A. The Survey Telescope

The survey was carried out with a telescope especially designed for this purpose. The infrared detectors were mounted at the prime focus of an f/1 mirror 62 inches in diameter. The reflecting surface of the mirror was a layer of aluminum deposited on an epoxy substrate. The epoxy substrate had been formed by allowing the liquid epoxy mixture to solidify in a parabolic aluminum frame which was being rotated about a vertical axis at a constant angular velocity chosen to give an f/1 surface. The imperfections in the mirror were such that the visible image of a star was blurred to a diameter one to two millimeters. At the focus of an f/1 system with a 62 inch mirror (aperture) the correspondence between distance in the focal plane and angular separation in the sky is such that

$$1 \text{ mm} = 2.2 \text{ minutes of arc } (') \, . \qquad [1]$$

Therefore, the imperfections in the mirror limited the angular resolution of the survey telescope to about three minutes of arc. The position of a star, i.e., the position of the center of the blur circle of a stellar image, could usually be determined to within less than a minute of arc.

B. Detectors and Amplifiers

The dimensions of the infrared detectors were compatible with the size of the blur circle of a stellar image. The detectors were mounted in an array as shown in Figure 1, which indicates the angular dimensions and the relative positions of the detector array projected onto the sky. The four pairs of detectors shown in Figure 1 are lead sulfide cells used to detect radiation of wavelength 2.0μ to 2.4μ. The longer, solitary detector is a silicon cell used to detect radiation in the 0.7μ to 0.9μ wavelength range. When the telescope was in operation for surveying the sky it was held at a constant north-south position (constant declination) and was moved either west to east (increasing right ascension) or east to west (decreasing right ascension) with respect to the stars. As a star's image moved across a detector it gave rise to an electrical signal which was amplified and recorded on a chart recorder. In order to have a signal which could be distinguished as well as possible from the noise arising from background radiation and random electrical fluctuations the stellar image was moved back and forth in the east-west direction 20 times per second. This "chopping" at 20 hertz was done by vibrating the mirror about a

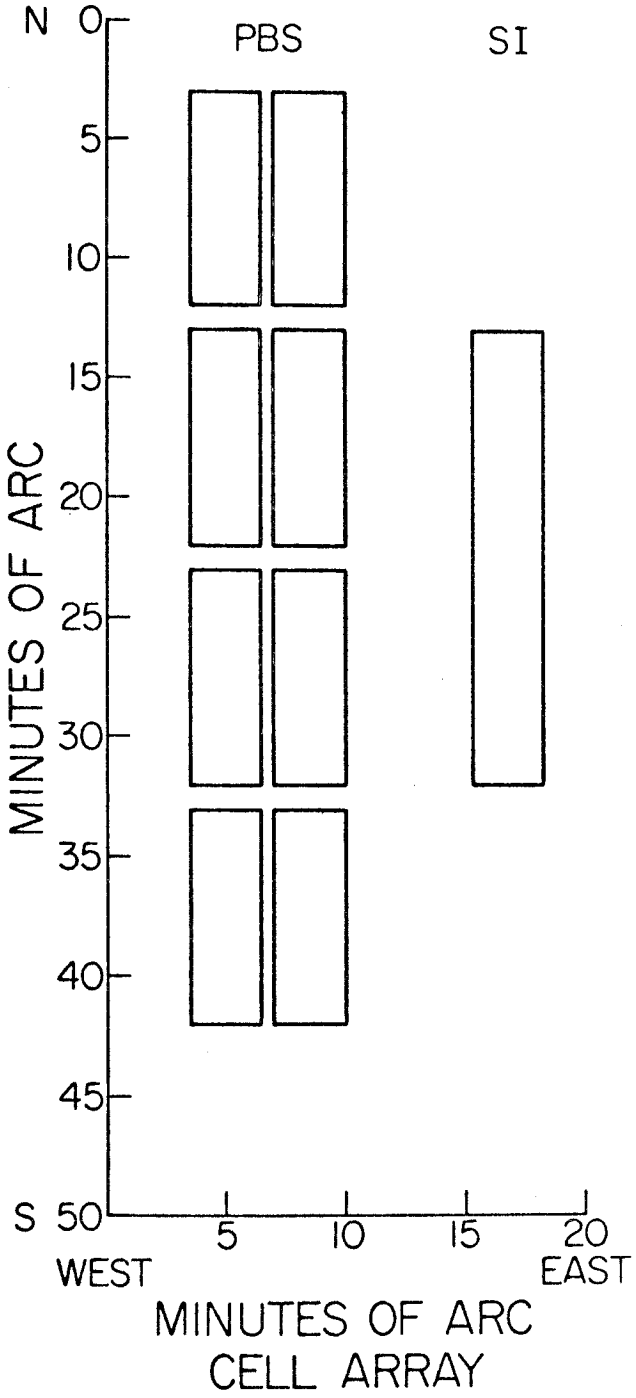

Figure 1.--The Detector Array

north-south axis. The amplitude of vibration was such that the image of a star oscillated through a distance approximately equal to the separation of the two halves of one of the double cells shown in Figure 1. For carrying out the survey the telescope was generally moved east-west at a rate of about 15' per minute, so it took about 1.5 seconds for the center of the image to move across the 3 millimeter (equals about 6') width of a double cell. Thus the vibration period was about one thirtieth of the time it took a star image to cross a double cell.

The entire detector array, lead sulfide (PbS) and silicon (Si) cells, was mounted in a dewar containing liquid nitrogen. The low temperature was required for the efficient operation of the PbS cells. The PbS cell array was covered by an interference filter which transmitted only the 2.0μ to 2.4μ range of wavelengths. The Si cell was covered by a filter which blocked the wavelengths shorter than about 0.7μ. The long wavelength cutoff was provided by the drop in sensitivity of the Si cell itself. The cells looked out of the dewar at the mirror through a light baffle system and a quartz window. The signal from each of the four PbS cells was picked up at the midpoint between the two halves. The maximum amplitude of the signal occurred when the stellar image was oscillating between the center of one half and the center of the other. A signal one half the maximum occurred when the image was oscillating between the center of either half and a position not on the cell at all. The Si cell, of course, had its maximum signal when the image oscillated between on the cell and off the cell. The signal from each of the five cells was filtered, amplified,

and phase detected before being displayed on the chart recorder. The phase detection circuitry discriminated against any component of the "signal" which had a frequency of 20 hertz but was not in phase with the true signal, which was that caused by a stellar image on the cell. As a result of the phase detection the PbS and Si signals which were finally displayed on the chart record have the appearance shown in Figure 2, which is described below.

C. Recording of Data

Figure 2 shows some PbS and Si signals as they appear on the chart record from a normal scan in right ascension. In scan n the telescope is moving to the east at the usual speed with respect to the sky of 18 times the sidereal rate. The regular spikes along the trace at the top of the figure indicate minutes of right ascension from 20h 00m through 20h 31m. At 20h 22m there is a PbS signal on cell A. Because of the phase detection the signal is negative at first as the stellar image oscillates on and off the eastward-looking half of the cell. As the image moves across the cell the signal becomes positive and attains twice the amplitude of the negative peak when the image is oscillating between the two halves of the cell. A second negative peak occurs when the image oscillates on and off the westward-looking half of the cell. In scan n + 1 the signal from the same star appears on cell B because the telescope has been moved 15' north. The Si signal from this same star occurs in scan n + 1 and is displayed on the chart recorder channel at the bottom of the figure. It is displaced

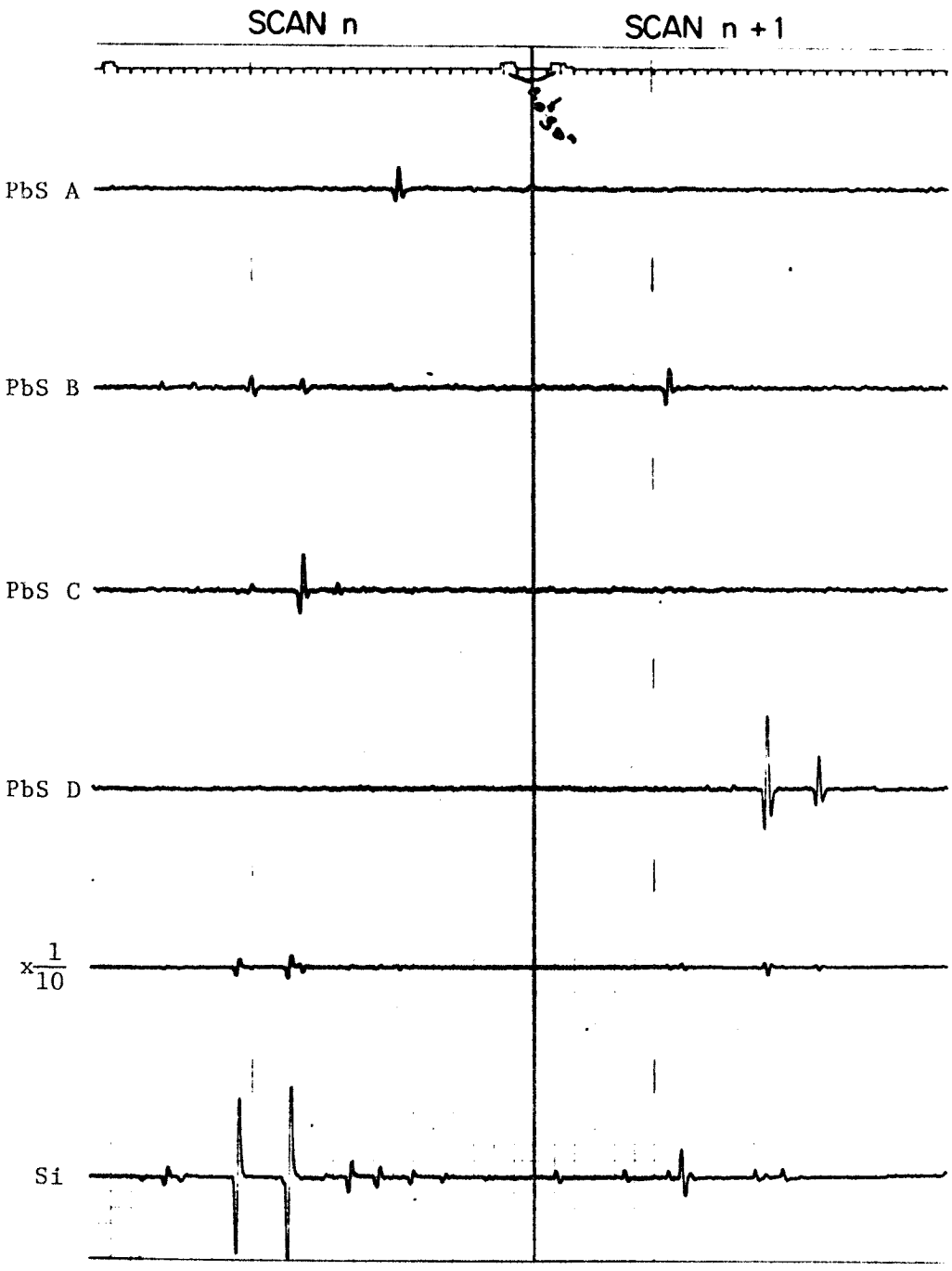

Figure 2.--Chart Record from the Survey

from the cell B peak by about one minute of right ascension. In this case the phase detection results in the signal being positive, while the image oscillates between the cell and a position just off the cell to its westward-looking side, and then negative, while it oscillates on and off the cell on the other side. There is no Si signal from this star in scan n because the Si cell does not extend to cells A and D.

Just above the Si channel on the chart there is a channel labeled "x 1/10" which is used to display the output of an amplifier designed to give one tenth of the sum of all the cells, the four PbS plus the Si. In scan n in Figure 2 there is a Si signal which is off scale on the Si channel but can be measured as about 8 divisions peak to peak on the x 1/10 channel. This would be called a 40 division Si signal. The PbS signal from this star with the off scale Si signal is the largest peak on cell C. This peak on cell C would be measured as about 11 divisions. The noise level on the four PbS channels can be seen to be 1/2 to 1 division. Using the x 1/10 channel it is possible to measure PbS signals which are about 250 divisions, i.e., on the order of 300 times the noise level. Another channel (not shown in Figure 2) was used during most of the survey to display the Si signal multiplied by 10. The minimum Si signal which could be detected was not determined by the electrical noise, as were the PbS signals, but was determined by the surface density of stars bright enough to give a measurable Si signal.

An automatic scanning system controlled the motion of the

telescope for gathering regular survey data. Operating under this system the telescope would scan east or west in right ascension until it tripped a microswitch that would stop its east-west motion when it was about half an hour of right ascension either side of the meridian. A declination drive motor would then move the telescope 15' north before it would again be moved in right ascension back toward the meridian. The east-west motion of the telescope with respect to the sky was either 15 or 18 times the sidereal rate at declinations south of +56° and was either 30 or 36 times the sidereal rate at declinations north of +56°. Thus the scanning rate in angular displacement per unit time varied as the cosine of the declination, and it was always about 4 minutes of arc per second or slower. At a scanning rate of 18 times the sidereal rate it was possible to do 14 right ascension scans, moving 15' north after each one, and then have ample time to manually move the telescope south 3-1/2 degrees back to the declination of the first scan, in time to start a new right ascension scan which overlapped the first one. The pattern traced out in the sky by this scanning procedure is shown in Figure 3. The patterns for scanning rates of 15, 30, and 36 times the sidereal rate were similar, but they covered 3, 6, and 6-1/2 degrees of declination respectively. As a result of this procedure, a normal night of survey data would cover a parallelogram in the sky with an altitude of about 3 (or 6) degrees of declination and a base of about n hours of right ascension, where n is the number of hours of time it was possible to take data that night.

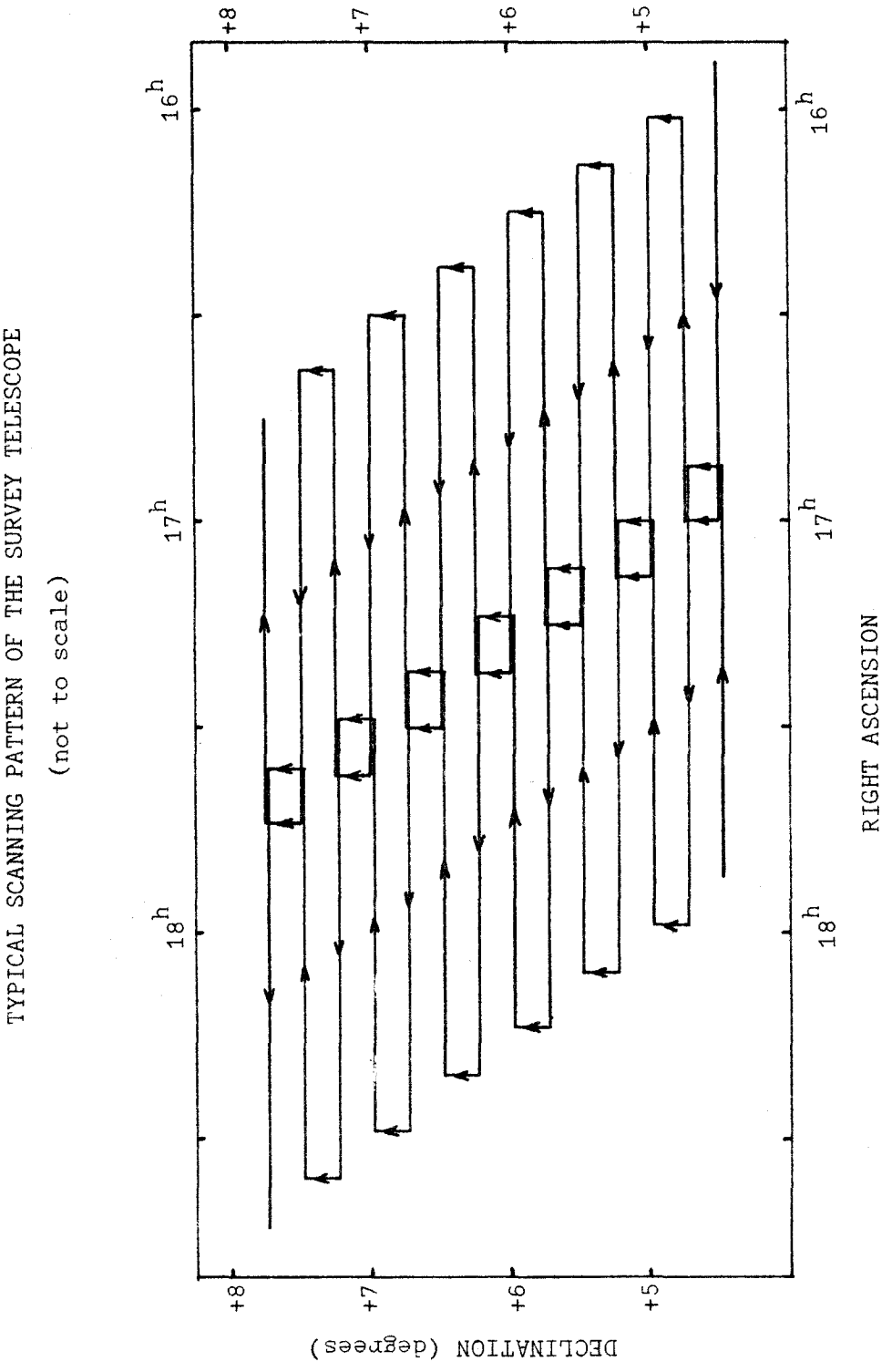
TYPICAL SCANNING PATTERN OF THE SURVEY TELESCOPE
(not to scale)
+8
+7
+6
+5
16h
17h
18h
DECLINATION (degrees)
RIGHT ASCENSION

Figure 3

D. Digitizing the Data

The minimum unit of data accepted for the data reduction process was a single set of the 14 right ascension scans separated by the 15' declination intervals. (Actually the number of scans in a set could also be 12, 24, or 26 if the scanning rate were 15, 30, or 36 times the sidereal rate rather than the 18 times which was most often used.) The first step in the data reduction was that of putting the information contained on the chart record into a digitized form suitable for processing by the IBM 7040-7094 data processing system at the California Institute of Technology. To carry out this step a chart reading table was designed and built, which has two sliding carriages, each coupled to a potentiometer, for measuring position coordinates x,y on the chart paper and two pairs of adjustable edges, each pair coupled to a potentiometer, for measuring the size of PbS and Si signals. The voltage on each of the four potentiometers is read by a digital voltmeter and punched onto paper tape which can be handled by a digital computer. The person operating the digitizing equipment can set the x and y carriages at the position of a PbS signal, open one pair of adjustable edges a distance equal to the height of the central peak of the PbS signal, open the other pair of adjustable edges a distance equal to the peak to peak amplitude of the Si signal associated with the PbS signal, and then push a foot pedal which causes all four voltages to be read and punched one after another. The computer can convert the voltages to distances or scale divisions using parameters which are determined by calibration.

Defining x as the coordinate measuring distance across the chart paper and y as the coordinate measuring distance along the length of the chart paper (see Figure 2), it is clear that x can indicate the channel (cell) on which a PbS signal occurs and y can be used to measure the right ascension of the PbS signal. The chart reading table is long enough to display the entire chart record for one east-to-west or west-to-east scan. This unit of chart record is called a frame. The first step in digitizing the data in each frame is to digitize the y positions of four right ascension minute marks (see Figure 2), whose right ascension values can be exactly established by the fact that the four are required to be the first and last minute marks of the frame plus two others exactly on the hour or half-hour. The four known points can be used by the computer to establish the best linear conversion of y position into right ascension for that frame.

E. The Calculation of the Positions and Brightnesses of the Stars

The preceding description should be sufficient to suggest how the information was converted from lines on a chart record to a list, stored in the computer, giving the PbS signal in divisions, the Si signal in divisions, the right ascension, the frame number, and the cell for each PbS signal which was large enough to be recognized by the person operating the digitizing equipment. The next stage in the data reduction process involved the grouping together of all the PbS signals which were due to the same star and the calculation of the position and brightness (at both 2.2μ and 0.8μ) of the star. Henceforth, the term

"peak" will be used for referring to one of the group of PbS signals which are due to the same star, and the term "signal" will be reserved for what is finally calculated as the actual brightness of the star. A single star could give rise to several PbS peaks because the cell array covered 40' of declination (see Figure 1) while the telescope was moved only 15' of declination between right ascension scans (frames). A group of peaks which had the same right ascension, within a certain tolerance, and the same declination, again within a certain tolerance, was very likely due to a single star. The computer found such groups and then calculated the position and PbS signal of the star which could give rise to such a group. The declination of a peak was taken to be the declination of the midpoint of the cell on which the peak occurred. For instance a peak on cell C in the fourth right ascension scan of a set, frame 4, would have had a nominal declination 40' (3 times 15' minus 5') north of the center of the cell array on frame 1. The declination of the center of the cell array on frame 1 was recorded by the observer at the telescope and punched onto the paper tape by the digitizer.

The nominal declination of a peak gives an estimate of the declination of the star which is good to within ±5'. A considerably more accurate determination of the declination is made by comparing the sizes of the peaks which are due to the same star. Figure 4 shows the sensitivity profile of the cells as a function of declination. The ordinate is labeled in minutes of declination ranging from 0 at the northern end of the array (cell A) to 50 at the southern end (cell D).

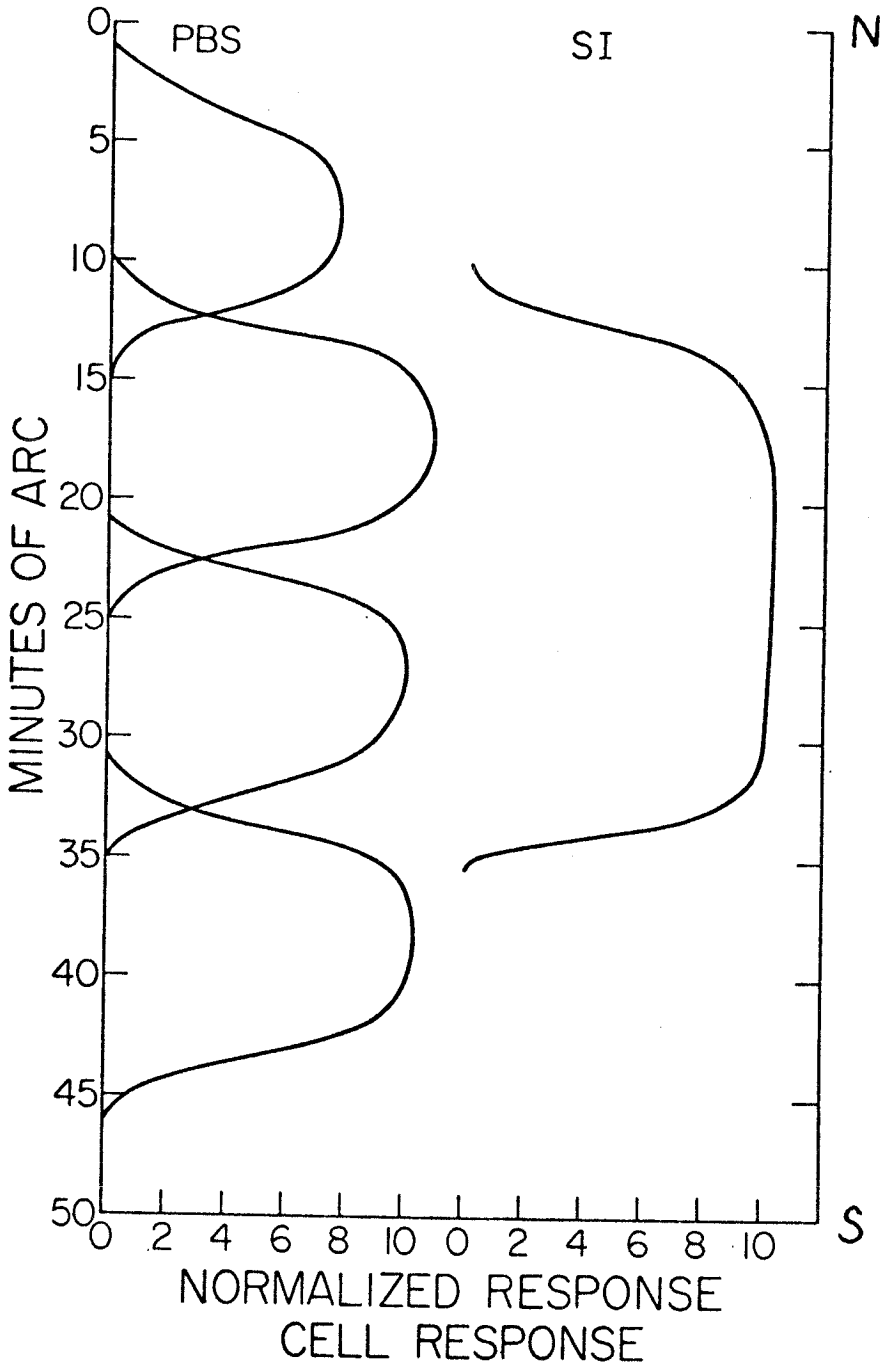

Figure 4.--Cell Sensitivity versus Declination

The abscissa is normalized to unity at the center of cell C. A single example should be sufficient to indicate how a more accurate declination can be calculated with the help of the declination profile. A star which first is detected when the center of its image is at the 2' position on the profile will give rise to another PbS peak on the next right ascension scan when the center of its image will be at the 17' position. This is because the telescope is moved 15' north in between the right ascension scans. From the declination profile it can be seen that the first peak occurs on cell A and the second occurs on cell B. The peak on cell B is about ten times as large as the peak on cell A (1.10/0.11). On the next scan the center of the star's image will cross the cell array at the 32' position, and the result will be a peak on cell C about one half of the previous scan's peak on cell B and one on cell D less than an eighth of the cell B peak. From these relative peak sizes quite an accurate determination of the star's position on the declination profile can be made. The inaccuracies are due to uncertainty in peak height measurements and in the shape of the declination profile. The number of peaks which are available to be used in determining the star's position depends on where the star happens to cross the declination profile and on how large a signal it gives. In the example used here the star would have to give a peak larger than about ten divisions on cell B in order for its cell A occurrence in the previous right ascension scan to give a peak large enough to be recognizable against the noise of about one division. (This noise level can be seen in Figure 2.)

Once a star's position on the declination profile has been determined each PbS peak caused by it can be used to calculate the size of the peak it would have given had it occurred on the center of cell C. The computer program which reduced the data took the weighted average of such calculations, with peaks less than a quarter the size of the largest being excluded, to be the PbS signal from the star. The knowledge of where the star had crossed the declination profile was also used to calculate the Si signal of the star, Si signal being defined as the size of the Si peak which would have resulted if the star had occurred on the center of cell C.

The right ascensions and declinations calculated by the above procedure had to be corrected to account for any inaccuracy in setting the telescope's right ascension and declination dials. This was done as a part of the computer processing of a night's data by identifying stars detected on the survey with a catalog of stars expected to be bright enough to be detected. The catalog used for this purpose consisted of about 25,000 stars selected from the *Smithsonian Astrophysical Observatory Star Catalog* (16) by R. G. Walker and A. P. D'Agati of the Air Force Research Laboratory at Cambridge, Massachusetts. This catalog was kept on disk storage in the computer. The correction of the coordinates of the stars was carried out by an iterative process in which each step consisted of making identifications on the basis of coordinate agreement and then finding corrections to make the coordinates agree better. The process terminated when the root mean square deviations in both right ascension and declination were within

prescribed limits.

The data reduction process described so far would produce a list of the stars observed in a set of scans (usually 14 scans) giving for each star the right ascension, the declination and the sizes of the PbS and Si peaks it would give crossing the declination profile at the center of cell C. In order to compare PbS and Si signals measured on one night with those measured on other nights, standard stars of known brightness were measured each night that survey data were being taken. The PbS and Si signals of two or three of these standard stars were measured every hour during the time available between the sets of right ascension scans. The operator would position the telescope so that the image of the standard star was at the center of cell C on the declination profile and then scan across it in right ascension at the usual scanning rate. The standard stars used on a particular night would be chosen by the operator to be as close as possible to the area of sky being surveyed. They would be chosen from a list of 450 stars known as the "survey standards." From these measurements of survey standards it was possible to determine the sensitivity of the night relative to that of an arbitrarily defined standard night. The sensitivities of the night for 2.2μ and 0.8μ signals were among the input data for the computer processing of the digitized data from a night of infrared survey. Therefore, the computer processing of a night's data (a "night" consisting of anywhere from two to twelve sets of right ascension scans) would give the normalized PbS and Si signals of the stars detected. The normalized signal strengths were converted

to K (2.2μ) and I (0.8μ) magnitudes through the relationships defining the standard night, i.e., that a PbS signal of 40 divisions corresponds to a K magnitude of 0.00 and a Si signal of 50 divisions corresponds to an I magnitude of 4.00.

F. The Calculation of Estimated Errors and Weighted Averages

In addition to the positions and normalized signals of the stars the computer processing of a night's data also produced an estimate of the uncertainty in each of the declinations, PbS signals, and Si signals calculated. These estimates of uncertainty or error were calculated from errors assigned *a priori* to individual peaks and to the declination profile. Statistical checks of the consistency of calculated declinations and signal strengths indicate that these assigned errors may be slightly large but are certainly not far from correct.

The final positions and signal strengths of the stars were obtained by calculating the weighted averages of the results from the individual nights. The weighting factors used in the averaging process were the reciprocal squares of the error estimates mentioned above. The computer processing of individual nights of data did not produce right ascension error estimates but it did give the number of PbS peaks which made up each star. The right ascension error was then taken to be 1.25' divided by the square root of the number of PbS peaks. The computer program which carried out this final averaging for each star first decided what stars from different nights, or from different sets

of scans on the same night, were actually the same star. This decision was made on the basis of the positions of the stars from the individual nights. To see if the correct group of stars had been put together for the final calculation of a single star, a check was made to see whether the star appeared either fewer or more times than its position had been surveyed. After the average right ascension, declination, PbS signal, and Si signal of a star had been calculated, the consistency of the data from the individual stars was checked by calculating a χ^2 for each of these four measured quantities. For a star which had n independent measurements x_i, each with an estimated error ε_i, resulting in an average value of x equal to $\bar{x}$ the χ^2 was calculated according to

$$\chi^2 = \sum_{i=1}^{n} \frac{(x_i-\bar{x})^2}{\varepsilon_i^2} \quad . \qquad [2]$$

The computer gave a warning message whenever a χ^2 was so large that the probability of its arising purely from random errors was less than one tenth. A warning was also given when an individual measurement x_i differed from the average $\bar{x}$ by more than two and a half times its estimated error ε_i. The output of the computer program which did all of this combining, averaging, and checking of the results of the individual nights of survey was read by members of the research group and appropriate corrections were made. This corrected output was used in the final version of the infrared star catalog.

G. Identifications with Visual Star Catalogs

The catalog gives some information which was not obtained from the infrared sky survey. This additional information, which includes the visual (V) magnitudes and the spectral types of many of the stars, was obtained by identifying them with stars given in various catalogs based on observations at visible wavelengths. One of these catalogs was the Walker-D'Agati selection from the *Smithsonian Astrophysical Observatory Star Catalog* (SAO) which, as mentioned above in section E, was also used to make corrections to the original coordinates of the survey stars. The other catalogs used for making identifications were the *Yale Catalogue of Bright Stars* (17), the *General Catalogue of 33342 Stars for the Epoch 1950* (18), and the *General Catalogue of Variable Stars* (19). The identifications with stars in these catalogs were made using punched card output from the averaging program described above to input the survey stars and using magnetic tape to input the visual star catalogs other than the Walker-D'Agati one. In some cases these identifications were helpful in correcting the output of the averaging program. The infrared star catalog was produced from the corrected output of the averaging program and the results of the identification programs.

It should be noted that the final published version of the infrared catalog (3) makes use of identifications from the complete SAO. This results in 241 identifications in addition to the 3569 identifications made with the Walker-D'Agati selection from the SAO. The analysis presented in this thesis makes use of SAO identifications

only for stars in the Walker-D'Agati selection. No use is made in this thesis of the identifications with stars in the *General Catalogue of Variable Stars*.

CHAPTER III

DEFINITIONS AND ACCURACY OF THE QUANTITIES MEASURED

The preceding discussion has been concerned with the gathering of data and the reduction of data. It is the purpose of this chapter to make more explicit the definitions of the infrared fluxes measured and to present quantitative indications of the accuracy of the data.

A. Definition of the K and I Magnitudes

The PbS and Si signals from a star are normalized to a "standard night" and are presented in the infrared star catalog as K and I magnitudes respectively. The standard night was defined above as one on which a star whose K magnitude is 0.00 would give a 40 division PbS signal and a star whose I magnitude is 4.00 would give a 50 division Si signal. Since a magnitude scale is a logarithmic one on which an increase in brightness by a factor of 100 corresponds to a change in magnitude of -5, the relationships between the normalized PbS and Si signals, $s(2.2\mu)$ and $s(0.8\mu)$, and K and I magnitudes are:

$$s(2.2\mu) = 40\times10^{-0.4(K-0.00)} \qquad [3]$$

$$s(0.8\mu) = 50\times10^{-0.4(I-4.00)}. \qquad [4]$$

The catalog gives the infrared fluxes in terms of K and I magnitudes.

The wavelength range of radiation included in the K band on the survey was determined by the interference filter which covered the PbS cells. This filter had its 50 percent transmission points at 2.0μ

and 2.4μ. The K band was intended to give K magnitudes in agreement with the K magnitude defined in the photometric system of H. L. Johnson (20). A comparison of the survey K magnitudes with Johnson's K magnitudes for 407 stars observed in common verifies that the two K bands are very nearly the same. The average value of the difference K_{survey}-$K_{Johnson}$ is -0.02 mag and the standard deviation is 0.07 mag. The difference does not vary significantly with either K magnitude or color index I-K. These data are published with the infrared catalog (3).

The wavelength range of the radiation included in the survey I band was determined by the Kodak No. 70 Wratten filter, which passed radiation with wavelength greater than 0.7μ, and by the long wavelength cutoff of the Si cell near 1.0μ. The resulting I magnitudes were found to be consistent with those of Kron, White, and Gascoigne (21), although comparisons could be made only over a limited range of spectral types. Stars from Kron, White, and Gascoigne's list of standards were used to set the survey I magnitude scale. It should be noted that the survey I magnitude system differs from that of Johnson (20) in both the color and the zero point. The effective wavelength of Johnson's I band is 0.88μ (22), which is definitely to the red side of 0.80μ, the effective wavelength of the survey I band.

The stars tabulated by Kron *et al.* (21) and Johnson (23) were used to determine the I and K magnitudes of the 450 survey standards, whose role in measuring the sensitivity of each night relative to the standard night has been described in Section E of Chapter II. This calibration of the survey standards was accomplished by devoting an

entire night about once a month to measuring all accessible survey standards together with the stars tabulated by Kron *et al.* (21) and Johnson (23). The criteria for choosing the survey standards were that they be fairly uniformly distributed throughout the sky and that they give signals which could be measured easily on the chart record with the amplifier gains set as for regular survey scanning. As a result of the second criterion the survey standards had magnitudes typically in the ranges $0.8 < K < 2.0$ and $2.5 < I < 3.8$. Eighty percent of them had a color index I-K between 1.3 and 2.6.

B. Accuracy of the K and I Magnitudes

The accuracy of the K and I magnitudes given in the infrared catalog varies from one star to another depending on the number of times the star was measured and on the brightness of the star in the K and I bands. As mentioned in the description of the data processing, estimates of the error have been calculated for each K and I magnitude given. These estimates were based on the assumption that, unless the signal was distorted by one from a nearby star, each peak had an intrinsic error of ε scale divisions given by

$$\varepsilon = \sqrt{\varepsilon_n^2 + \varepsilon_f^2} \quad , \qquad [5]$$

where ε_n was the constant error of about half a scale division due to noise (see Figure 2) and ε_f was an error equal to a constant fraction (0.07) of the peak height. The estimated errors in the final magnitudes are typically 0.05 mag to 0.08 mag in K and 0.07 to 0.15 mag

in I. The χ^2 defined by Equation [2] in Section F of Chapter II, which was calculated for the K and I magnitude of each star in the catalog to check the consistency of the measurements made on different nights, was greater than the 10 percent χ^2 level for only 6 percent of the K magnitudes and for only 9 percent of the I magnitudes. The 10 percent χ^2 level is the value of χ^2 which would be exceeded 10 percent of the time if the errors were normally distributed with standard deviations comparable to the estimated errors in K and I magnitudes. Since some of the stars actually are variable and could therefore have a χ^2 greater than the 10 percent level due to systematic changes in K or I, the number of stars found to have χ^2 greater than the 10 percent level is fewer than would be expected if the estimated errors were indeed indicative of the standard deviations of the actual errors. The relatively small number of stars whose K and I magnitude measurements have a χ^2 greater than the 10 percent level suggests that the estimated errors in K and I magnitudes are somewhat too large on the average.

For the K magnitudes, one further clue to the accuracy of the values given in the infrared catalog is the fact cited above that for 407 stars observed in common the mean difference between the catalog K magnitude and that given by Johnson *et al.* (29) is 0.02 mag and the standard deviation of these differences is 0.07 mag.

For some of the stars in the infrared catalog the major source of error in measuring the K or I magnitude was neither the noise level ε_n nor the fractional error ε_f referred to in Equation [5] but was the presence of another star close enough to have its image on the PbS

or Si cell at the same time. This confusion of two sources of radiation is more of a problem for the I magnitude measurements than for those of K, because the Si cell was twice as long in declination as a PbS cell and because estimates based on the density of sources observed suggest that about three times as many stars were detectable at I. One way of estimating the number of stars with K or I magnitudes contaminated by a nearby star is to compare the number of stars per unit area with the area of the PbS or Si cell. For K magnitudes this estimating procedure proceeds as follows: There are about 5600 stars in the infrared catalog; i.e., 5600 stars brighter than K = 3.00. To estimate the number of stars brighter than K = 4.00 multiply 5600 by 4.0. This last step assumes that the number of stars per unit volume is a constant, since then one magnitude fainter means a factor of $[10^{0.4(1.0)}]^{1/2}$ farther which means a factor of $[10^{0.4(1.0)}]^{3/2}$ = 4.0 more volume of space. A star of fourth magnitude in K would give a 1 division signal on a standard night and would be just barely detectable above the noise on the PbS cells. Since the survey covered about 32,000 square degrees, this leads to the estimate that there is about one star with K < 4.00 in every 1-1/3 square degrees. This 1-1/3 square degrees is 160 times the area of a PbS cell (10' by 3') and leads to the prediction that about 35 stars (5600/160) have K magnitudes affected by a nearby star. This can be only a rough estimate, because the actual distribution of the catalog stars is greatly concentrated toward the galactic plane and there are various degrees of being "affected" by a nearby star.

A similar estimate of the number of I magnitude measurements affected by a nearby star has been made based on the surface density of stars brighter than magnitude 7.0 in I, i.e., giving Si signals greater than about 2 divisions. In the general area of the galactic north pole the surface density of stars with I < 7.0 was found to be about 1 star per square degree. In regions along the galactic equator the surface density of such stars was found to be about 3 stars per square degree. Adopting a surface density estimate of one star for every half of a square degree and a Si cell area of 20' x 3' leads to the prediction that about 1 star out of every 30 would have its signal affected by another star with I < 7.0. This would mean about 190 stars out of 5600.

Another estimate of the number of stars with K or I magnitudes affected by a nearby star was made using the SAO catalog of about 250,000 stars (16). The relationship between spectral type and the color indices V-K and V-I was determined by identifying stars in a preliminary version of the infrared catalog with stars in the Walker-D'Agati selection from the SAO as described in Chapter II. Then for each star in the infrared catalog a search of the SAO was performed on the computer to find any star which (1) was close enough to the infrared star to contribute to the measured K or I magnitude, (2) was not identified as the sole source of the flux measured in the K or I band, and (3) had a spectral type and a V magnitude which would predict either a flux in the K band exceeding 10 percent of that measured or a flux in the I band exceeding that corresponding to K = 7.0 as well as

10 percent of that measured. This search procedure found that 100 of the K magnitudes given in the infrared catalog were affected by a nearby star meeting these criteria and that 319 of the I magnitudes were so affected. In some cases the obscuring or distortion of the Si signal by another star was obvious to the person digitizing the data, and this fact was recorded on the digitized input to the computer. As a result the I magnitudes of 65 stars not included among the 319, whose possible I magnitude confusion was revealed by the search of the SAO, are known to be contaminated by the 0.8μ radiation of nearby stars. There are 10 stars in the catalog for which no measurement of the I magnitude was possible because the Si signal was obscured by that from another star every time it appeared on the survey.

C. Estimates of the Effects of the Contamination of K and I Magnitudes by Background Stars

From these estimates of the extent to which K and I magnitudes given in the infrared catalog have been affected by nearby stars it is reasonable to conclude that the effect on I magnitudes is more serious than that on K magnitudes, but that neither effect is large enough to alter significantly the conclusions to be drawn from the analysis of the following chapters. For the K magnitudes the above estimates suggest that less than 1 percent of the catalog stars have K magnitudes affected by the presence of another star whose K magnitude is brighter than K = 4.00 and that approximately 2 percent have K magnitudes affected by another star which is more than 10 percent as bright. It should be noted that a 10 percent effect on a star with K = 3.00

corresponds to a PbS signal of 2.5/10 = 0.25 scale division which is half the effect of the noise. An estimate of the number of stars affected by 25 percent would have to be based on background stars a magnitude brighter than those causing a 10 percent effect; therefore, the number affected by 25 percent is about a quarter the number affected by 10 percent. The conclusion is that the effect of background stars on the K magnitudes given in the catalog is comparable to that of the noise on the PbS cells for less than 1 percent of the stars measured.

As far as the I magnitudes are concerned, the above estimates suggest that several hundred of the stars in the catalog have I magnitudes affected by more than 10 percent by background stars whose I magnitude is brighter than 7.0. Again using the rule that to go one magnitude fainter is to increase the number of stars by a factor of four, the estimates of contamination due to stars brighter than I = 7.0 point to near certainty that there is a star brighter than I = 9.0 available to affect any I magnitude measurement. This was taken into account in the estimated error calculated for each star's I magnitude measurement by the *a priori* assignment of a constant error of half a scale division to each Si peak. (On a standard night an I magnitude of 9.0 would give a Si signal of $50 \cdot 10^{-0.4(9.0-4.0)} = 0.5$ scale division according to Equation [4].) Thus the estimates given here point to the conclusion that some fraction, possibly approaching 10 percent, of the catalog stars have I magnitudes contaminated by stars two magnitudes brighter than the general background star.

The crucial question is whether or not the degree of contamination of I magnitudes suggested by the estimates given here can have a significant effect on the analysis of the data which follows in Chapters IV and V. The only use of I magnitudes in that analysis is in the separation of the stars into four groups based on their color indices I-K. The I-K ranges of the groups and the number of stars in each group are:

Group No.	Range of I-K	Number of Stars	Median I-K
1	< 2.33	1012	1.84
2	2.33 to 2.87	1012	2.62
3	2.87 to 3.38	1012	3.12
4	> 3.38	2576	4.21

Now in the vast majority of cases ($\sim$95 percent) the effect of a nearby star is to increase the observed Si signal over what it would have been in the absence of the contaminating star. Therefore, stars whose I magnitudes are contaminated have erroneously small values of I and I-K. For the purpose of estimating the number of stars in each I-K group which would be in a redder group were it not for a coincidence with a background star, it will be assumed that each of the first three I-K groups consists of 1012 stars which all have a K magnitude of 2.5 and a color index I-K equal to the median of the group. It will also be assumed that there are 300 catalog stars which coincide in position to within the area of the Si cell with background stars having I < 7.0 and that these 300 stars are distributed in I-K

the same as the rest of the catalog stars. Thus the number of coincidences with background stars brighter than I = 7.0 in each of the first three I-K groups will be taken to be 60 (one fifth of 300). A final assumption will be that the number of coincidences with background stars of brightness other than I < 7.0 may be scaled according to the factor of four per magnitude rule, so the number of background stars with $I < I_o$ coincident with catalog stars in each of the first three I-K groups is given by

$$N(I<I_o) = 60 \cdot 4^{(I_o-7.0)} . \qquad [6]$$

Table 1 gives the results of some calculations of the number of stars in the wrong I-K group. The calculations are based on the assumptions just given. As an example, one of these calculations is worked out in the following paragraph.

The third I-K group is assumed to consist of 1012 stars with K = 2.5 and I = 5.6. To calculate the number of these stars which actually have I-K > 3.4 (K = 2.5 and I > 5.9) is to calculate the number which are coincident with background stars having $I < I_o$ where I_o is given by

$$10^{-0.4(5.9)} + 10^{-0.4I_o} = 10^{-0.4(5.6)} , \qquad [7]$$

which yields the result $I_o = 7.1$. The number coincident with background stars having I < 7.1 is

$$60 \cdot 4^{(7.1-7.0)} = 69. \qquad [8]$$

TABLE 1

ESTIMATES OF NUMBERS OF STARS IN WRONG I-K GROUP
DUE TO CONTAMINATION OF I MAGNITUDES

Group	I-K range	Median I-K	Median I	I_o to make I-K > : 2.3	2.9	3.4	Number with I-K > : 2.3	2.9	3.4
1	< 2.3	1.8	4.3	5.4	4.8	4.4	7	3	2
2	2.3-2.9	2.6	5.1	-	6.6	5.8	-	35	11
3	2.9-3.4	3.1	5.6	-	-	7.1	-	-	69

Explanation:

If a star is contaminated by one with $I < I_o$, then its I-K is greater than that indicated (i.e., greater than 2.3, 2.9, or 3.4) rather than equal to the median I-K for its group. For example, a star in group 2 is assumed to have an I-K of 2.6 and must be contaminated by a star with $I < 5.8$, if its actual I-K is greater than 3.4. The estimate given in this table is that there are 11 such cases.

Therefore, as is shown in Table 1, this procedure leads to the estimate that there are 69 stars with I-K between 2.9 and 3.4 which actually have I-K greater than 3.4 but are in I-K group 3 because the measured I magnitude includes 0.8μ radiation from a sufficiently bright background star. The other values in Table 1 are to be interpreted similarly. For example, it is estimated that 35 of the stars with I-K between 2.3 and 2.9 are coincident with background stars having I < 6.6 and, therefore, actually have I-K greater than 2.9. In this case 11 of the 35 actually have I-K greater than 3.4.

According to the estimates presented in Table 1 the most serious effect of the contamination of I magnitudes by background stars is found in I-K group 3 (2.87 < I-K < 3.38) where about 7 percent of the stars would be in group 4 if it were not for the contamination. It should be noted that the number of stars per unit area with I < 7.0 was taken to be 3 per square degree, the value given on page 30 based on data taken near the galactic equator. This was the basis for the figure of 300 coincidences with I < 7.0 which was used in the above calculations. The surface density value near the galactic pole was about one third of that near the equator.

D. Accuracy of the Identifications and Positions

The identification of stars found on the infrared survey with stars in other catalogs has been mentioned previously, but the accuracy of the identifications made has not yet been discussed. The star catalogs searched in order to identify the stars in the infrared catalog and the number of stars identified in each are given below:

Bright Star Catalogue (17)	1613
General Catalogue (18)	2340
Walker-D'Agati selection from SAO (16)	3569
Variable Star Catalog (19)	1055

This thesis does not make use of the identifications made with stars in the *General Catalogue of Variable Stars*. The procedure used in making the identifications in the first three catalogs was to say that an identification existed whenever two stars were found to be within 3' north-south and 3' east-west of each other. If more than one of the visual catalog stars were within these limits from an infrared star, the K magnitude (2.2μ) of each of the visual stars was predicted from its V magnitude (0.55μ) and spectral type, and the star predicted to be brightest at 2.2μ was taken for the identification. Spectral data were not used in the identification process except to resolve such ambiguities. Thus, no identification made on the basis of the positional agreement given above was invalidated because the spectral type and V magnitude were not consistent with the infrared star's K and I magnitudes.

The accuracy of the positions of the stars in the infrared catalog can be indicated statistically by the differences between the coordinates of the infrared stars and the visual catalog stars identified with them. Histograms of the differences in declination and the differences in right ascension of the infrared coordinates and the SAO coordinates show that over 2/3 of the right ascension differences fall within ±0.6' and over 2/3 of the declination differences fall within

±0.3' (3). Clearly, then, the 3' tolerances used in making identifications were wide enough to find all identifications.

Some additional information concerning the accuracy of the data in the infrared catalog has been published by Neugebauer and Leighton in the introduction to the catalog (3).

CHAPTER IV

THE DISTRIBUTIONS OF THE COLORS, SPECTRAL TYPES, AND POSITIONS OF THE INFRARED STARS

A. Some Data from the Work of Other Authors

This chapter will present the data from the infrared survey. The significance of the data can be better understood if one is aware of the types of stars which might be expected to be seen on the survey. Tables 2, 3, and 4 present data based on the work of other authors which have a bearing on the number and the spatial distribution of stars of various spectral-luminosity classes. From Table 2 it is clear that very few main sequence stars are expected to appear on the survey and that those which do appear should be distributed isotropically on the celestrial sphere since the distances to which they can be seen (r_{max}) are less than the distances from the galactic plane at which their space densities fall appreciably below their densities in the plane (σ). Similar data for the giant stars (luminosity class III) given in Table 3 lead to the expectation that the giant stars earlier than spectral type M0 are distributed isotropically. From Table 3 one would conclude that only the very late M giants are likely to be seen at distances r_{max} well beyond the characteristic half-width of their space density function σ. The total number of stars seen on the survey (5612) is close enough to the total number of giant stars predicted in Table 3 to be consistent with the hypothesis that almost all of the survey stars are giant stars of spectral type K or M. Table 4

TABLE 2

SOME DATA ON STARS OF LUMINOSITY CLASS V

Sp.	M_V	Max. dist. (pc) if visual mag. is <6.5	<8.5	$(V-K)_o$	M_K	r_{max} (pc) K<3.0	D_o number per $10^6 pc^3$	Number within r_{max}	σ (pc)
O	-5.5	2500	6300	-1.0	-4.5	320	0.02	2	50
B0	-4.4	1500	3800	-0.9	-3.5	200	0.2	7	
B2	-2.5	630	1600	-0.7	-1.8	91	3	8	60
B5	-1.0	320	790	-0.5	-0.5	50	6	3	
B8	0.1	190	480	-0.2	0.3	35	33	6	
A0	1.0	125	320	0.0	1.0	25			
A2	1.2	115	290	0.1	1.1	24*	570	33	115
A5	1.8	87	220	0.4	1.4	21			
A7	2.0	80	200	0.5	1.5	20			
F0	2.4	66	166	0.8	1.6	19			
F2	2.8	55	138	0.9	1.9	17*	2,200	46	190
F5	3.2	46	115	1.1	2.1	15			
F8	4.0	32	80	1.3	2.7	12			
G0	4.4	26	65	1.4	3.0	10			
G2	4.7	23	57	1.4	3.3	8.5*	4,300	11	340
G5	5.1	19	48	1.5	3.6	7.5			
G8	5.5	16	40	1.6	3.9	6.5			
K0	5.9	13	32	1.8	4.1	6.0			
K2	6.3	11	28	2.2	4.1	6.0	10,000	5	350
K5	7.2	7	18	2.8	4.4	5.0*			
K7	8.1	5.0	12.0	3.2	4.9	4.0			
M0	8.7	3.5	9.0	3.6	5.1	4.0			
M1	9.4	2.5	6.5	4.0	5.4	3.5*	65,000	12	350
M2	10.1	2.0	5.0	4.3	5.8	3.0			
M3	10.7	1.5	3.5	4.6	6.1	2.5			
M4	11.2	1.0	3.0	4.9	6.3	2.0			

The absolute visual magnitudes M_V are from Blaauw (24).

The intrinsic colors $(V-K)_o$ are from Johnson (25).

The numbers of stars within r_{max} are from Gliese (26) for spectral types later than B8, and from counting bright stars in the FK4 (27) for types O and B. The numbers per 10^6 cubic parsecs D_o were calculated from the numbers within r_{max}, using the r_{max} values marked *.

The characteristic half-widths σ are from Allen (28).

TABLE 3

SOME DATA ON STARS OF LUMINOSITY CLASS III

Sp.	M_V	Max. dist. (pc) if visual mag. is <6.5	Max. dist. (pc) if visual mag. is <8.5	$(V-K)_o$	M_K	r_{max} (pc) K<3.0	D_o number per $10^6 pc^3$	Number within r_{max}	σ (pc)
G5	0.4	166	417	2.1	-1.7	87	4.5	12	1100
G8	0.4	166	417	2.2	-1.8	91	26.	83	300
K0	0.8	138	347	2.4	-1.6	83	140.	340	150
K1	0.8	138	347	2.5	-1.7	87	100	295	125
K2	0.8	138	347	2.6	-1.8	91			
K3	0.1	191	478	2.9	-2.8	145			
K4	-0.1	209	525	3.2	-3.3	180	7.5	190	500
K5	-0.3	229	575	3.7	-4.2	275			
M0	-0.3	229	575	3.8	-4.3	290	4.1	412	
M1	-0.5	250	630	3.9	-4.6	330	1.6	243	
M2	-0.8	290	725	4.1	-5.1	420	1.4	425	250
M3	-1.1	330	830	4.6	-5.9	600	1.1	1000	
M4	-1.0	320	795	5.2	-6.4	760	0.5	915	
M5	-0.9:	300	760	6.1	-7.2	1100	0.2	1100	
M6	-0.9:	300	760	7.0	-8.1	1660			
M7	-0.9:	300	760						

: means "value uncertain"

References:

The absolute visual magnitudes M_V are from Blaauw (24) for spectral types earlier than M0 and are from Blanco (7) for M0 or later.

The intrinsic colors $(V-K)_o$ are from Johnson (25), but for purposes of converting M_V to M_K for M stars the $(V-K)_o$ values have been increased by 0.2 to correct for a difference between visual magnitude and V magnitude.

The numbers per 10^6 cubic parsecs are from Upgren (42) for the G and K stars and from Blanco (7) for the M stars.

The characteristic half-widths σ are from Upgren (42) for the G and K stars and from Blanco (7) for the M stars.

Note: Corrections have been applied to Upgren's data in some cases where he used a value of M_V different from that given here.

TABLE 4

SOME DATA ON STARS OF LUMINOSITY CLASS I

Sp.	$(V-K)_o$	M_K for subclass Ia	M_K for subclass Ib	r_{max} (pc) for subclass Ia	r_{max} (pc) for subclass Ib
O9	-0.9	-5.3	-5.2	460	440
B0	-0.8	-5.4	-5.0	480	400
B2	-0.5	-6.3	-5.2	730	440
B5	-0.2	-6.8	-5.5	920	500
B8	-0.0	-7.1	-5.6	1050	530
A0	0.1	-7.2	-5.3	1100	460
A2	0.2	-7.7	-5.2	1400	440
A5	0.4	-8.1	-5.2	1700	440
F0	0.6	-9.1	-5.3	2700	460
F2	0.8	-9.2	-5.4	2800	480
F5	0.9	-9.1	-5.5	2700	500
F8	1.2	-9.2	-5.8	2800	580
G0	1.4	-9.4	-5.9	3100	600
G2	1.7	-9.7	-6.2	3500	700
G5	1.9	-9.9	-6.4	3900	760
G8	2.0	-10.0	-6.5	4100	800
K0	2.2	-10.2	-6.6	4500	840
K2	2.4	-10.4	-6.8	4900	920
K5	3.7	-11.7	-8.1	8700	1700
M0	3.8				
M1	3.9				
M2	4.1	-11.1	-8.9	6600	2500
M3	4.6				
M4	5.2				
M5	6.0				

References:

The intrinsic colors $(V-K)_o$ are from Johnson (25).

The absolute K magnitudes M_K were obtained by applying Johnson's $(V-K)_o$ to the absolute visual magnitudes M_V given by Blaauw (24).

gives an idea of the distances to which supergiant stars may be seen on the survey, but no predictions of numbers of these stars can be made because overall space densities for supergiants are not known. In fact, an overall space density for supergiants is not expected to be a meaningful number anyway, since these stars are thought to be located primarily in special regions of the galaxy where star formation has recently occurred or is now occurring (31). The columns of Tables 2 and 3 showing the maximum distances at which stars can be seen provide an indication of the sensitivity of the infrared survey relative to visual surveys as far as the detection of various types of stars is concerned. More will be said about this later.

B. The Correlation of Color Index I-K with Spectral Type

In order to relate the information in Tables 2, 3, and 4 to the survey results to be presented in this chapter, it is necessary to have some idea of the relationship between the color of a star as measured on the survey by I-K and the spectral type of the star. Spectral types are known for stars in the infrared catalog which have been identified in the *Yale Catalogue of Bright Stars* (17). The mean colors I-K and V-K for these identified stars of various spectral types are given in Figure 5. Figure 6 shows how the 5612 survey stars are distributed in I-K. Since many distribution functions will be displayed in a form similar to Figure 6, a description of the method used to calculate the data points and error bars is given in Appendix B. A comparison of Figure 6 with Figure 5 shows that about half of the survey

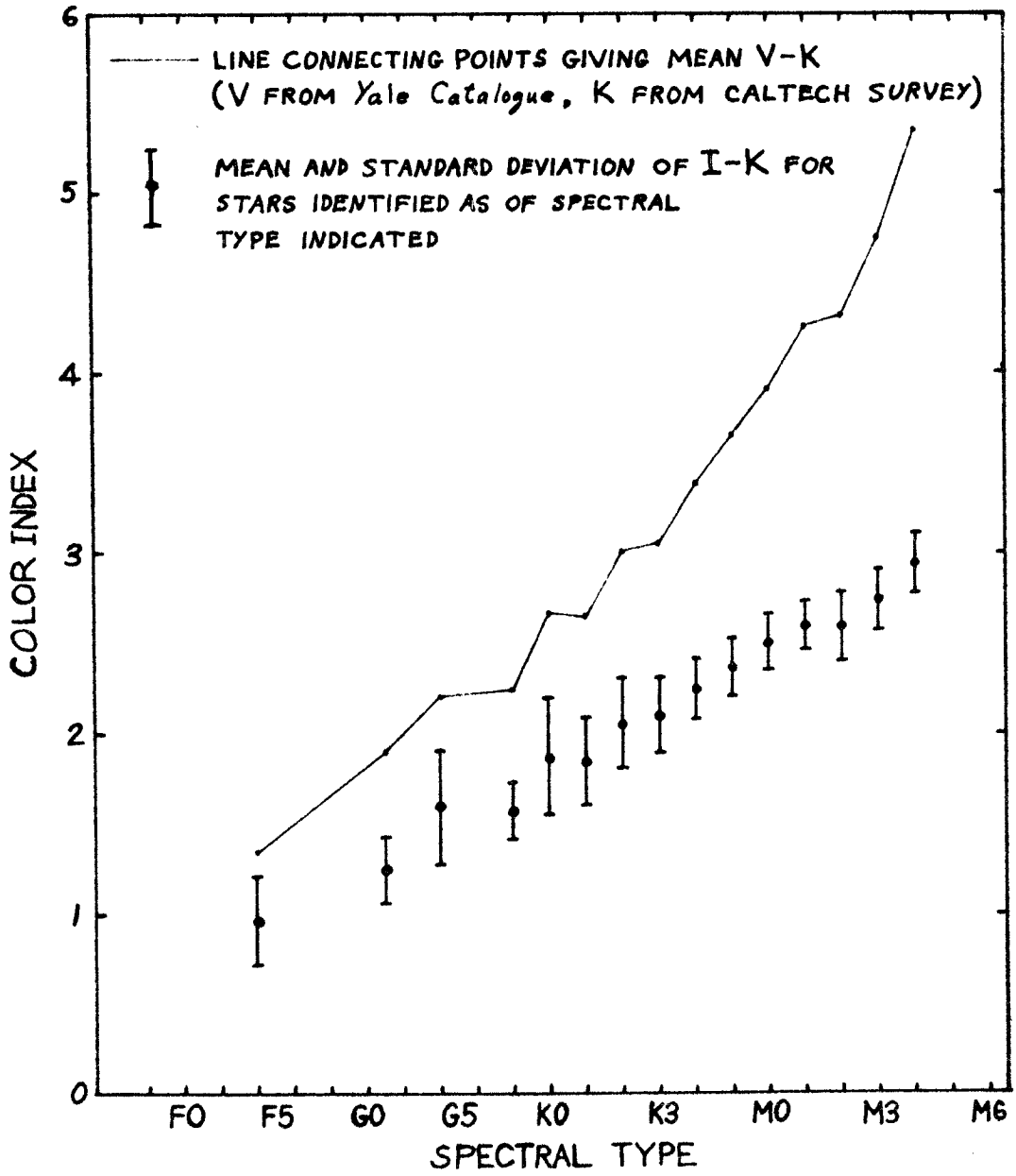

Figure 5.--Color Index versus Spectral Type for Stars Identified in the *Yale Catalogue of Bright Stars*.

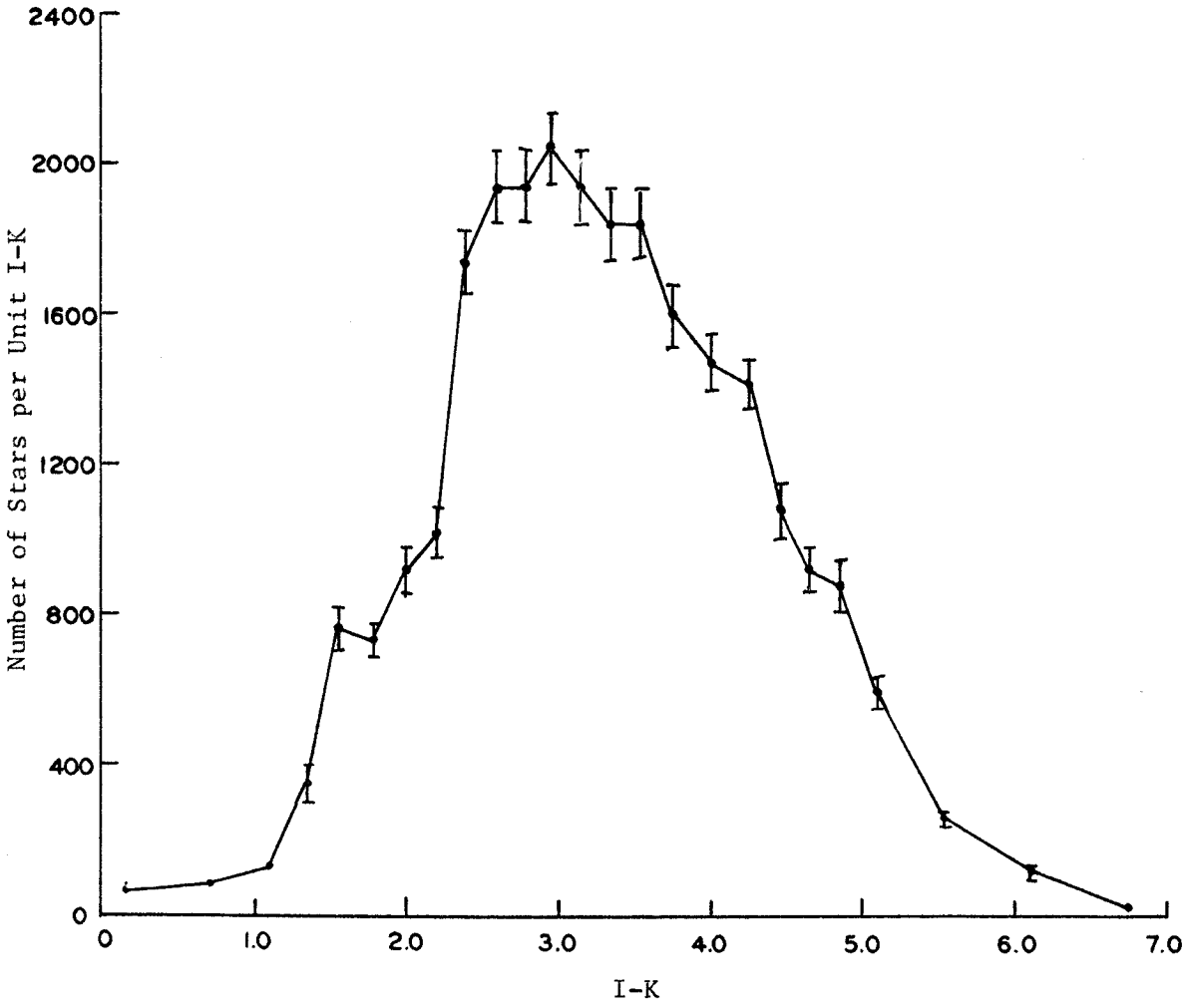

Figure 6.--I-K Distribution of the Stars in the Infrared Catalog

stars are red enough to be of spectral type M5 or later; i.e., about half the area under the curve in Figure 6 is contained in the region I-K > 3.2 and this I-K value is well into the late M spectral types of Figure 5. However, this does not allow us to conclude that half the stars must be later than M4 because such a conclusion would neglect the possible effects of catalog selection criteria and interstellar reddening on the observed I-K values. Identifications of survey stars with catalogs which are more complete than the *Yale Catalog of Bright Stars* show that a significant proportion of earlier M stars have I-K greater than 3.2. A more modest conclusion regarding the spectral type of the redder half of the survey stars can be drawn from the comparison of Figures 5 and 6, if one also introduces some reasonable assumptions about interstellar reddening. Figure 5 shows that stars earlier than M0 have I-K less than about 2.5, and Table 3 shows that most of these stars must be within 300 parsecs of the sun. Now, in order for a star this close to the sun to be reddened by 0.7 magnitude in I-K, the interstellar absorption in the visible wavelength band (V) would have to be about twice as great, corresponding to a rate of more than 4 magnitudes per kiloparsec. (See Appendix A, especially Table 16, on interstellar absorption at different wavelengths.) There is no evidence for such a large amount of interstellar absorption in the solar vicinity. A value of 1-2 magnitudes of visual absorption per kiloparsec in the galactic plane is more like the average (32,33). Therefore, it is safe to conclude that in general the survey stars with I-K greater than 3.2 are of spectral type later

than M0.

C. The Completeness of the Infrared Catalog Relative to the Visual Catalogs

Three star catalogs have been searched in order to make identifications of the infrared survey stars. The identification searches were described in Chapters II and III. The catalogs searched were the *Yale Catalogue of Bright Stars* (17), the *General Catalogue of 33342 Stars for the Epoch 1950* (18), and the special catalog of infrared stars compiled by Walker and D'Agati from the SAO (16). As one might expect, the survey stars which are reddest in I-K are generally not found in any of these catalogs, while those which are least red are found in all three of them. This result is shown in Figure 7 where the fraction of stars identified in each of the three catalogs is shown as a function of I-K. Each of these three curves will now be considered in the light of the information in Tables 2 and 3 and the completeness of the visual catalogs involved.

Figure 7 shows that all stars with I-K less than 2.1 are identified in the *Yale Catalogue of Bright Stars*. According to Figure 5 this would mean that all stars earlier than K3 which are seen on the survey are found in the Yale Catalogue, which is said to be complete to visual magnitude 6.5 (34). All this is in agreement with Table 3 which says that for giant stars of type later than K2 the maximum distance for inclusion in the infrared catalog (r_{max}) is greater than the maximum distance for detection by a visual survey complete to magnitude 6.5.

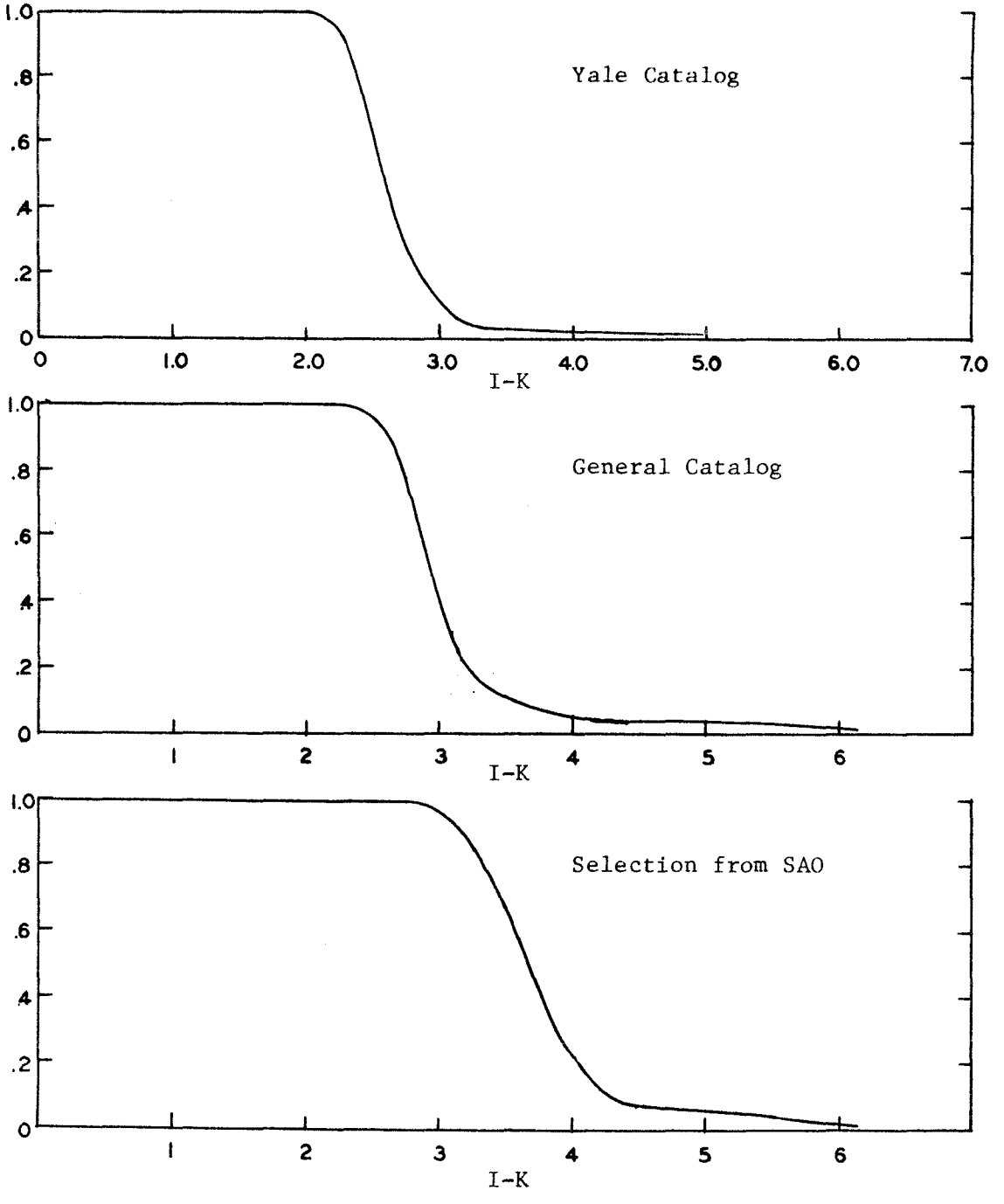

Figure 7.--Fraction Identified versus I-K

For the General Catalogue, Figure 7 shows complete identification of the survey stars out to an I-K of 2.4, which would mean all stars earlier than K5 according to Figure 5. The completeness of the General Catalogue is not as well defined as that of the Yale Catalogue. Trumpler and Weaver (34) say it is nearly complete to visual magnitude 7.5. Using 7.5 as the completeness limit of the General Catalogue, Table 3 would predict 100 percent identification for all stars earlier than M0 or K5.

For identifications with the Walker-D'Agati selection from the SAO, Figure 3 shows 100 percent out to an I-K of 2.9, which would mean all survey stars earlier than M5 are found in the SAO if Figure 5 is applied to convert I-K to spectral type. But the M giants earlier than M5 may well be about 500 parsecs away, and, therefore, may be reddened by several tenths of a magnitude in I-K. (See Table 3 and Appendix A.) A more reasonable conclusion would be that the infrared catalog stars earlier than M3 are all found in this visual catalog. It is impossible to compare this conclusion with one arrived at by using Table 3 together with the visual completeness of the SAO as was done for the other two catalogs, because the completeness of the SAO is not known. The selection criteria used by Walker and D'Agati in compiling their catalog from the SAO were generous enough to make it likely that any K or M star in the SAO which could be seen on the infrared survey would be in their selection, but identifications made with the entire SAO did find over 200 infrared stars which could be identified with SAO stars not included in the Walker-D'Agati selection. What is important

for purposes of comparison with the survey is the completeness of the Walker-D'Agati SAO for K and M stars. One way of estimating this is to use the data shown in Figure 8 which are based on the infrared stars identified in the Walker-D'Agati SAO. This figure shows K magnitude plotted versus V magnitude for various spectral types of stars identified in the Walker-D'Agati SAO catalog. In such a plot a line at 45° is a constant V-K line. The effect of interstellar reddening would be to make the more distant stars appear redder; i.e., to make those with larger K magnitudes have larger V-K. None of the spectral type groups in Figure 8 shows such a reddening tendency. In fact, the groups of stars of type M1 and later show the opposite tendency; i.e., the fainter Ks are associated with the smaller V-K values. This result can be explained by the incompleteness of the Walker-D'Agati SAO. The stars later than M0 which have V magnitudes faint enough to keep the data points on or to the right of the constant V-K line are simply not in the Walker-D'Agati SAO catalog. The incompleteness effect becomes evident at a V magnitude somewhere between 8.0 and 8.5 according to Figure 8. Table 3 predicts that the survey would become more complete than a catalog of limiting visual magnitude 8.5 for stars later than M4. But the direct evidence of Figure 8 is that the Walker-D'Agati SAO becomes incomplete with respect to the survey for stars later than M0.

There are inconsistencies in spectral types as determined by different observers, so some of the disagreement mentioned above could be accounted for by such differences. For instance, in a group of 17 stars which were called M0 in the SAO the spectral types assigned in

K VERSUS V FOR STARS IDENTIFIED IN
THE WALKER-D'AGATI SAO CATALOG

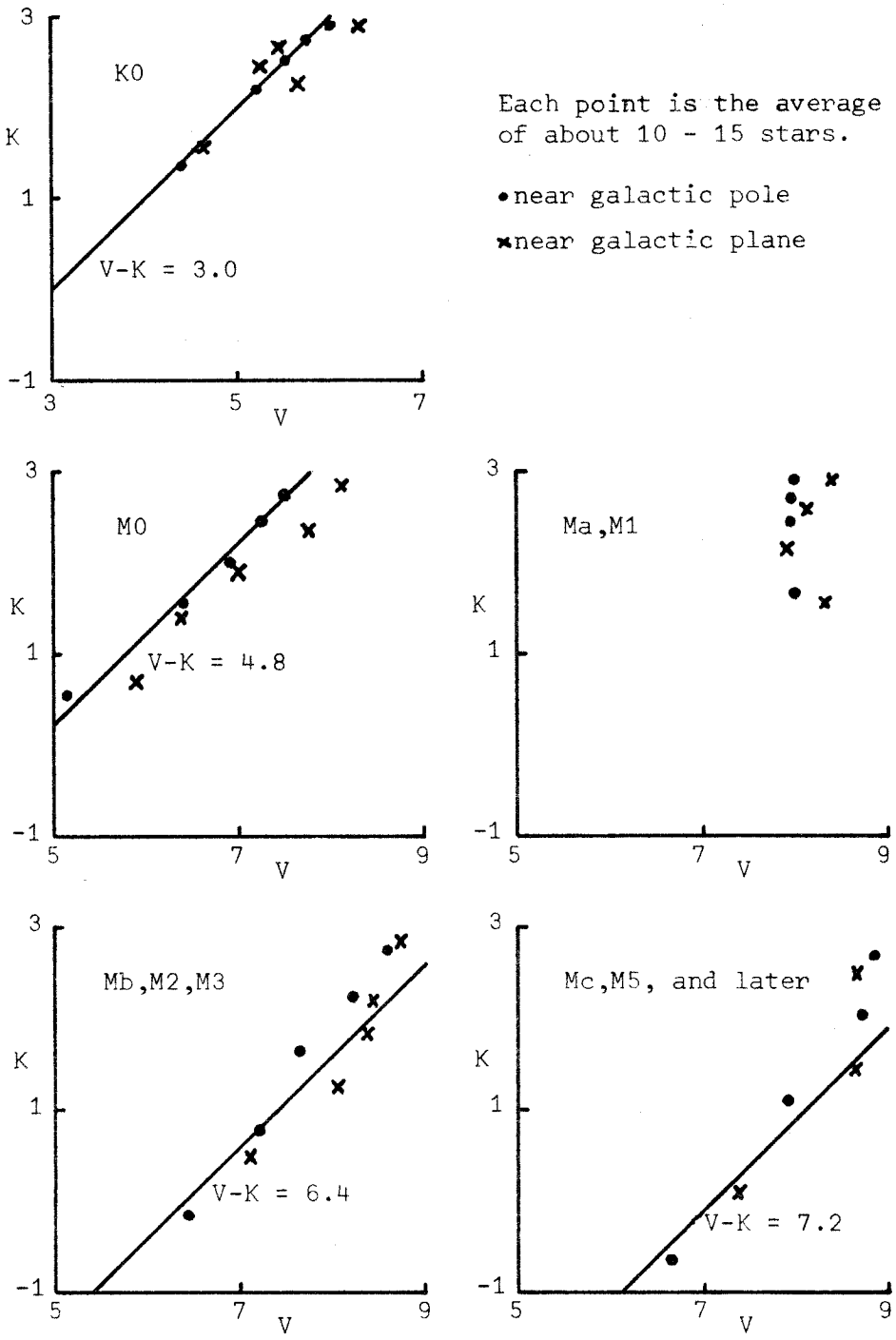

Each point is the average of about 10 - 15 stars.

•near galactic pole

×near galactic plane

Figure 8

the *Yale Catalogue of Bright Stars* were distributed as follows: one M0, seven M1, three M2, five M3, and one S5. Thus the average Yale Catalogue type was nearly 2 subtypes later than the SAO type in this sample.

D. Distribution of Spectral Types within Various I-K Ranges

Further data on the relationship between the color I-K and the spectral type of the survey stars are presented in Figure 9, parts a and b. This figure was constructed by dividing the survey stars into groups of various I-K range and plotting the percentage of the identified stars in each range which have the spectral types indicated. The numbers in the upper left hand corner of each histogram give the I-K range, the number of identified stars in that I-K range, and the total number of stars in that I-K range. Many of the stars, especially those with small I-K, are identified in two or three of the catalogs. In such cases the order of preference used in assigning the spectral type was as follows: *Yale Catalogue of Bright Stars*, *General Catalogue of 33342 Stars for the Epoch 1950*, and *Smithsonian Astrophysical Observatory Star Catalog*. Therefore, according to the percent identified versus I-K plots in Figure 7, one can assume that nearly all the spectral types for stars with I-K less than 2.33 are from the Yale Catalogue and that most of them for stars with I-K greater than 2.87 are from the SAO.

E. Positions of the Stars Plotted on Galactic Coordinate Maps

The positions of the infrared catalog stars on the celestial

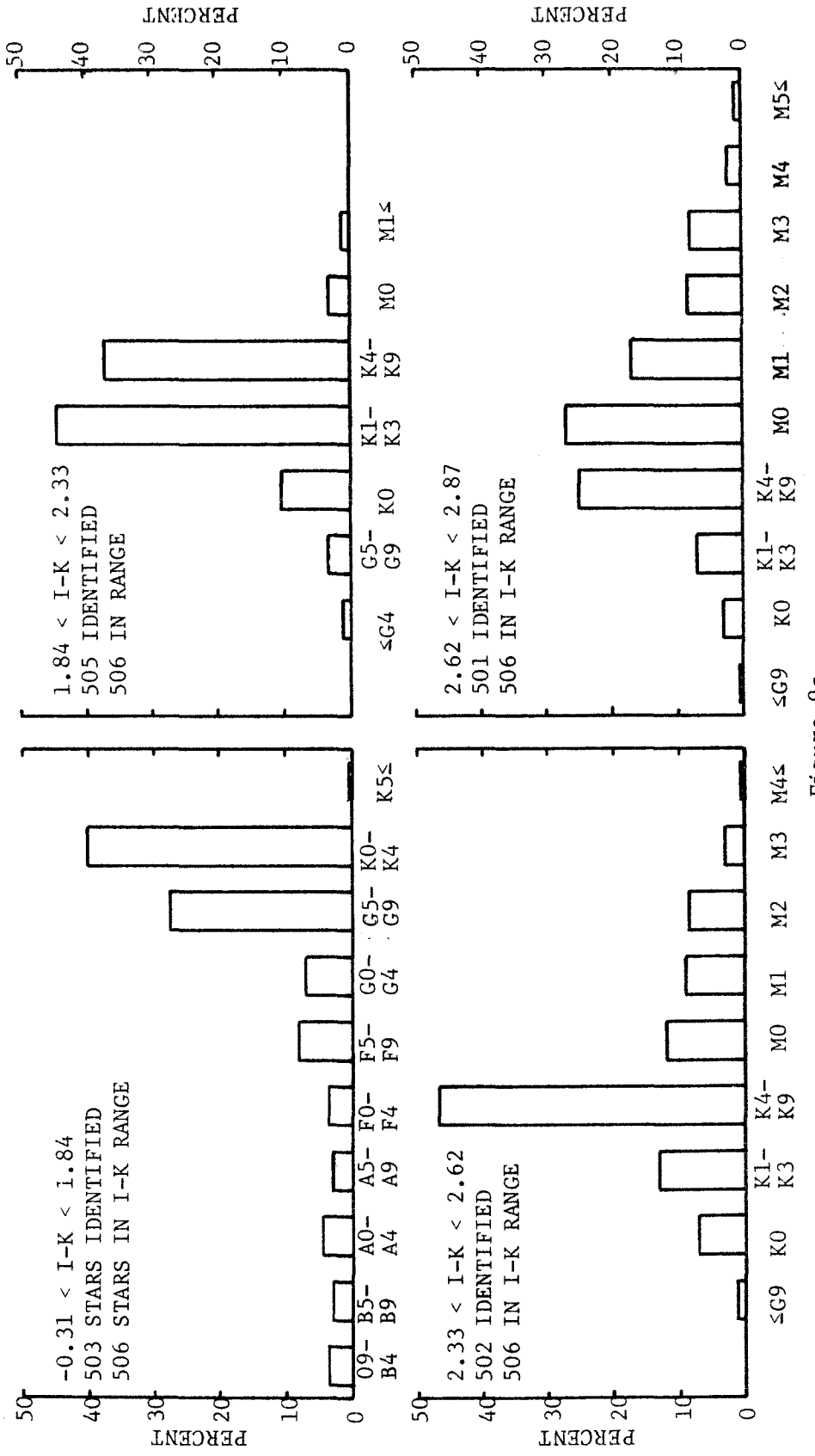

Figure 9. Spectral Type Distribution within I-K Groups

Figure 9a

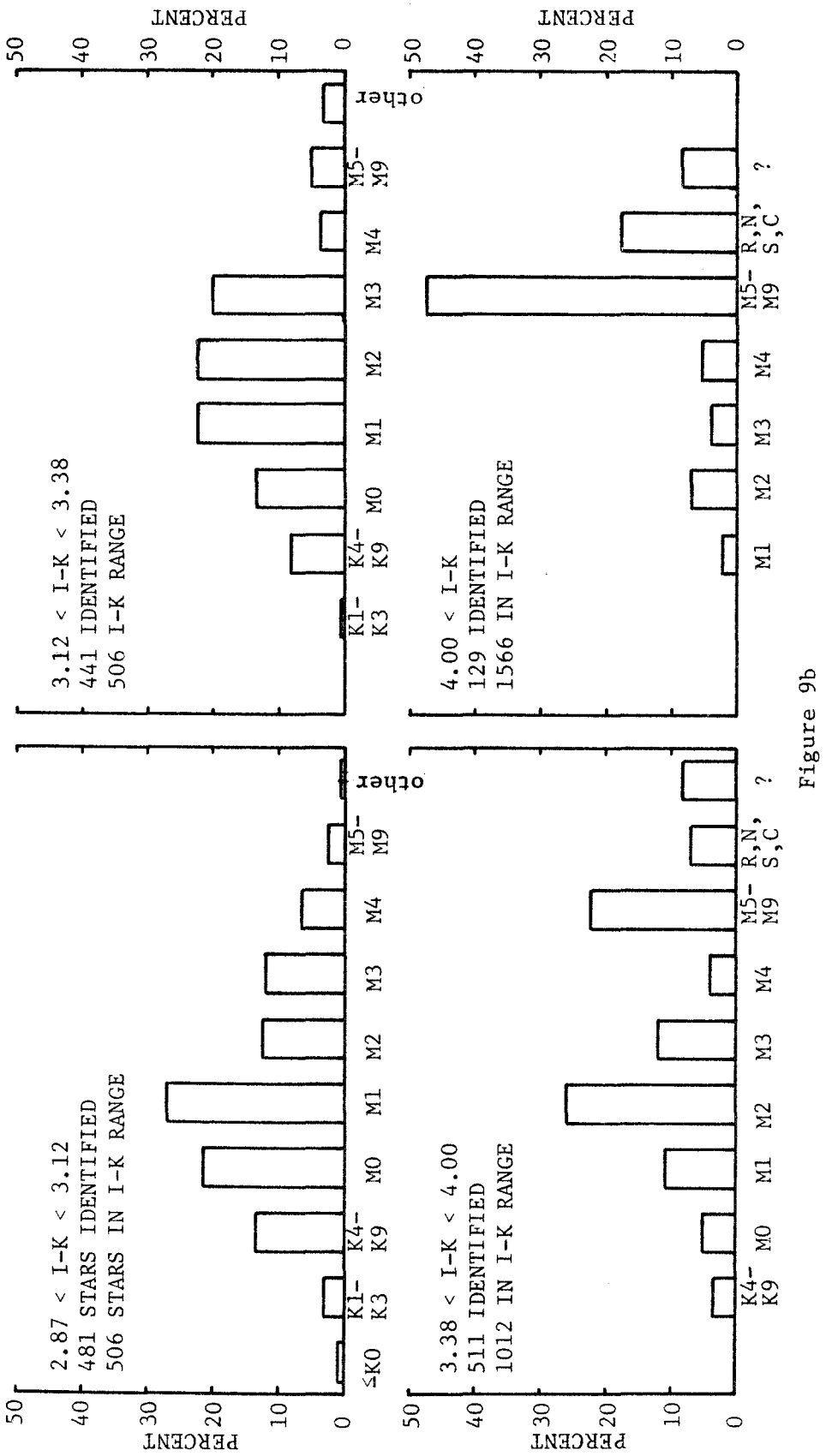
2.87 < I-K < 3.12
481 STARS IDENTIFIED
506 STARS IN I-K RANGE
3.12 < I-K < 3.38
441 IDENTIFIED
506 I-K RANGE
3.38 < I-K < 4.00
511 IDENTIFIED
1012 IN I-K RANGE
4.00 < I-K
129 IDENTIFIED
1566 IN I-K RANGE
PERCENT
0
10
20
30
40
50
≤K0
K1- K3
K4- K9
M0
M1
M2
M3
M4
M5- M9
R,N, S,C
?
other

Figure 9b

sphere are shown in Figures 10 through 13. The positions of the stars are shown in the new galactic coordinate system ℓ^{II}, b^{II} (35). The north galactic pole is at the top of each figure. The direction of the galactic center is in the center of each figure. Longitude is increasing to the left. The grid lines mark 30 degree intervals of longitude and latitude. Two areas, one large and one small, which contain no stars are specially marked off. These are regions not covered by the infrared survey. The small area near longitude $\ell^{II} = 120°$ and latitude $b^{II} = +30°$ is the region of sky north of declination (1965.0) + 81°, and the large area is the region of sky south of declination (1965.0) -33°. The coordinate grid is constructed to make the map an equal area plot, so equal areas anywhere in the figure correspond to equal areas in the sky. Surface densities at different latitudes can be compared by counting the number of stars in equal areas in the figure.

The survey stars have been divided into groups based on color and brightness for purposes of plotting their positions. Each plot contains about 500 stars. All the survey stars brighter than K = 3.01 have been divided into three groups of about 1000 stars and one group of about 2500 on the basis of I-K. Within each I-K group the stars were sorted in order of K magnitude. The groups of 1000 were separated into the brightest half and the faintest half, and each half was plotted separately as part a and part b of the figure. This procedure produced Figures 10, 11, and 12. The stars with I-K greater than 3.38 and K less than 3.01 form a group of 2532 stars which was divided in five

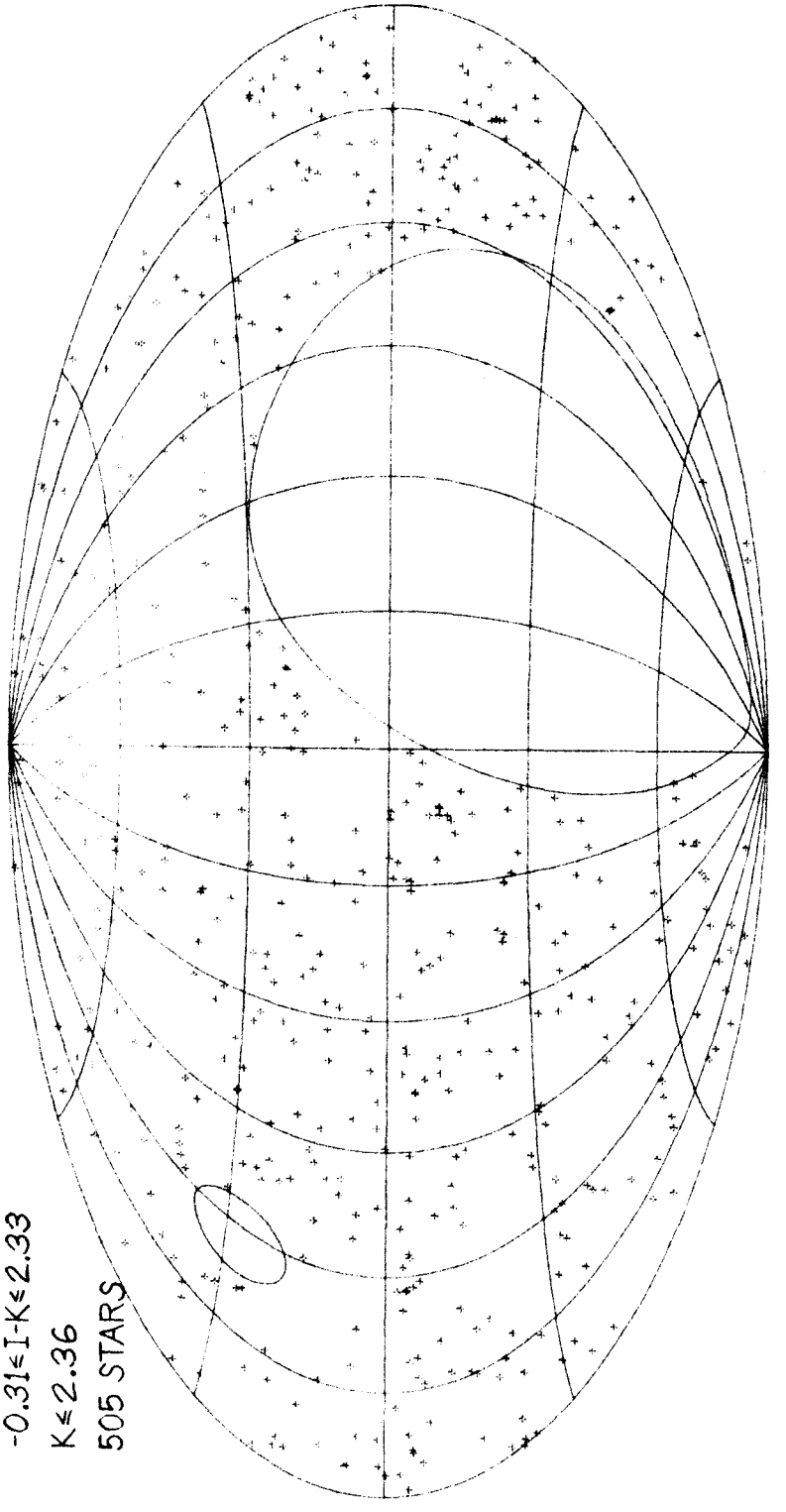

Figure 10a

Figure 10.--Galactic Coordinates of Stars with I-K < 2.33

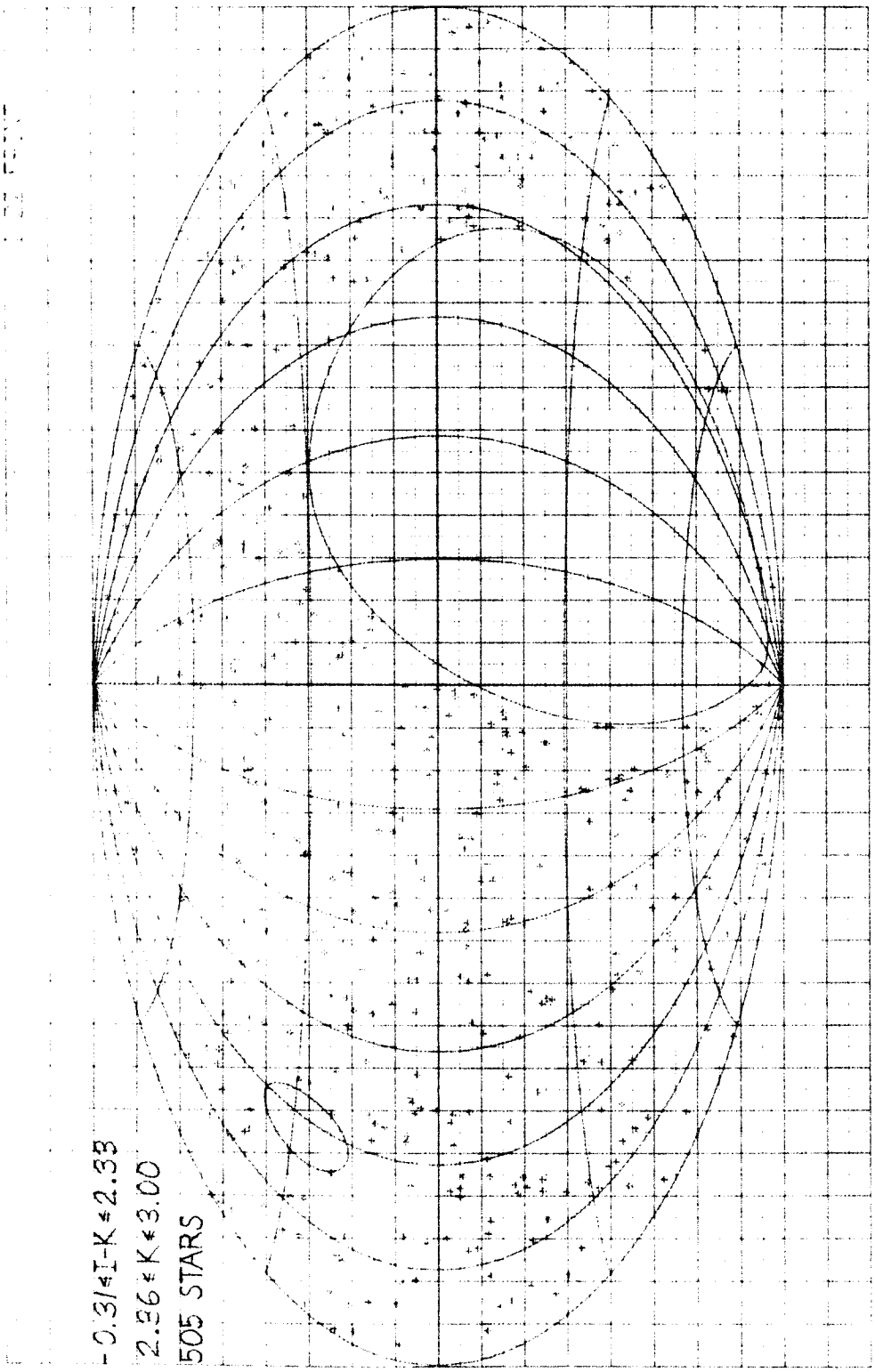

Figure 10b

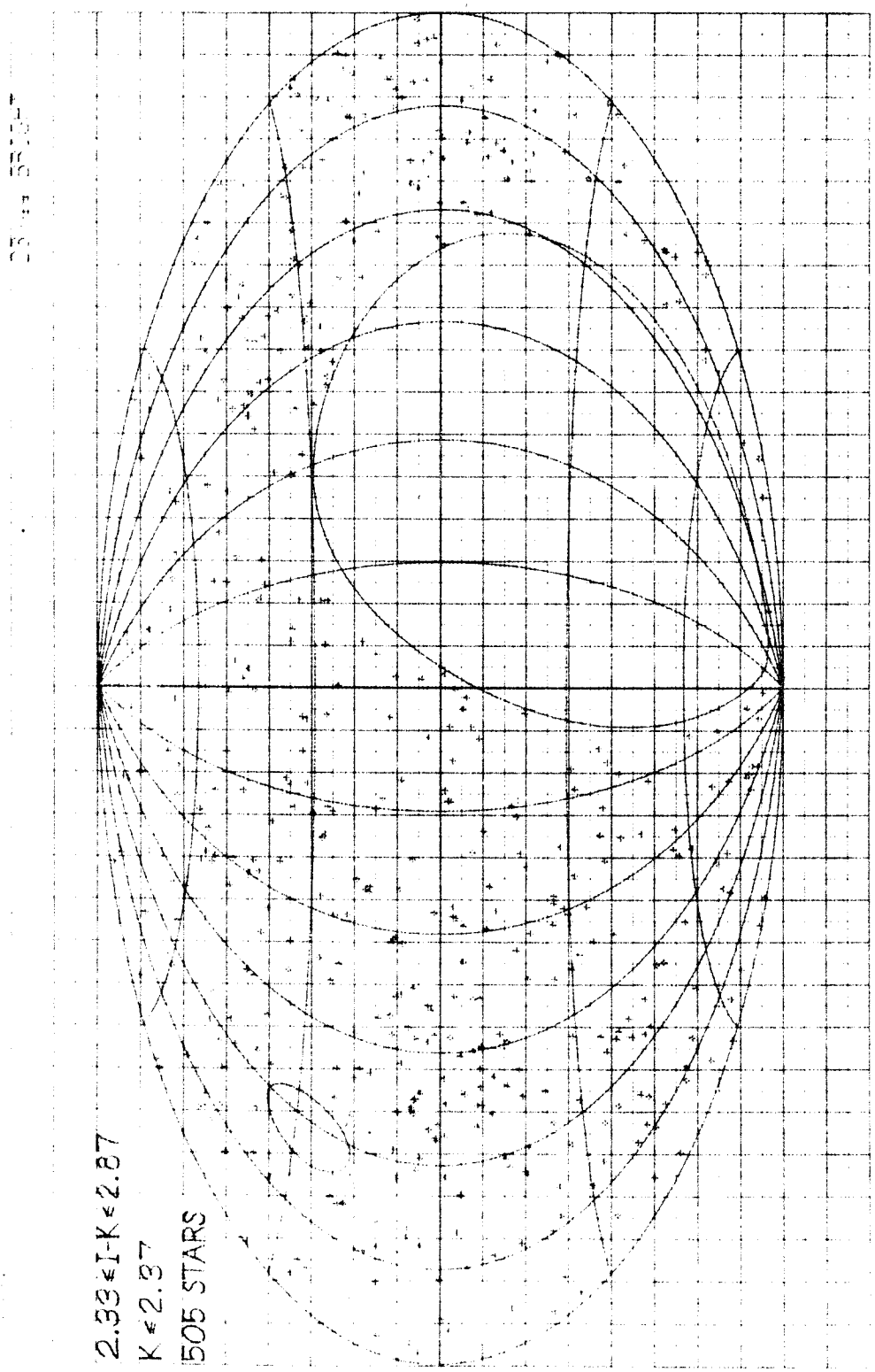

Figure 11a

Figure 11.--Galactic Coordinates of Stars with 2.33 < I-K < 2.87

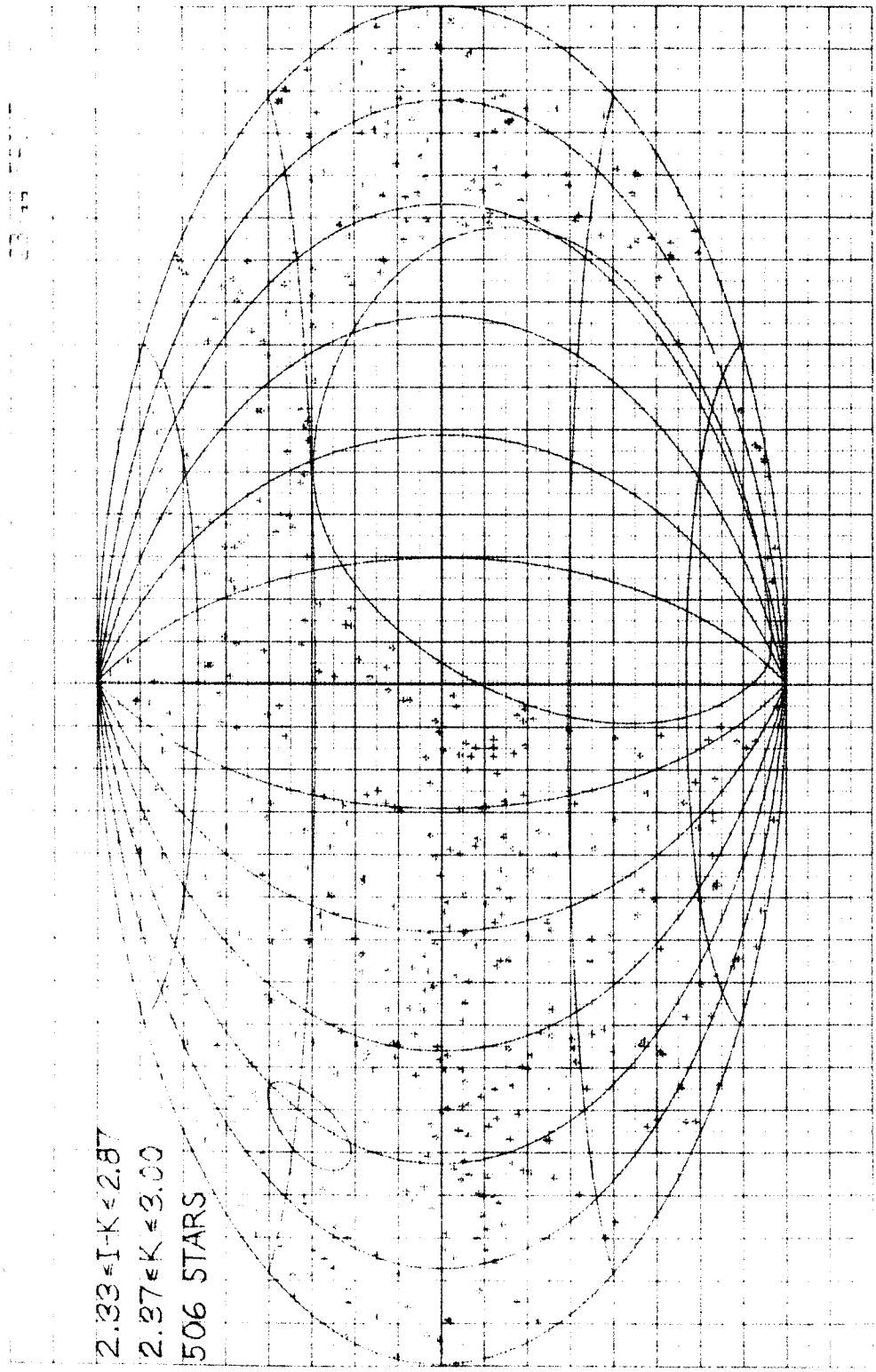

Figure 11b

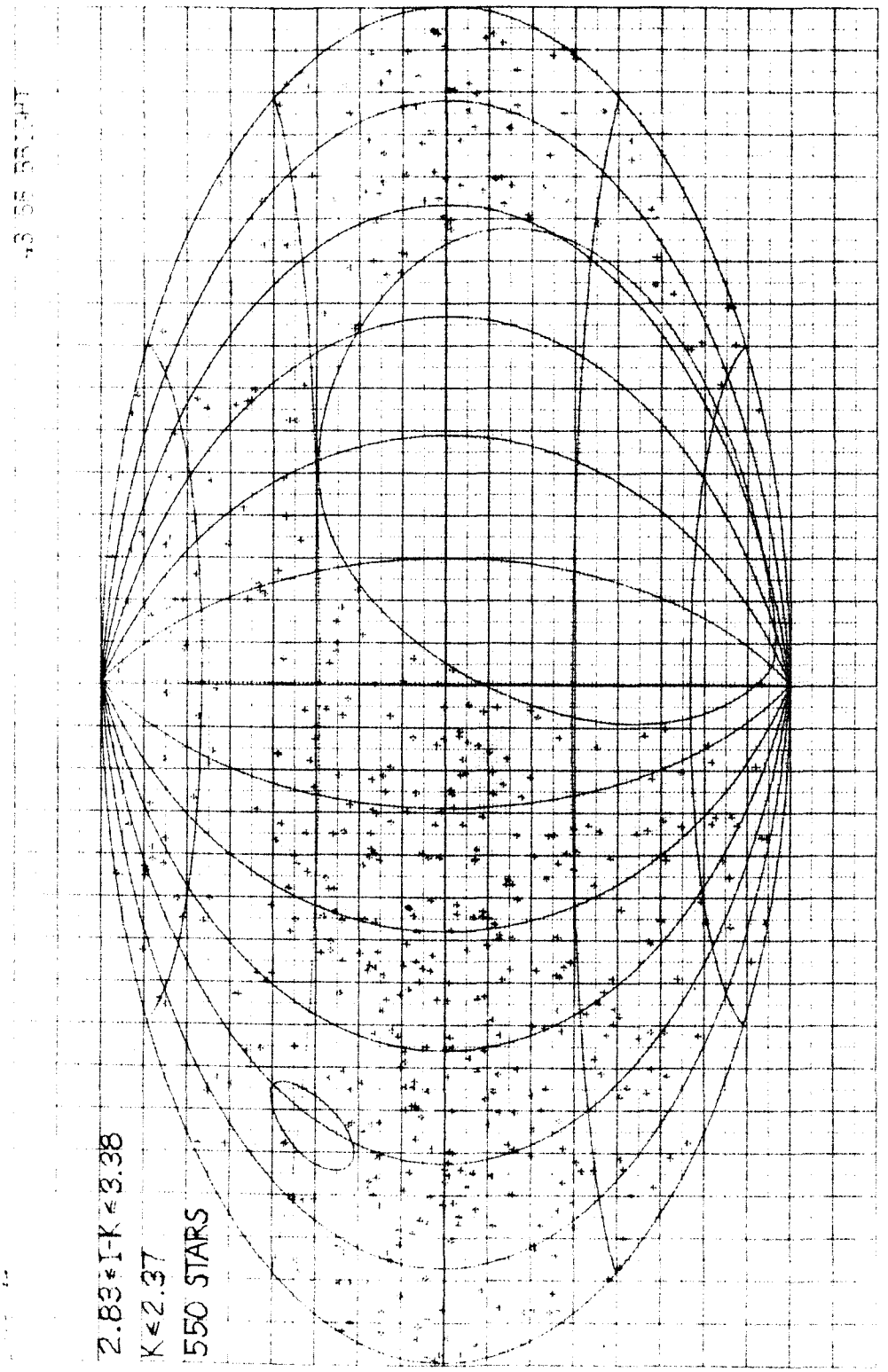

Figure 12a

Figure 12.--Galactic Coordinates of Stars with 2.83 < I-K < 3.38

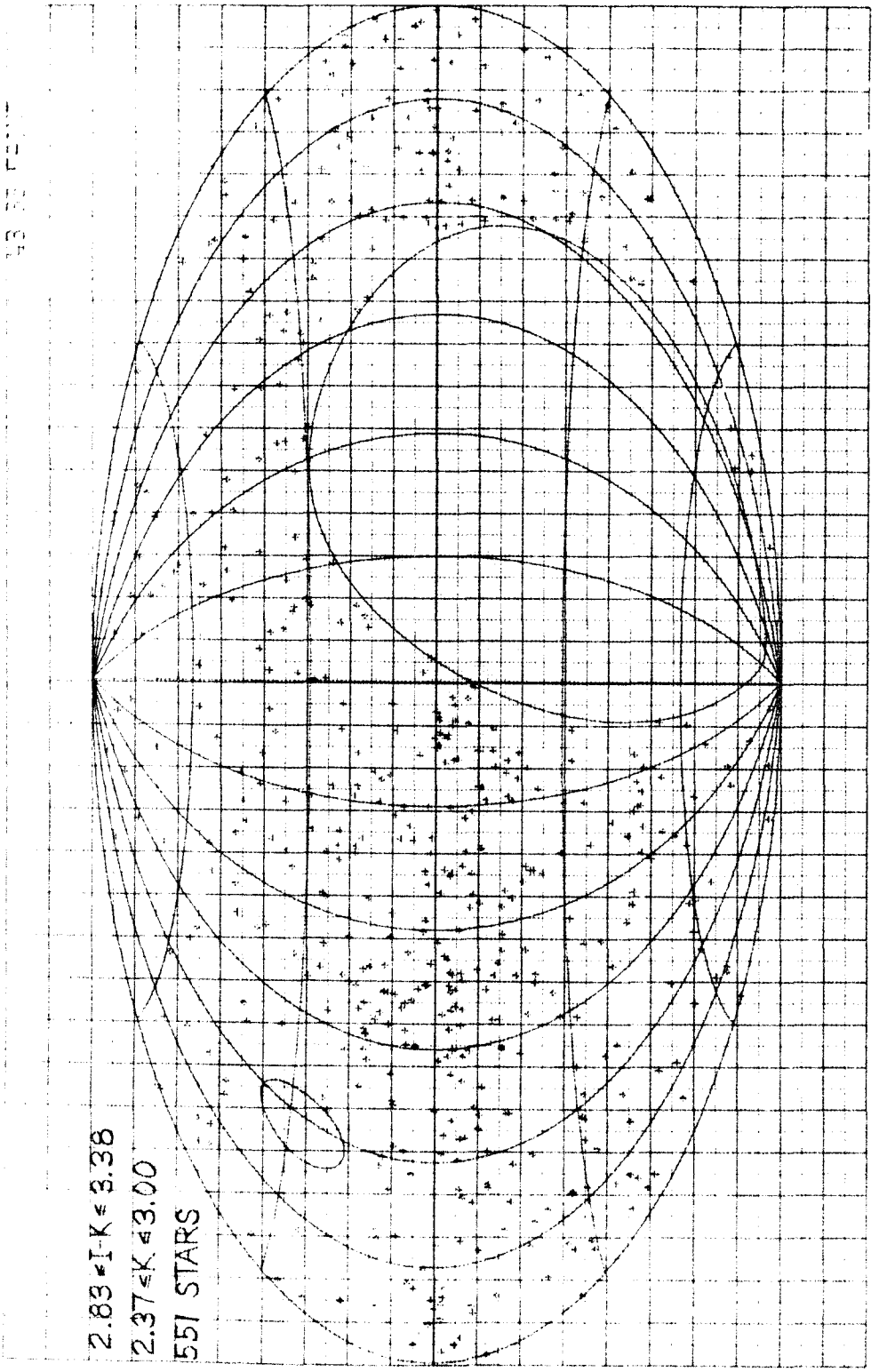

Figure 12b

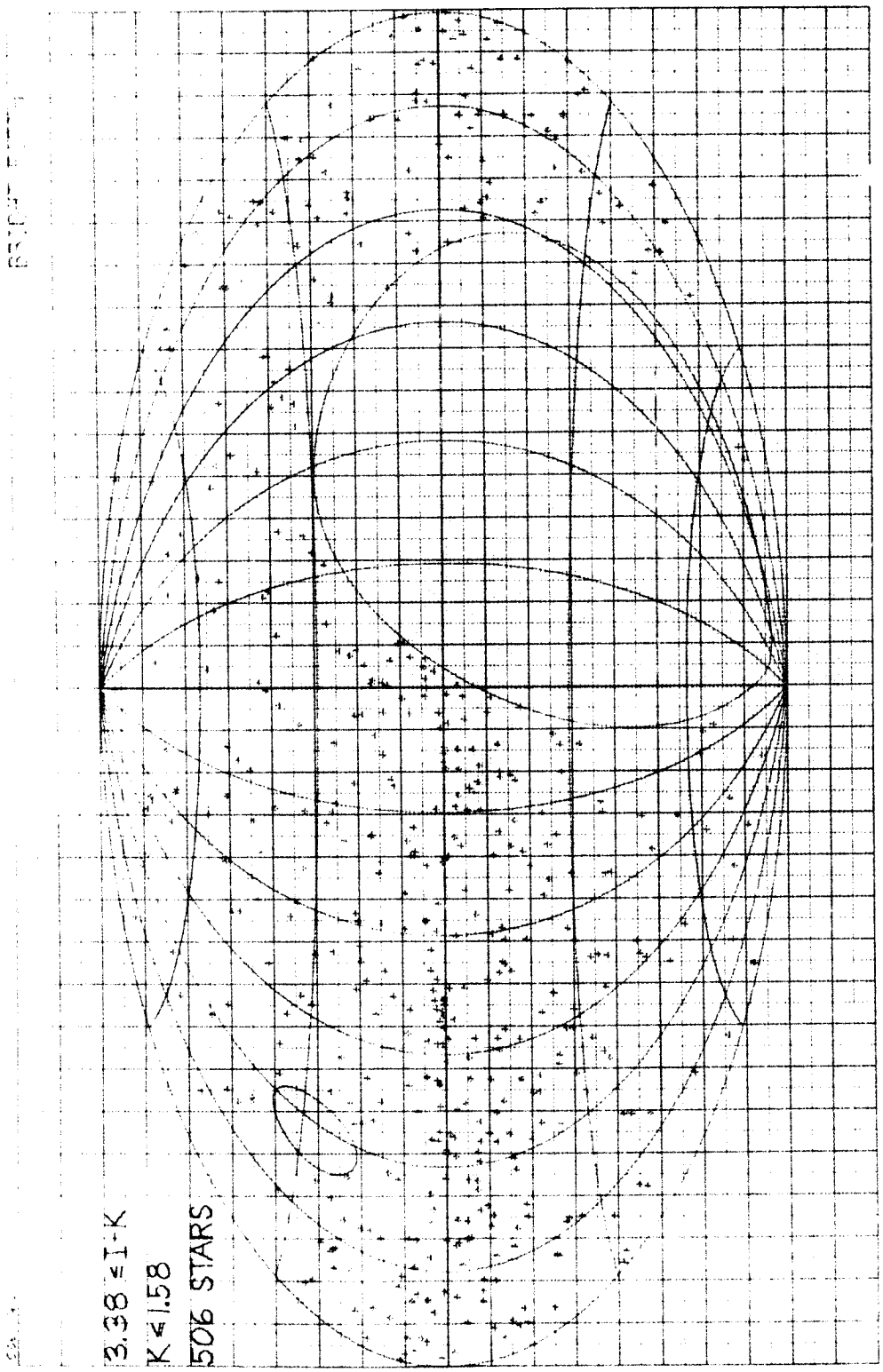

Figure 13a

Figure 13.--Galactic Coordinates of Stars with I-K > 3.38

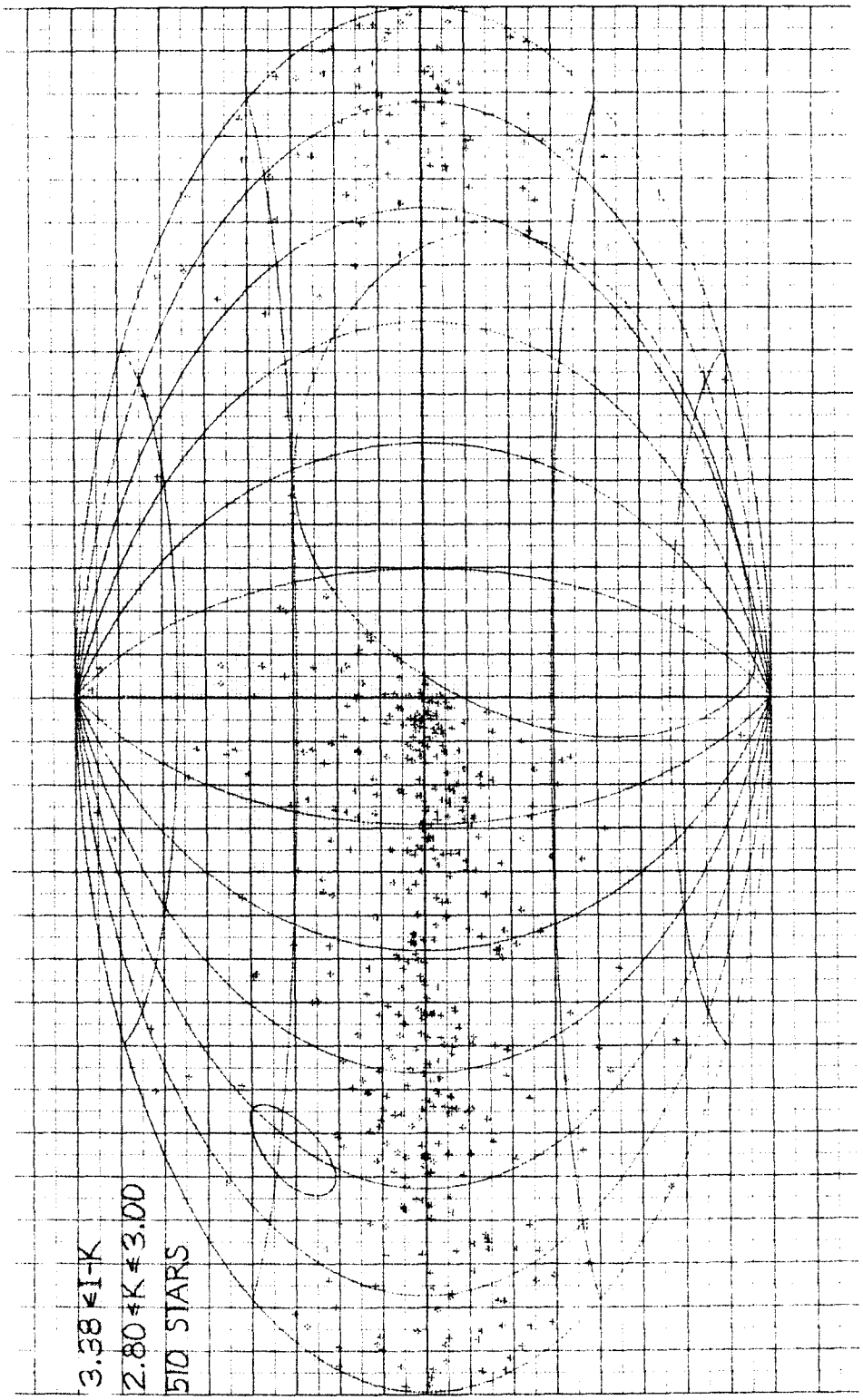

Figure 13b

subgroups based on K. Only the brightest fifth and the faintest fifth were plotted. These plots are shown in Figure 13, a and b.

F. The Distribution in Galactic Latitude

Figures 10 through 13 show an increasing degree of concentration of stars toward the galactic plane as the stars plotted increase in I-K. Some of the quantitative details of this concentration toward the plane are shown in Figure 14 which has resulted from counting the number of stars in various latitude zones and dividing the number in a zone by the area surveyed within that zone. In Figure 14 the latitude zones are indicated by a positive or negative integer depending upon whether the zone is in the northern or southern galactic hemisphere. The actual latitude range included in each zone is given in Table 5. The ordinate in the graphs of Figure 14 is the logarithm to the base 10 of the number of stars per 100 square degrees. The error bars on each point are indicative of the statistical uncertainty due to the finite number of stars in the zone. Thus, if the surface density in a particular zone is calculated from N stars found in that zone, it is plotted as having a fractional standard deviation of $1/\sqrt{N}$.

G. Discussion Based on the Distributions of the Spectral Types and Positions of the Stars in Each of Four I-K Groups

The spectral types of the stars whose positions are plotted in Figures 10 through 13 and summarized in Figure 14 can be determined in a statistical sense by referring to Figure 9. Thus it is possible to compare the observed latitude distribution of the infrared stars

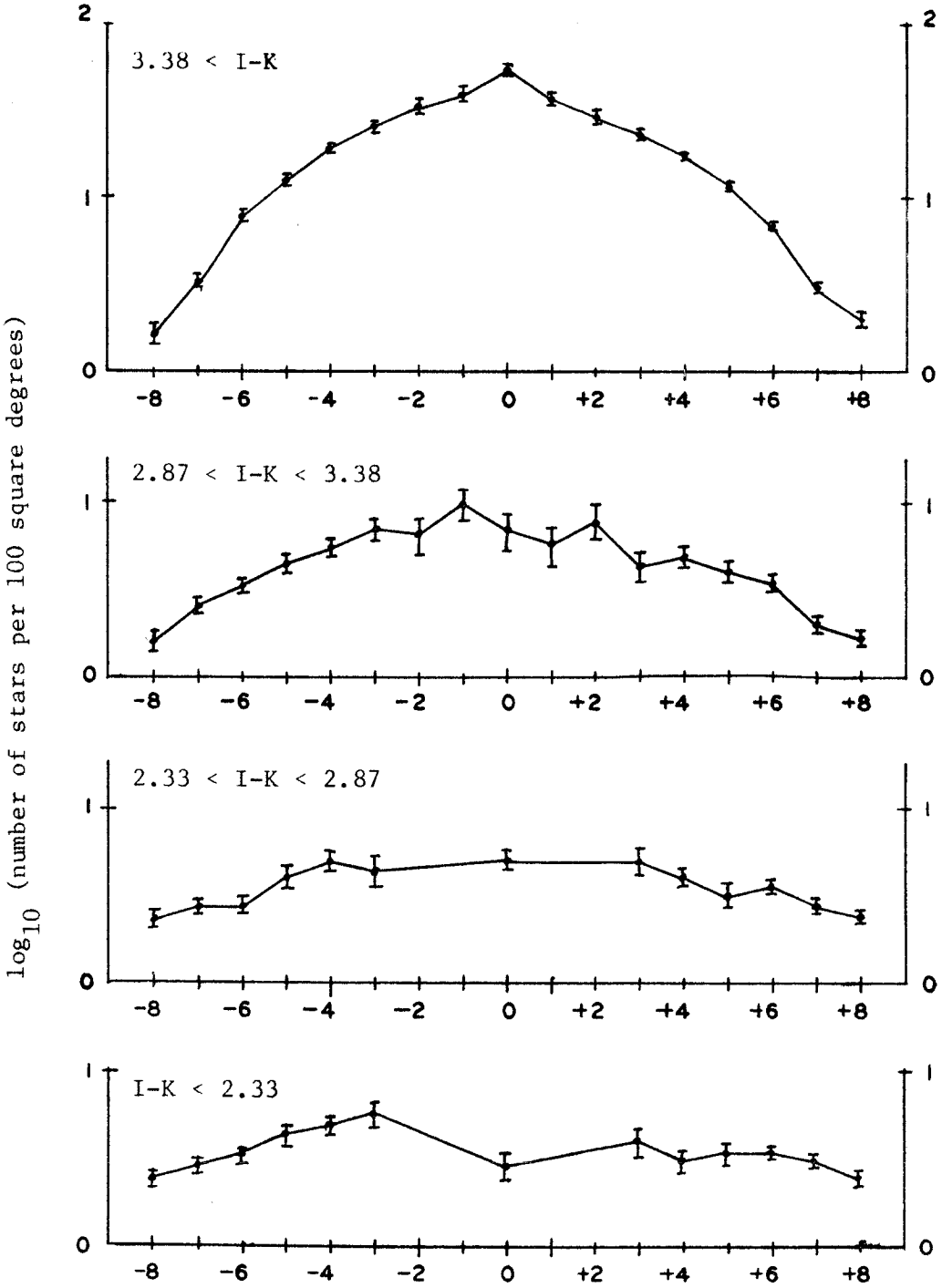

Figure 14. Galactic Latitude Distributions

TABLE 5

THE LATITUDE ZONES AND THE LATITUDE DISTRIBUTIONS

Zone	Latitude range in degrees	Area surveyed in sq. deg.	Number in zone for I-K group indicated:			
			<2.33	2.33-2.87	2.87-3.38	>3.38
+8	+90 to +50	4822	120	116	83	96
+7	+50 to +30	5407	167	149	111	164
+6	+30 to +15	4056	139	146	145	278
+5	+15 to +10	1346	46	43	56	156
+4	+10 to +5	1322	41	54	66	228
+3	+5.0 to +2.5	651	26	33	29	153
+2	+2.5 to +1.5	258	9	11	21	76
+1	+1.5 to +0.5	257	6	13	15	95
0	+0.5 to -0.5	256	9	15	18	140
-1	-0.5 to -1.5	254	4	16	26	101
-2	-1.5 to -2.5	252	9	11	17	84
-3	-2.5 to -5.0	626	36	28	45	159
-4	-5 to -10	1220	60	62	68	237
-5	-10 to -15	1178	51	48	54	148
-6	-15 to -30	3225	108	91	109	250
-7	-30 to -50	3406	97	94	90	113
-8	-50 to -90	3432	82	81	56	56

with that which would have been predicted on the basis of the data in Tables 2, 3, and 4 giving r_{max} the maximum distance for inclusion in the infrared catalog and σ the characteristic half-width of the space density distribution perpendicular to the galactic plane for various spectral types.

I-K < 2.33.--The stars with I-K less than 2.33 show very little tendency to be concentrated toward the galactic plane. Figure 14 shows a definite excess of these stars in the range $-10.0° < 2.5°$ compared to the same positive latitudes, but taking the average of both hemispheres results in a mean surface density of about 4 stars per 100 square degrees over the region within 30 degrees of the plane. Within 40 degrees of the poles the mean surface density is about 2.5 stars per 100 square degrees. According to Figure 9, almost 2/3 of these stars have spectral types from K0 to K9 and nearly all of the rest are earlier than K0. Tables 2 and 3 indicate that none (except 10 or 20 OB stars) of these spectral types are expected to be seen at distances r_{max} greater than their characteristic half-width σ. Therefore, the nearly isotropic distribution of these stars is consistent with predictions based on previous work at visible wavelengths.

2.33 < I-K < 2.87.--The survey stars with I-K between 2.33 and 2.87 do not show much more tendency to concentrate toward the galactic plane than the preceding I-K group. Figure 14 shows a surface density of about 5 stars per 100 square degrees throughout the latitude zones between $-10.0°$ and $+10.0°$. The surface density within 40 degrees of either pole is about 2.3 stars per 100 square degrees.

Figure 9 indicates that of the stars in this I-K range about a third are K4-K9, another third are M0-M1, and the other third are split quite equally into those which are earlier than K4 and those which are later than M1. Table 3 indicates that most of these stars have about the same ratio of r_{max} to σ as the somewhat earlier K giants which predominated in the group with I-K less than 2.33. Again the observed latitude distribution seems to be consistent with Table 3.

2.87 < I-K < 3.38.--The next group in order of redness is that plotted in Figure 12. These stars have I-K in the range 2.87 to 3.38. For this group there is an obvious concentration of stars within 20 or 30 degrees of the galactic plane when this region is compared to the polar regions. The quantitative data in Figure 14 show that the surface density of stars in this I-K range increases steadily in going from the south pole through the zone $-5.0° < b^{II} < -2.5°$. In the northern hemisphere the steady increase in surface density toward the galactic plane continues through the zone $+5.0° < b^{II} < 10.0°$. There is a definite asymmetry between the hemispheres in the latitude zones $\pm(30.0° - 50.0°)$, but in either hemisphere there is clearly an increase in surface density to within 10 degrees of the plane. The average surface density within 10 degrees of the plane is about 7 stars per 100 square degrees while that within 40 degrees of the poles is less than 2 stars per 100 square degrees. This I-K group must contain some stars which can be seen to distances well beyond the characteristic half-width of their space density function perpendicular to the plane. Figure 9 provides the following statistics concerning the types of stars

in this I-K group: 11 percent earlier than M0, 38 percent M0-M1, 31 percent M2-M3, 10 percent later than M3, and 10 percent not identified. Since there are no previous measurements of σ , the characteristic half-width of the space density function, for late M giants, Table 3 cannot confirm or deny the conclusion that the survey must be able to see M stars later than M2 to distances r_{max} definitely larger than σ . The latitude distribution and the spectral type identifications of the stars with I-K between 2.87 and 3.38 point to just that conclusion. A more quantitative argument leading to this conclusion will be presented in Chapter V.

I-K > 3.38.--A comparison of Figure 12b with Figure 13a shows that the brightest fifth of the stars with I-K greater than 3.38 are slightly more concentrated toward the galactic plane than the faint half of the stars with I-K between 2.87 and 3.38. Figure 13b gives the positions of the faintest fifth of this I-K group, and shows that these stars are extremely concentrated toward the plane, especially in some longitude ranges. The latitude distribution of all the stars with I-K greater than 3.38 is much more concentrated near the galactic plane than any of the other I-K groups. This is very obvious in Figure 14. The increase in surface density continues to within one half of a degree of the equator, as is shown by the fact that the point at latitude zone $-0.5° < b^{II} < 0.5°$ is significantly higher than the points at latitude zones $-1.5° < b^{II} < -0.5°$ and $+0.5° < b^{II} < +1.5°$. The actual numbers of stars in these zones are given in Table 5. The conclusion to be drawn from the latitude distribution of this group, the

reddest 45 percent of the survey stars, is that these stars can be seen to distances r_{max} which are large compared to the distance from the plane σ at which their space density is appreciably below what it is in the galactic plane. The data in Figure 9 show that only about a quarter of these stars have been identified in the star catalogs used to get spectral types. Virtually all of those identified are type M0 or later, and of these nearly 40 percent are very late type stars, i.e., classified as M5-M9, R, N, S, or C. In the discussion above concerning the stars with I-K in the range 2.87 to 3.38 it was pointed out that some stars in that group have spectral types later than M2, and the suggestion was made that such stars must account for the anisotropy of the latitude distribution of that I-K group. In the group with I-K greater than 3.38 the majority of the stars must be of these late spectral types. Some indication that this is the case is found in the fact that the stars of spectral types M5-M9, R, N, S, and C which are identified as such are among the brightest stars in this I-K group. Sixty-five percent of the 234 stars identified as belonging to these late spectral types are in the brightest fifth; i.e., 153 of the 234 have a K magnitude less than 1.58.

H. The Longitude Dependence of the Latitude Distribution of the Stars with I-K > 3.38

Looking at the positions of the faintest fifth of the reddest survey stars plotted in Figure 13b one can get the impression that two different groups of stars are represented in the plot. One group would be the stars which account for a moderate concentration of stars

within 10 or 20 degrees of the galactic equator. The effect of this group would be to make the latitude distribution at all longitudes resemble that in the longitude range from 120° to the survey limit near 240°. The second group would be the stars which account for the very high concentrations which are shown within 5 degrees of the equator at various longitudes between the galactic center direction and 120°. In order to examine such dependence of the latitude distribution on longitude in a more quantitative way Figure 15 has been constructed. This figure shows the logarithm of the surface density plotted versus latitude zone in the same manner as Figure 14, but in this case all of the stars have I-K greater than 3.38 and the figure is divided into eight graphs on the basis of longitude ranges. The latitude zones referred to in Figure 15 are the same as those defined in Table 5 and used in Figure 14.

An important feature of the distribution of the positions of the stars with I-K greater than 3.38 is revealed by Figure 15. This is the fact that the extreme concentration toward the galactic equator, which appeared in Figure 14 as a significant increase in surface density within 1/2 degree of the equator, is due almost entirely to stars between 0° and 30° of longitude. The longitude zone between 90° and 120° shows increasing surface density to within 1-1/2 degrees of the equator, and the longitude zones 30°-60° and 60°-90° show such increase to within 2-1/2 degrees of the equator. The longitude zone 120°-150° shows increasing surface density to within 5 degrees of the equator in both hemispheres, although there is a significantly greater surface

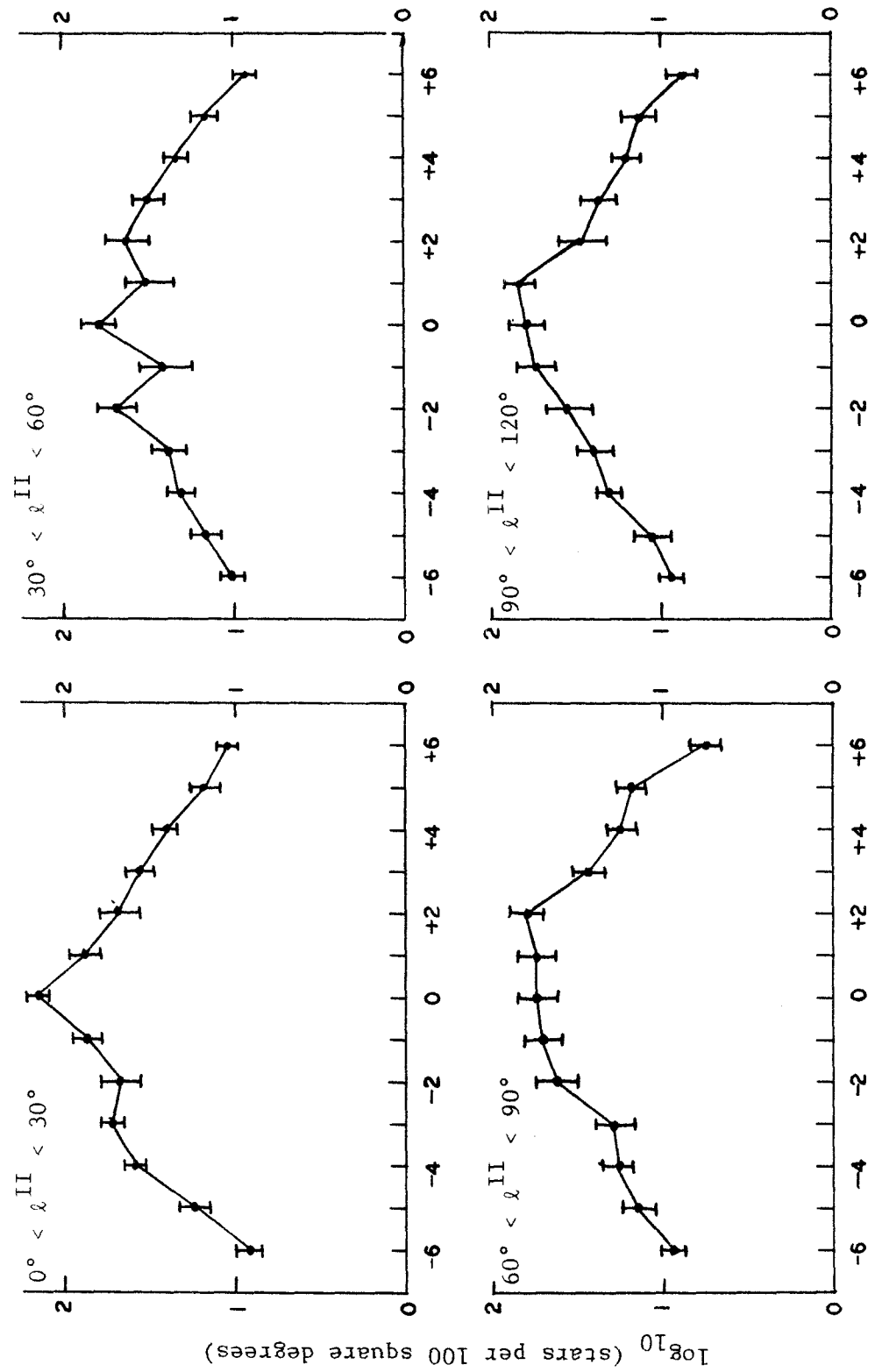

Figure 15a

Figure 15. The Latitude Distributions within Longitude Ranges for Stars with I-K > 3.38.

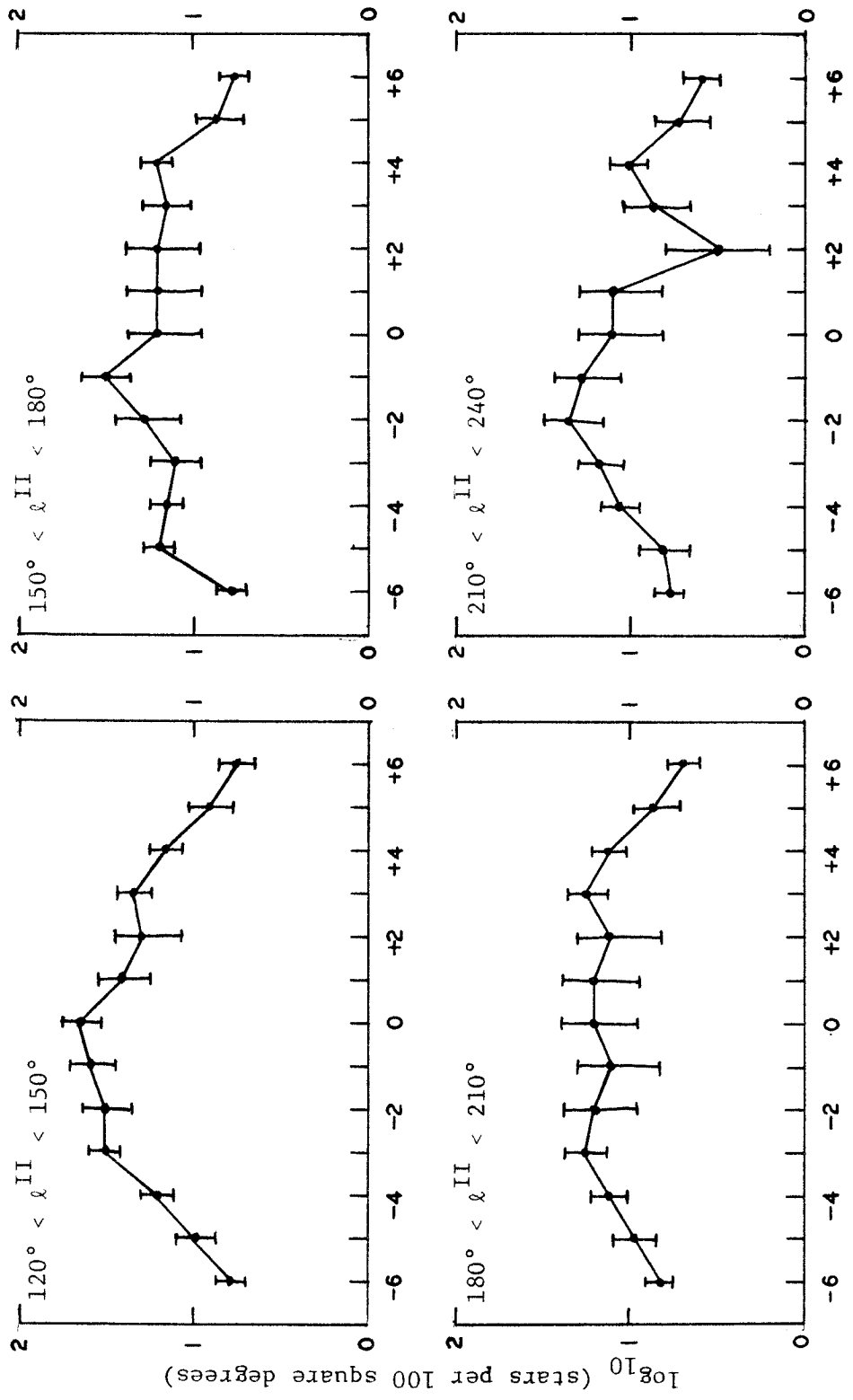
120° < ℓ^II < 150°
150° < ℓ^II < 180°
180° < ℓ^II < 210°
210° < ℓ^II < 240°
log10 (stars per 100 square degrees)
LATITUDE ZONE (defined in Table 5)

Figure 15b

density between latitudes -0.5° and -5.0° than between +0.5° and +5.0°. For the longitudes between 150° and the survey limit, the constant surface density within 10 or 20 degrees of the equator which was suggested by Figure 13 is on the whole confirmed by the last three plots in Figure 15. In this longitude range the increase in surface density ends about 10 degrees from the equator, and the surface density within this distance from the equator fluctuates around an average value of about 17 stars per 100 square degrees.

I. Interpreting the Extreme Concentration toward the Galactic Equator as Being Due to Supergiants

The significance of the latitude at which the surface density stops increasing can be illustrated using Figure 16. Assume that all the stars in a particular sample have the same luminosity, so they can all be seen to the same maximum distance r_{max}. Assume also that these stars are all located in space within a distance σ of the galactic plane and that within this distance they are uniformly distributed in space. Now if r_{max} is less than σ, as is shown in Figure 16a, the number of stars seen per unit solid angle will be the same in all directions. If r_{max} is greater than σ, a critical latitude b_c (or $-b_c$) can be defined as the latitude at which a sphere of radius r_{max} intersects the plane $z = \sigma$ (or $z = -\sigma$). Here z measures distance from the galactic plane. Now, because the space density of the stars is constant everywhere between $z = \sigma$ and $z = -\sigma$, the number of stars seen per unit solid angle is the same at all latitudes b such that $-b_c < b < +b_c$. But for

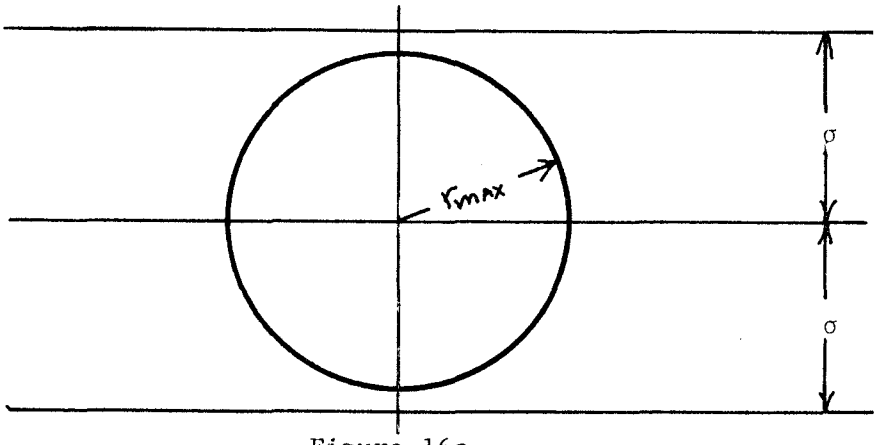

Figure 16a

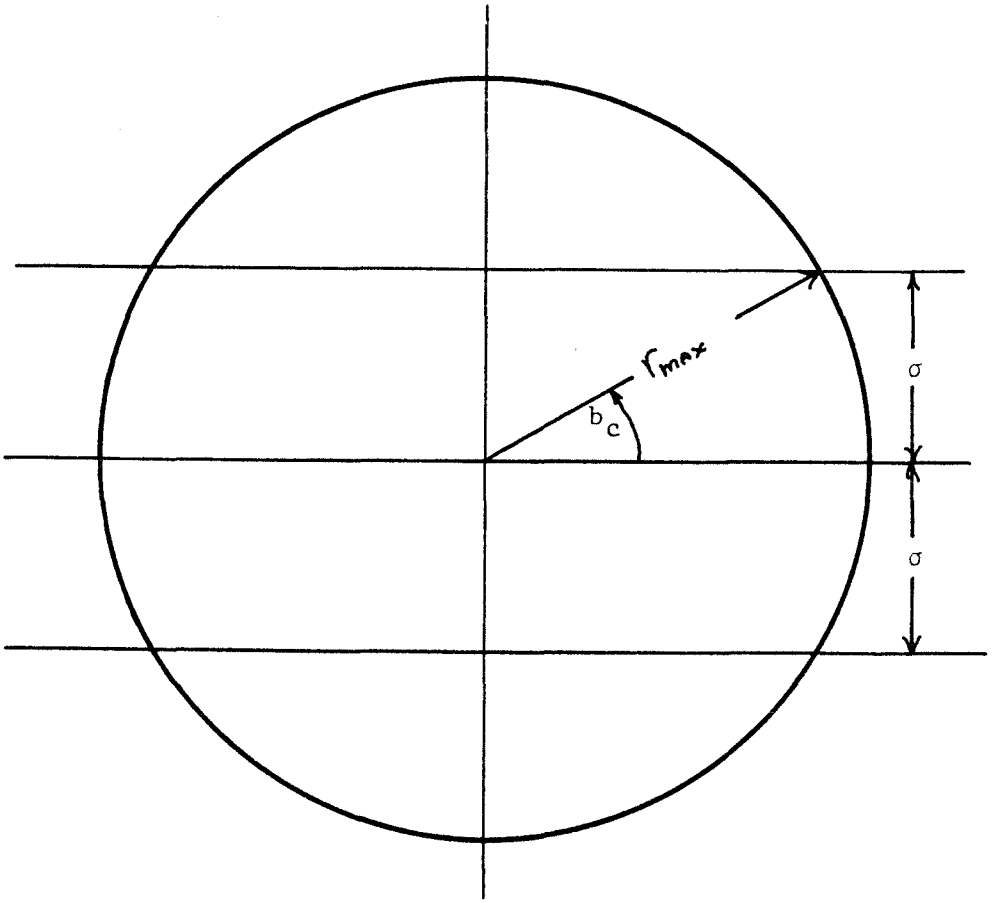

Figure 16b

Figure 16.--An Illustration for Interpreting Latitude Distributions

latitudes b outside of this range the number of stars seen per unit solid angle will decrease as b moves from equator to pole, because the effective volume over which stars can be counted will decrease. Thus, the latitude at which the surface density (i.e., number of stars per unit solid angle) becomes constant as one goes from pole to equator is b_c where $|\sin b_c| = \frac{\sigma}{r_{max}}$. This is illustrated in Figure 16b.

Therefore, the assumption that the group of stars with I-K greater than 3.38 consists of two components would lead to the following conclusions. The component which reaches a constant surface density at about 10 degrees from the equator contains a significant number of stars which can be seen to a distance r_{max} which is about six times σ the characteristic half-width of their space density distribution. This ratio of r_{max} to σ appears consistent with what Table 3 would predict for the very late M giants if the value of σ given for early M giants also applied to the very late types. The component which causes the very high surface density increasing to latitudes very close to the galactic equator would have to include stars at distances from 12 to 100 times σ, depending on the longitude zone. Such large values of r_{max}/σ are more consistent with supergiant stars than with giant stars. For instance, if σ is taken to be 200 parasecs a ratio of 50 would mean the stars being seen are 10 kiloparsecs away. Stars bright enough to be seen at such a distance would be supergiants like α Orionis, which has an absolute K magnitude of -11 and could be seen at a distance of 6 kiloparsecs (36). The estimates of r_{max} given in Table 4 for class Ia supergiants of spectral type K and M are

greater than 4 kiloparsecs. Assuming that the supergiants are young stars and are associated with O and B type stars (31), the characteristic half-width σ of 50 parsecs given in Table 2 for O stars should be applicable to supergiants. Using this value of σ, the latitude distribution shown in Figure 15 for the stars in the longitude range 0°-30° would imply that a significant number of these stars are 5 kiloparsecs away. Table 4 shows that such a maximum distance is not unreasonable for supergiants of spectral type M. But the ratio $r_{max}/\sigma = 12$ suggested for the longitude range 120°-150° is not consistent with the assumption that these are stars within 50 parsecs of the plane which are several kiloparsecs from the sun. Before concluding that supergiants do not contribute significantly to the latitude distribution in this latter longitude range, some information gained from the actual identification of supergiants in this region must be considered.

J. Identifications with Known M Supergiants Near the Clusters h and χ Persei

Eighteen of the stars with I-K greater than 3.38 and longitude between 120° and 150° have been identified with stars known to be supergiants of spectral type M associated with the association I Persei, which is centered on the double cluster h and χ Persei. The lists of these M supergiants used for making identifications are those published by Wildey (37) and Sharpless (38). The actual identifications are listed in Table 6. If these known M supergiants are removed

TABLE 6

INFRARED CATALOG STARS IDENTIFIED WITH
M SUPERGIANTS OF I PERSEI

CIT number	Wildey or Sharpless number	BD number	K mag.	I-K	ℓ^{II}	b^{II}	Sp.-lum. class
+60074	W- 4	+55°529	2.10	3.44	133.68	-4.66	M2 Ib
+60078	W-16	+56°512	2.28	3.86	134.52	-3.46	M3.5 Ib
+60079	W-19	+58°439	2.67	3.40	134.06	-2.00	M2 Iab
+60081	W-20	+58°445	2.55	3.75	133.95	-1.28	M1
+60082	W-21	+56°547	2.15	3.52	134.87	-3.80	M2.5 Iab
+60083	W-23	+56°551	2.54	3.54	134.89	-3.61	M1 Iab
+60085	W-24	+57°550	2.32	3.35	134.72	-2.93	M1 Ib
+60086	W-27	+55°597	1.50	3.44	135.21	-4.09	M3.5 Iab
+60087	W-29	+56°583	1.72	4.18	135.09	-3.61	M4.5 Iab
+60088	W-30	+57°552	1.31	4.39	134.62	-2.20	M4e Ia
+60089	W-33	+56°595	2.45	3.40	135.15	-3.47	M0 Iab
+60090	W-36	+56°609	1.95	3.63	135.33	-3.15	M3 Iab
+60091	W-39	+60°478	1.89	5.35	134.42	-0.02	M2 Iab
+60093	W-45	+56°673	2.17	3.35	137.12	-2.85	M2.5 Iab
+60094	S-WS1	+58°501	1.97	4.25	136.26	-0.44	M2 Iab
+60100	S-WS2	+57°647	2.11	4.11	138.32	-1.40	M2 Ia
+60111	S-WS91	+59°594	2.05	4.04	138.95	+1.93	M2 Ib
+60106	S-WS31		2.39	4.37	139.15	-1.31	M1 Iab:
+60110	S-WS33		1.43	5.16	141.23	-2.26	M3 Iab:
+50089	S-WS34		1.87	4.20	142.68	-2.38	M1 Ib

from the latitude distribution given in Figure 15b for the stars with longitudes between 120° and 150°, the resulting latitude distribution is that shown in Figure 17. A comparison of the two latitude distributions shows that the M supergiants associated with I Persei are responsible for the high surface density in latitude zones -3 and -2 in Figure 15b. The latitude distribution in Figure 17 could be attributed to a group of stars whose surface density is constant within 10 degrees of the galactic equator plus a group whose contribution to the surface density is significant only within a degree or so of the equator. This latter group could consist of some M supergiants which are more distant than those associated with I Persei. The average K magnitude of the identified M supergiants in I Persei is 2.05, which is bright enough to lead to the conclusion that a good proportion of such stars could be seen at distances 1-1/2 or 2 times as far as the I Persei association. The accepted distance for I Persei is 2.3 kiloparsecs (37), so the estimate of r_{max} for M supergiants derived from the I Persei identifications is over 3 kiloparsecs.

Therefore, once the identifications with known M supergiants are taken into account, the latitude distribution of the survey stars with I-K greater than 3.38 in the longitude range 120°-150° is not inconsistent with the assumption that both giant and supergiant stars contribute to the distribution. The identifications do suggest, however, that the statement made earlier to the effect that supergiants may be expected to be found within 50 parsecs of the galactic plane should not be taken too strictly. Most of the M supergiants in

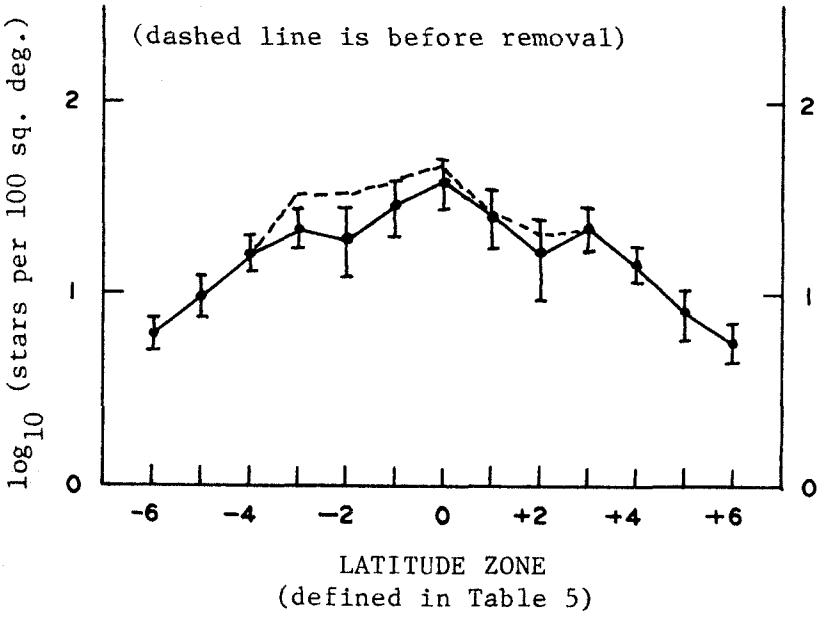

Figure 17.--Latitude Distribution of Stars with I-K > 3.38 and 120° < ℓ^{II} < 150° after Known M Supergiants from I Persei Association Have Been Removed.

I Persei are found at latitudes between -1° and -4° (see Table 6), which at a distance of 2.3 kiloparsecs would mean between 40 and 160 parsecs from the galactic plane.

K. Summary of This Chapter

This chapter has presented data taken directly from the infrared survey together with data based on other work done primarily at visible wavelengths. The conclusions which have emerged in the process of interpreting these data on colors, spectral-luminosity classes, positions, and mean absolute magnitudes may be summarized as follows. Most of the 2024 survey stars which have I-K values less than 2.87 are K giants and cannot be seen at distances r_{max} greater than their characteristic distance from the galactic plane. Most of the 1012 stars with I-K in the range 2.87 through 3.38 are giants of spectral type M0-M4 and some of them can be seen out to distances about six times their characteristic distance from the galactic plane. The survey stars with I-K greater than 3.38 can be seen at distances at least several times their characteristic distance from the plane. Such stars must be of late M spectral type, if they are of luminosity class III. Some of the stars in this I-K group are concentrated so close to the galactic equator that their ratio of maximum distance to characteristic distance from the plane suggests that they are supergiants of late spectral type.

CHAPTER V

DERIVATION OF THE LUMINOSITY DISTRIBUTIONS

In the previous chapter the relationship between the luminosities of the stars and their characteristic distance from the galactic plane was discussed on the basis of their latitude distribution. No attempt was made to take into account the apparent brightnesses (K magnitudes) of the stars. If interstellar extinction at 2.2μ is negligible, the observed latitude and the observed brightness at 2.2μ give a direct measurement of the ratio of the luminosity L of a star to the square of its distance z from the galactic plane. Thus, it is possible to derive a relationship between $D(z)$, the space density function in the z direction, and $p_L(L)$, the luminosity function (i.e., the probability density function for luminosity L).

In this chapter it is shown that the functions $D(z)$ and $p_L(L)$ are related to the distribution function $n(t)$ of an observable quantity

$$t = \frac{2}{5}(3.0-K) + 2 \log_{10}|\csc b^{II}| \qquad [9]$$

by the integral equation

$$n(t) = (\log_e 10)\pi \frac{10^t-1}{10^{3t/2}} \int_{-\infty}^{\infty} \sigma^3 D[z(v-t)]p_v(v)10^{3v/2}dv \qquad [10]$$

where

$$L = \sigma^2 10^v , \qquad [11]$$

$$p_v(v) = p_L(L)\frac{dL}{dv} , \qquad [12]$$

$$z(v-t) = \sigma 10^{(v-t)/2}, \qquad [13]$$

and σ is the distance scale factor. This equation is used to calculate distribution functions n(t) assuming a particular form of D(z) with characteristic distance σ and a gaussian form of $p_v(v)$ with the mean and the standard deviation taken as parameters. The parameters which result in the calculated n(t) that best fits the observed n(t) are determined by applying a χ^2 test. As a result of this analysis the range of luminosity distributions which are consistent with the observed n(t) distribution is obtained for each of the three groups of stars with I-K greater than 2.33. The luminosities so obtained are in units of σ^2, so the absolute luminosity scale is not known unless the characteristic half-width of the z distribution is known.

A. Derivation of the Integral Equation

Let s be the apparent brightness of a star at 2.2μ measured as a ratio to the minimum brightness included in the catalog. Since the minimum brightness included in the catalog is a K magnitude of 3.00, this definition of s means

$$s = 10^{0.4(3.0-K)} . \qquad [14]$$

Defining luminosity L in units such that

$$s = \frac{L}{r^2} \quad \text{(no interstellar extinction)}, \qquad [15]$$

we can write

$$s_{min} \equiv 1 \equiv \frac{L}{r^2_{max}} \qquad [16]$$

so this definition expresses the luminosity of a star as the square of the maximum distance at which the star would appear bright enough to be included in the catalog. Expressing the distance r in terms of the distance from the plane z gives the relationship

$$s = \frac{L}{z^2 \csc^2 b} , \qquad [17]$$

so the observed quantity $s \csc^2 b$ is equal to the square of the ratio r_{max}/z for each star. Figure 18 illustrates the quantities involved here. (It is assumed that the sun is in the plane of the galaxy. This assumption is justified by the fact that various ways of measuring the distance of the sun from the galactic plane give results ranging from 4 to 20 parsecs north of the plane (39,40,41), results which are small compared to the characteristic half-width $\sigma > 200$ parsecs suggested by the data given in Table 3 for late K and M giants.)

The distribution function of the observed quantity $s \csc^2 b$ can be expressed as an integral over the product of the space density function and the luminosity function. Define a space density function $D(r,\Omega)$ and a luminosity function $p_L(L)$ as follows:

$D(r,\Omega)$ = number of stars per unit volume in the region of space at distance r in the direction Ω

$P_L(L)$ = probability per unit luminosity that a star has luminosity L

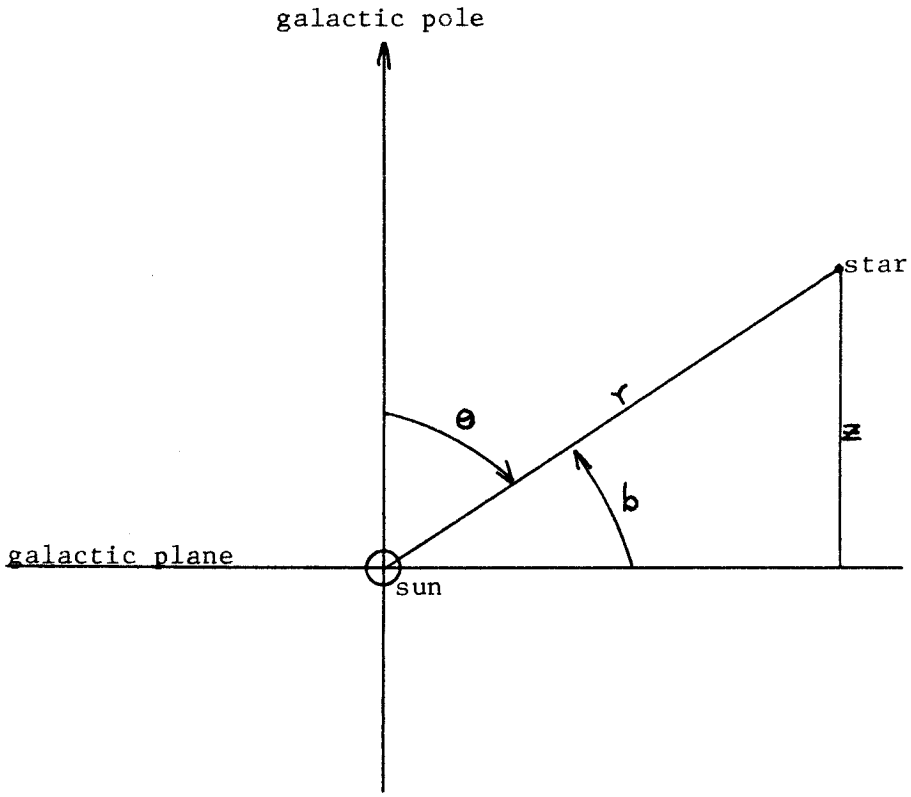

Figure 18.--An Illustration for Defining Some Symbols

Then the number of stars in a volume element dV located at distance r in direction Ω with luminosity in the range L to L + dL is

$$D(r,\Omega)dVp_L(L)dL = D(r,\Omega)r^2drd\Omega p_L(L)dL \qquad [18]$$

where $d\Omega$ is an element of solid angle. Since $L = sr^2$ the number of stars in the volume element which will give a signal in the range s to s + ds is

$$D(r,\Omega)p_L(sr^2)r^2\left|\begin{matrix}\frac{\partial L}{\partial s} & \frac{\partial r}{\partial s} \\ \frac{\partial L}{\partial r} & \frac{\partial r}{\partial r}\end{matrix}\right|drdsd\Omega = D(r,\Omega)p_L(sr^2)r^4drdsd\Omega \ . \qquad [19]$$

Integrating this expression over all distances r gives the number of stars in solid angle $d\Omega$ in direction Ω which have a signal in the range s to s + ds. Calling this number $n(s,\Omega)dsd\Omega$ we can write the distribution function for brightness s and position Ω as

$$n(s,\Omega) = \int_0^\infty D(r,\Omega)p_L(sr^2)r^4dr \ . \qquad [20]$$

This is the integral equation which must be solved to find the space density as a function of distance along a line of sight in direction Ω when a luminosity function is assumed and the distribution in apparent brightness is observed.

In the present case there are not enough stars within solid angles small enough to be considered a single direction to use successfully Equation [20] to determine either the space density or the luminosity function. In order to combine the data from all directions

(latitudes) it is useful to take the distribution function for the quantity x defined as

$$x \equiv s \csc^2 b = \frac{L}{r^2} \frac{1}{\sin^2 b} = \frac{L}{z^2} . \qquad [21]$$

The distribution function for x may be obtained by integrating the distribution function $n(s,\Omega)$ over the strip in the s,θ plane which contains the stars having $s \csc^2 b$ (i.e., $s/\cos^2\theta$) in the range x to $x + dx$. Here direction Ω is being indicated by the single coordinate θ (the colatitude) because the space density $D(r,\Omega)$ is assumed to be a function of distance from the plane z only.

$$D(r,\Omega) = D(z) = D(r \cos \theta) . \qquad [22]$$

The integral in the s,θ plane must exclude the region $s < 1$, since stars with $s < 1$ are too faint to be included in the catalog. Figure 19 illustrates the integration used to get $n(x)dx$, the number of stars with x in the range x to $x + dx$. Assuming north-south symmetry, $D(z) = D(-z)$, $n(x)$ is given by

$$n(x)dx = \int_0^{\theta_c} n(s,\theta) d\Omega ds + \int_{\pi-\theta_c}^{\pi} n(s,\theta) d\Omega ds$$

$$= 2 \int_0^{\theta_c} n(s,\theta) d\Omega ds$$

$$= 4\pi \int_0^{\theta_c} n(s,\theta) \sin \theta \, d\theta \, ds \qquad [23]$$

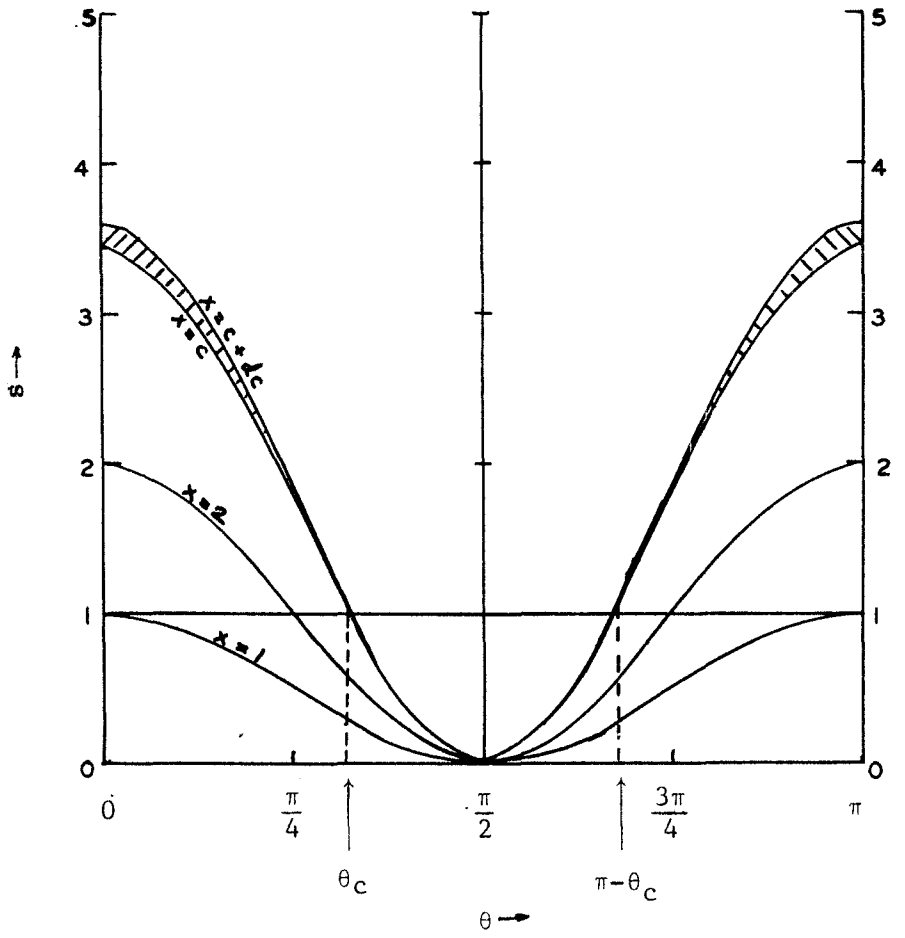

θ_c is used in Equation [23].

Figure 19.--Integration in the s,θ Plane

Now, θ_c is determined by the fact that s, which is related to x by

$$s = x \sin^2 b = x \cos^2\theta \qquad [24]$$

is equal to unity at θ_c, therefore giving

$$\theta_c = \cos^{-1}\sqrt{1/x} \; . \qquad [25]$$

Using Equations [20] and [24] in Equation [23] gives

$$n(x)dx = 4\pi \int_0^{\theta_c} \int_0^{\infty} D(r \cos\theta) p_L(xr^2\cos^2\theta) r^4 dr \sin\theta \, d\theta \cos^2\theta \, dx, \qquad [26]$$

where the change of variables from s,θ to x,θ has been

$$ds \, d\theta = \begin{vmatrix} \frac{\partial s}{\partial x} & \frac{\partial \theta}{\partial x} \\ \frac{\partial s}{\partial \theta} & \frac{\partial \vartheta}{\partial \theta} \end{vmatrix} dx \, d\theta = \cos^2\theta \, dx \, d\theta \; . \qquad [27]$$

Changing variables from r,θ to L,θ where

$$r = \sqrt{L/s} = \frac{1}{\cos\theta} \sqrt{L/x} \qquad [28]$$

results in the expression

$$n(x) = 2\pi \int_0^{\theta_c} \int_0^{\infty} D(\sqrt{L/x}) p_L(L) \frac{L^{3/2}}{x^{5/2}} \frac{\sin\theta}{\cos^3\theta} \, dL \, d\theta, \qquad [29]$$

after the differentials have been transformed according to

$$dr\ d\theta = \begin{vmatrix} \frac{\partial r}{\partial L} & \frac{\partial \theta}{\partial L} \\ \frac{\partial r}{\partial \theta} & \frac{\partial \theta}{\partial \theta} \end{vmatrix} dL\ d\theta = \frac{dL\ d\theta}{2\ \cos\ \theta\ \sqrt{xL}} \ . \qquad [30]$$

Finally, carrying out the integration over θ in Equation [29] and expressing θ_c in terms of x according to Equation [25], the distribution function for x is

$$n(x) = \pi \frac{x-1}{x^{5/2}} \int_0^\infty D(\sqrt{L/x}) p_L(L) L^{3/2} dL \ . \qquad [31]$$

Because the space density function D(z) takes a simple form when z is replaced by a logarithmic variable, the following transformation will be made:

$$t = \log_{10}(x) \qquad x = 10^t \qquad [32]$$

$$u = \log_{10}(\frac{z^2}{\sigma^2}) \qquad z = \sigma 10^{u/2} \qquad [33]$$

$$v = \log_{10}(\frac{L}{\sigma^2}) \qquad L = \sigma^2 10^v \qquad [34]$$

The parameter σ used in this transformation is to be a characteristic distance associated with the space density function D(z). It may be viewed as a measure of the width of D(z). Carrying out this transformation on Equation [31] gives

$$n(t) = n[x(t)]\frac{dx}{dt} = n[x(t)](\log_e 10)10^t$$

$$= (\log_e 10)\pi\frac{10^t-1}{10^{3t/2}}\int_{-\infty}^{\infty}\sigma^3 D[\sigma 10^{(v-t)/2}]p_v(v)10^{3v/2}dv \qquad [35]$$

where $p_v(v)dv$ is the probability of a star having a luminosity L such that $\log_{10}(\frac{L}{\sigma^2})$ is in the range v to v + dv. In fact

$$p_v(v)dv = p_L(L)dL \qquad [36]$$

with L(v) given by Equation [34]. The complicated argument of the space density function in Equation [35] is removed by defining the function

$$K(u) \equiv D[z(u)]/D(0) = D[\sigma 10^{u/2}]/D(0) \ , \qquad [37]$$

which results in

$$D[\sigma 10^{(v-t)/2}] = D(0)K(v-t) \ . \qquad [38]$$

Then Equation [35] becomes

$$n(t) = (\log_e 10)\pi\frac{10^t-1}{10^{3t/2}}\int_{-\infty}^{\infty}\sigma^3 D_o K(v-t)p_v(v)10^{3v/2}dv \ , \qquad [39]$$

where D(0), the space density in the galactic plane, has been written as D_o.

This equation can be put in the standard form for a Fredholm equation of the first kind by defining the functions

$$f(t) = \frac{4}{3(\log_e 10)} \frac{10^{3t/2}}{10^t - 1} n(t) \qquad [40]$$

and

$$U(v) = D_o \frac{4}{3}\pi\sigma^3 10^{3v/2} p_v(v) \ . \qquad [41]$$

With these definitions Equation [39] becomes

$$f(t) = \int_{-\infty}^{\infty} K(v-t)U(v)dv \ . \qquad [42]$$

In what follows the integral equation will be used in the form of Equation [42], taking f(t) as a function known from the observed n(t) distribution, the kernel K(u) as a function assumed known from previous work on the z distribution of red giant stars, and U(v) as the unknown function to be determined. Notice that because $L = r_{max}^2 = \sigma^2 10^v$ (from Equations [16] and [34], U(v) can be written

$$U(v)dv = \frac{4}{3}\pi r_{max}^3(v) D_o p_v(v)dv \ . \qquad [43]$$

This way of writing U(v) shows that U(v)dv is the product of $D_o p_v(v)dv$, the number of stars per unit volume in the galactic plane with a luminosity characterized by v to v + dv, and $\frac{4}{3}\pi r_{max}^3$, the volume of the sphere throughout which they would appear bright enough to be included in the infrared catalog.

B. The Limiting Case of a Sharp Cutoff in D(z) and K(u)

As an illustration of the relationship among the functions

f(t), K(u), and U(v), consider the limiting case where there is a constant space density of stars out to some definite distance from the plane but no stars are found beyond that distance. In this case, the obvious choice for the parameter σ would be the distance at which the space density falls to zero, so D(z) and K(u) would be given by

$$D(z) = \begin{cases} D_o & z < \sigma \\ 0 & z > \sigma \end{cases} \qquad [44]$$

and

$$K(u) = \begin{cases} 1 & u < 0 \\ 0 & u > 0 \end{cases} \qquad [45]$$

This form of K(u) makes the solution of the integral Equation [42] trivial. That equation is

$$f(t) = \int_{-\infty}^{\infty} K(v-t)U(v)\,dv$$

$$= \int_{-\infty}^{t} U(v)\,dv \ . \qquad [46]$$

Therefore,

$$U(v) = \left.\frac{df}{dt}\right|_v = f'(v) \ . \qquad [47]$$

Thus, in the case of a sharp cutoff in the z distribution the luminosity function can be obtained from the first derivative of f(t).

C. Adoption of an Analytic Expression for K(u)

Unfortunately for purposes of determining the luminosity function of the stars in the infrared catalog the actual space density function D(z) does not have a sharp cutoff. Some curves of $D(z)/D_o$ for various kinds of late type giant stars are shown in Figure 20. These curves taken from the work of various authors are all derived from star counts at high or intermediate latitudes with the exception of the curve derived by Oort for K giants (44). Oort's curve is derived from dynamical considerations as well as star counts. When Oort's $D(z)/D_o$ function is transformed into the function K(u) given in Equation [37] taking the characteristic width σ to be 210 parsecs, the resulting K(u) can be closely approximated by the normal error function as is shown in Figure 21. The approximation is

$$K(u) \simeq \frac{1}{0.7\sqrt{2\pi}} \int_u^\infty e^{-\frac{x^2}{2(0.7)^2}} dx \qquad [48]$$

where

$$u = 2 \log_{10}\left(\frac{z}{210 \text{ pc}}\right) . \qquad [49]$$

That a normal error function with a standard deviation of 0.70 is also a fair approximation for most of the other $D(z)/D_o$ curves is demonstrated in Figure 22. This figure shows the K(u) derived from each of the $D(z)/D_o$ curves shown in Figure 20 using a characteristic width σ of 200 parsecs in each case. The ordinate in Figure 22 is scaled so that a normal error function is a straight line with a slope

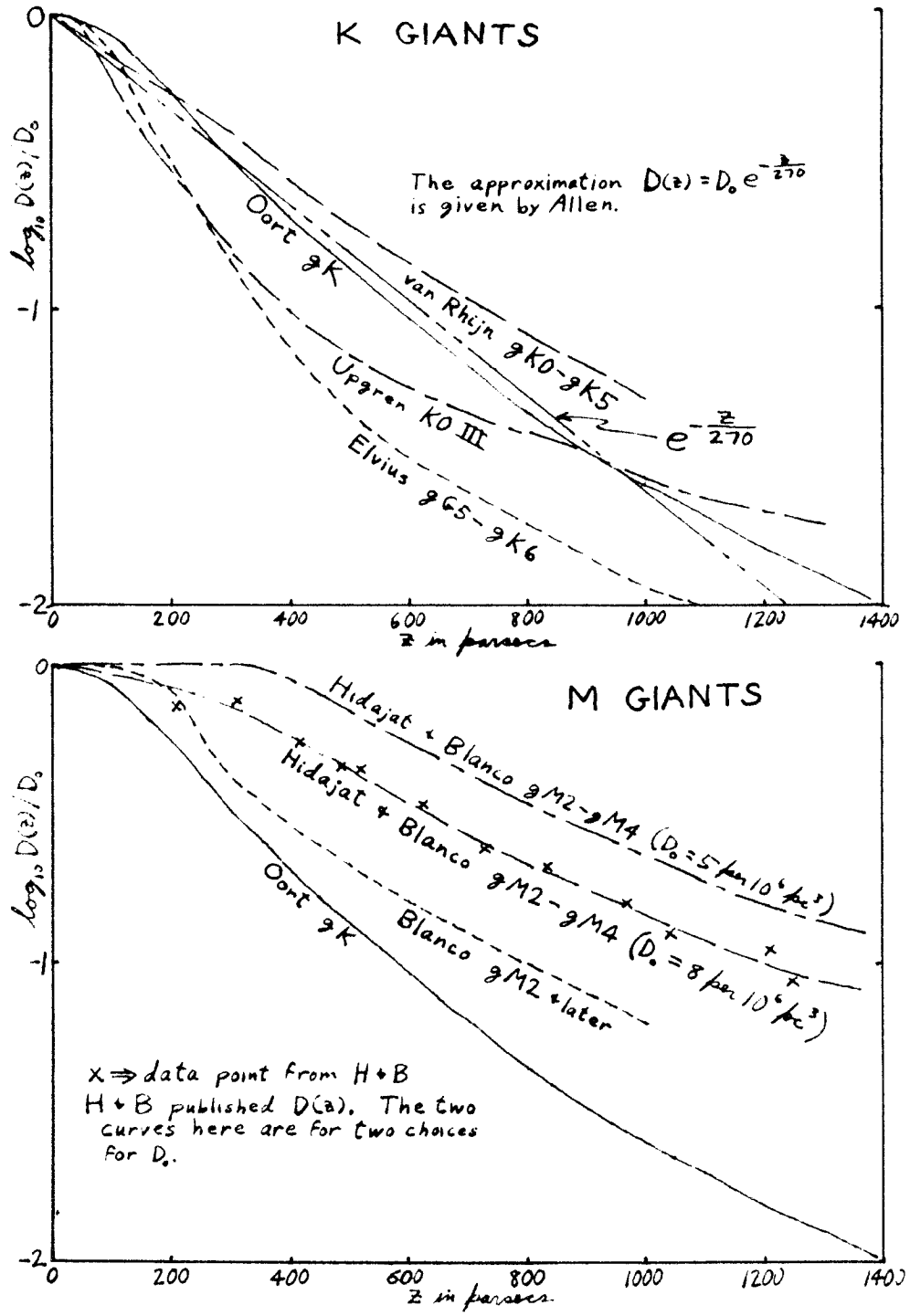

References: Allen (28), Blanco (7), Elvius (41), Hidajat and Blanco (45), Oort (44), van Rhijn (43), and Upgren (42).

Figure 20.--$D(z)/D_0$ Curves for K and M Giants

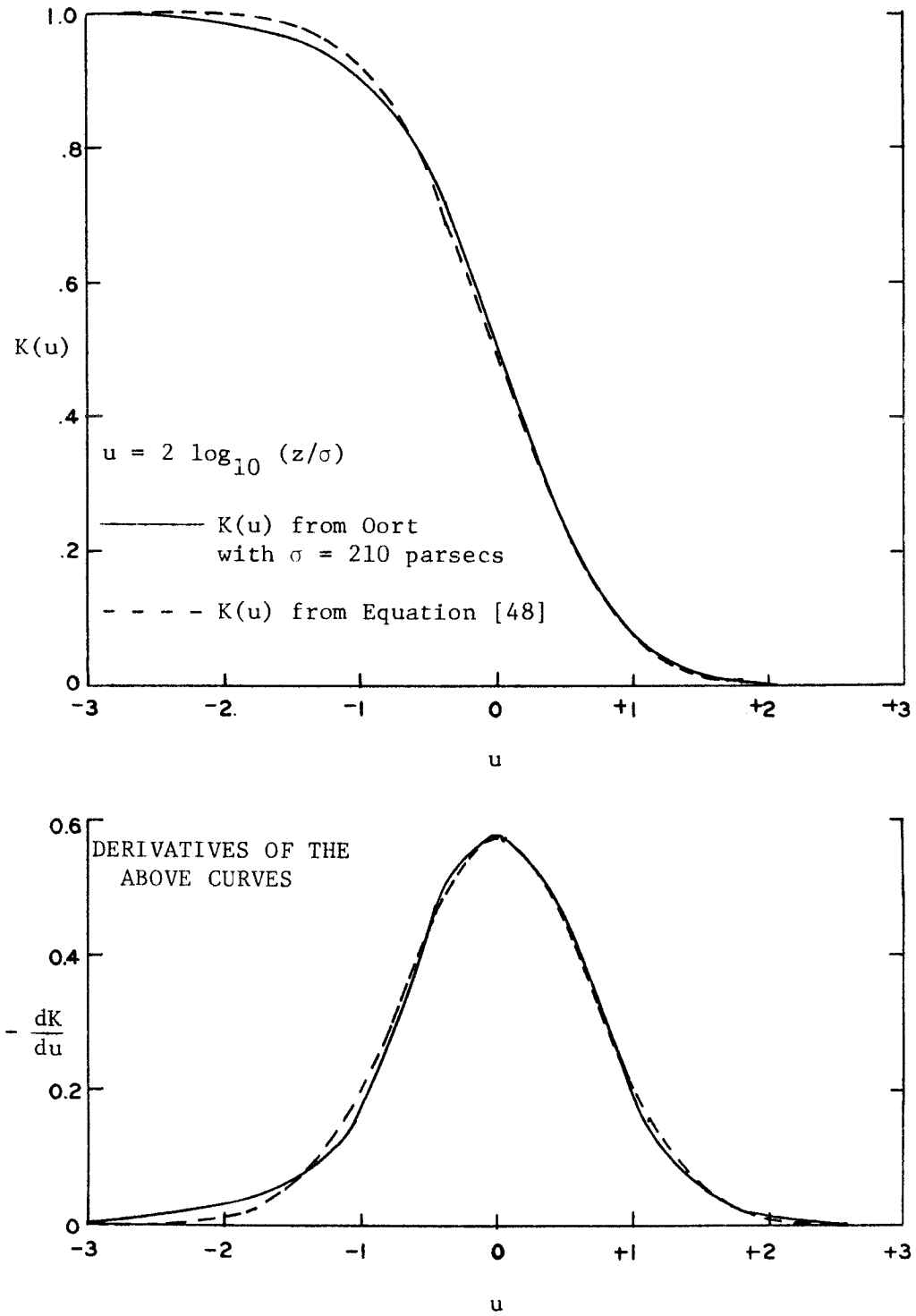

Figure 21.--K(u) from Oort's $D(z)/D_o$ Curve Compared to the Normal Error Function.

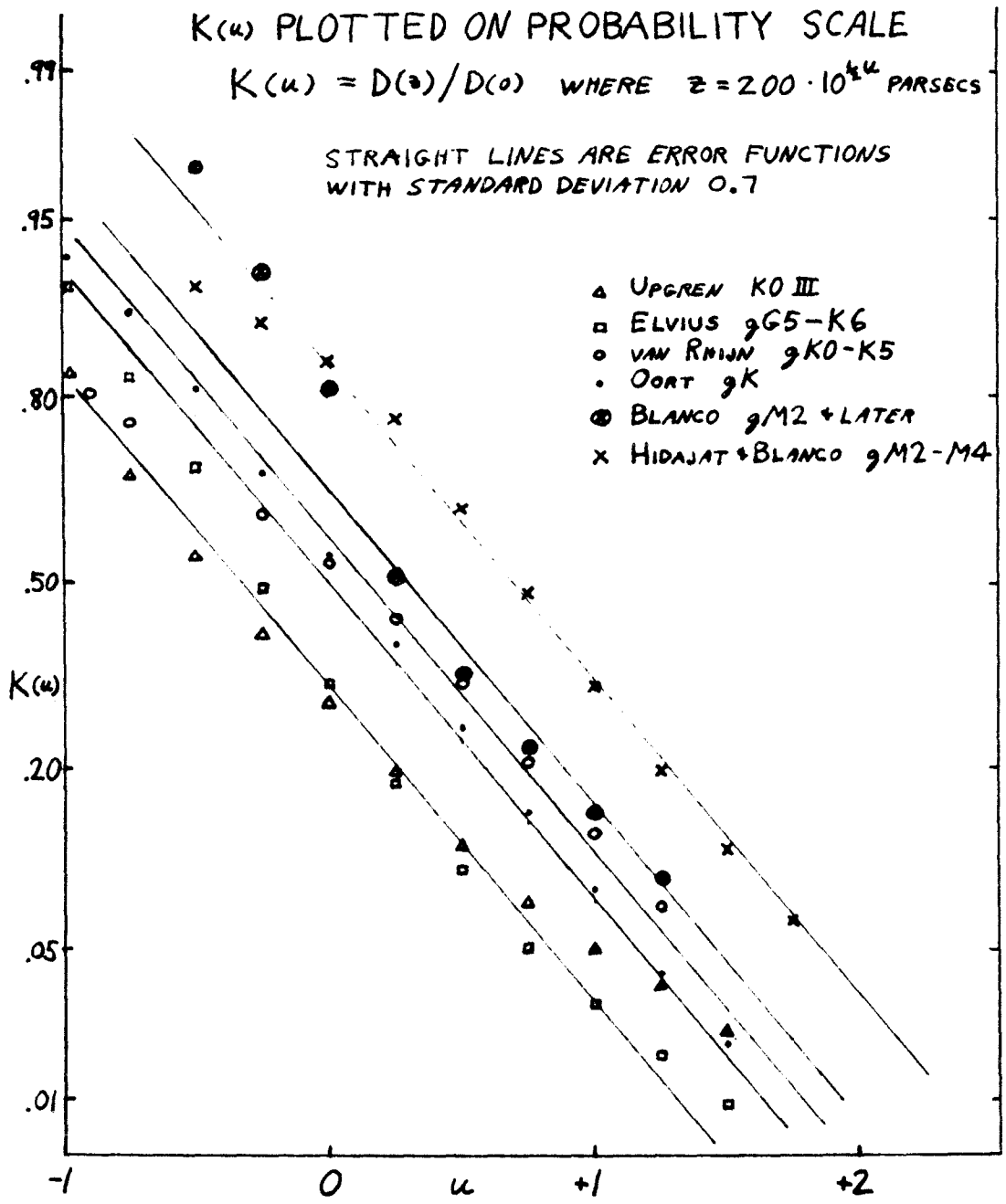

References: The same as given in Figure 20.

Figure 22.--K(u) Data from Various Authors Plotted on a Probability Scale.

determined by its standard deviation. The lines drawn in the figure have the slope for a standard deviation of 0.70. The fact that the value of u where K is equal to one half is not zero in many cases indicates that a characteristic half-width other than 200 parsecs should be used in these cases in order to approximate K(u) by Equation [48]. The conclusion to be drawn from Figure 22 is that Equation [48] is a reasonable way to express the space density function as long as σ is viewed as an adjustable parameter indicative of the distance scale of D(z). Values of σ suggested by Figure 22 for the various types of stars shown there are given in Table 7.

D. Observed n(t) Distributions Compared to the Limiting Case of Constant Space Density

In Section I of Chapter IV it was pointed out that the galactic latitude below which the surface density of stars assumes a constant value provides an indication of the ratio of distance to characteristic z thickness for the most distant stars included in the selection. The same information may be obtained from the observed distribution function n(t) for a group of stars by comparing it to $n_o(t)$, the distribution function which would result from a constant space density of stars. Constant space density would mean

$$K(u) = \text{constant} = 1 \ , \qquad [50]$$

so the distribution $n_o(t)$ would be given by

$$n_o(t) = \frac{3}{4}(\log_e 10)\frac{10^t - 1}{10^{3t/2}}\left[f(t)\right]_{K=1} = \frac{3}{4}(\log_e 10)A\frac{10^t - 1}{10^{3t/2}} \ , \qquad [51]$$

TABLE 7

VALUES OF σ WHICH WOULD GIVE BEST FIT FOR THE DATA OF VARIOUS AUTHORS SHOWN IN FIGURE 22

Author	Type of stars	u at which line of 0.7 std. dev. crosses K = 0.5	σ (pc) which puts crossing at u = 0.00
Upgren	K0 III	-0.38	129
Elvius	gG5-K6	-0.38	129
Oort	gK	0.05	212
van Rhijn	gK0-K5	0.15	238
Blanco	gM2 and later	0.30	282
Hidajat & Blanco	gM2-M4	0.70	448

where A is the constant which results from setting K(v-t) equal to unity in Equation [42]. In fact,

$$A = \int_{-\infty}^{\infty} U(v)dv \qquad [52]$$

the area under the U(v) curve. Figure 23 shows the functions $n_o(t)$ and $\log_{10} n_o(t)$ normalized to a maximum value $n_o = 1000$ at $t = 0.5$. The constant space density form of the distribution n(t) will be applicable whenever K(v-t) is equal to unity over the range of v which contributes significantly to the area under U(v). Thus, for stars which cannot be seen to distances comparable to their characteristic z thickness (i.e., $r_{max} << \sigma$), n(t) will go as $n_o(t)$ even at t = 0. Notice that as a result of Equations [21] and [32]

$$t = \log_{10}\left[\frac{\text{signal from star}}{\text{minimum signal in catalog}} \csc^2 b\right], \qquad [53]$$

so t = 0 corresponds to a star of minimum apparent brightness located at the galactic pole. If a group of observed stars contains a significant number which can be seen to distances $r_{max} \gtrsim \sigma$, then n(t) for these stars will not go as $n_o(t)$ until t is large enough to make

$$z = \sqrt{L/x} = \sqrt{\sigma^2 10^v / 10^t} = \sigma 10^{(v-t)/2} \qquad [54]$$

small compared to σ. The larger the ratio (from Equations [16] and [34])

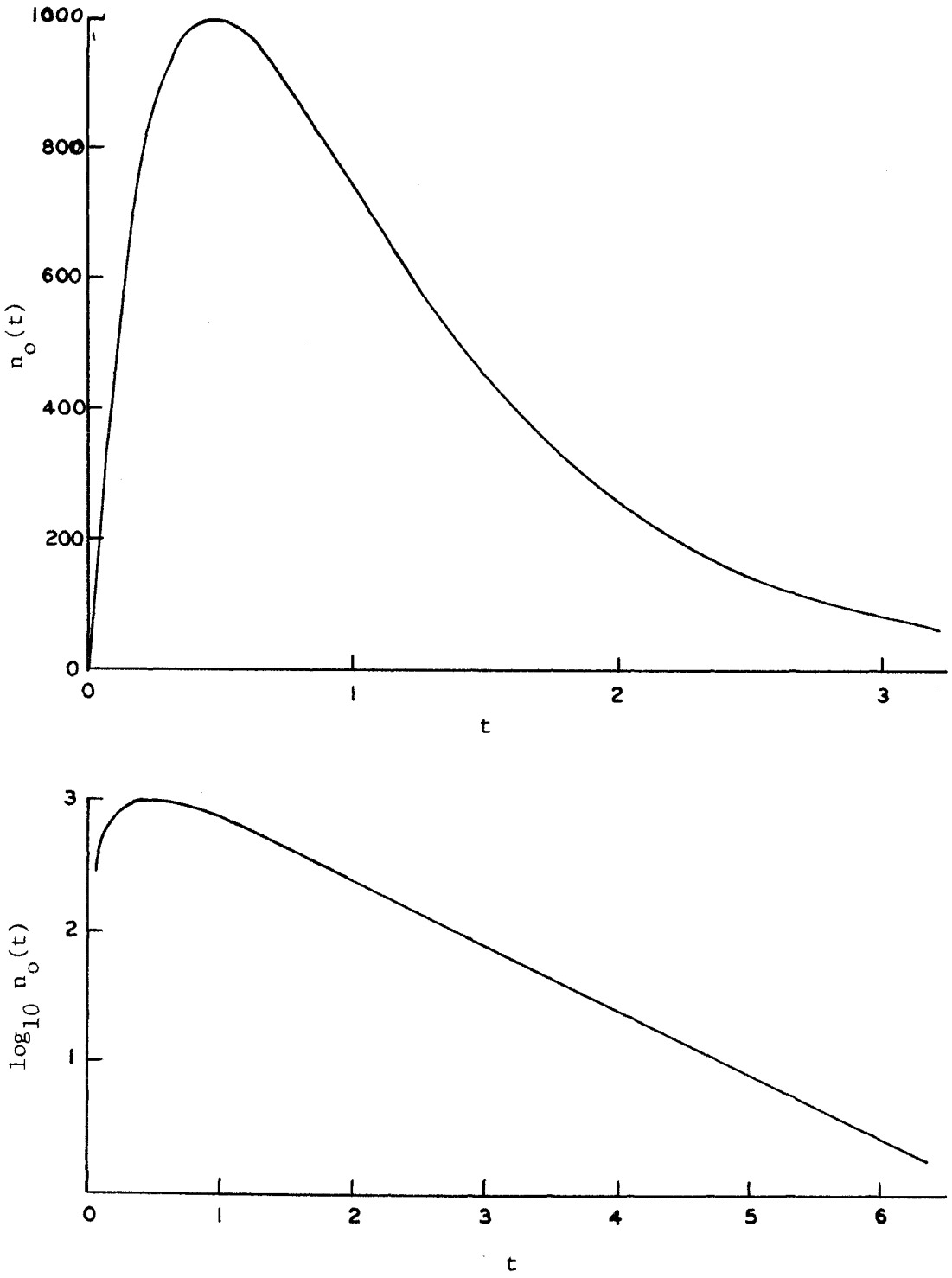

Figure 23.--$n_o(t)$, The Constant Space Density Limit

$$\frac{r_{max}}{\sigma} = 10^{v/2} \qquad [55]$$

for stars in the selection the greater the value of t at which K(v-t) becomes equal to unity.

The observed n(t) distributions for the three groups of catalog stars with I-K less than 3.38 are shown in Figure 24. The procedure used to construct these observed n(t) distributions is described in Appendix B. As explained there, all of the n(t) distribution to be presented are extrapolations to the whole sky (4π steradians) from the fraction of the sky actually covered by the infrared catalog. The integral equation (Equation [39]) was derived on the assumption that stars in all directions are counted. The plots of $\log_{10}n(t)$ versus t in Figure 24 show the tendency for n(t) to go as $10^{-t/2}$ at large enough values of t, which is expected according to Equation [51] and the discussion following it. The constant space density curve $\log_{10}n_o(t)$, fitted by eye to each of the $\log_{10}n(t)$ curves over the linear range where n(t) is proportional to $10^{-t/2}$, has been drawn in for purposes of comparison.

The vertical positions of the $\log_{10}n_o(t)$ curves in Figure 24 are of course arbitrary, reflecting the value of normalization constant A in Equation [51]. The $\log_{10}n_o(t)$ curves actually drawn in Figure 24 are close to the observed distributions $\log_{10}n(t)$ for t approximately in the range 1.0-2.5. Because the observed n(t) distributions are significantly above these $n_o(t)$ curves for some

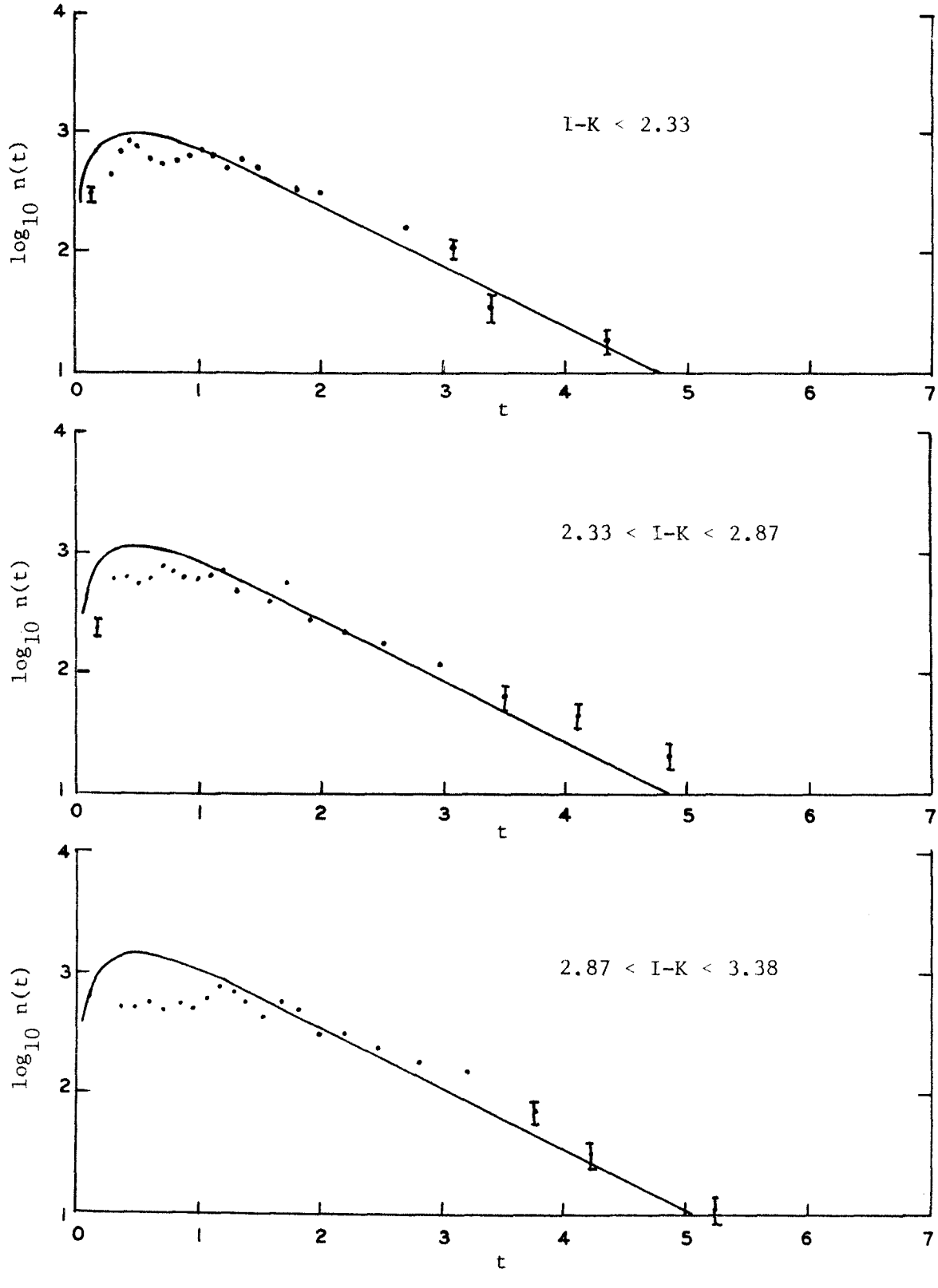

Figure 24.--Observed n(t) Compared to $n_o(t)$ on a Logarithmic Scale

values of t greater than 2.5, larger values of the normalization constant A would be required to make $n_o(t)$ ($\sim 10^{t/2}$) consistent with the observed n(t) for all t greater than some critical value t_c. The significance of another choice of normalization will become clear in the following interpretation of the n(t) and $n_o(t)$ curves shown in Figure 24.

For stars with I-K less than 2.33 the observed distribution n(t) becomes consistent with the constant space density distribution $n_o(t)$ shown in Figure 24 at $t \simeq 1.0$. Since according to Equations [40], [42], and [51]

$$n(t) = n_o(t)\frac{\int_{-\infty}^{\infty} K(v-t)U(v)dv}{\int_{-\infty}^{\infty} U(v)dv} , \qquad [56]$$

this means that there are not a significant number of stars with I-K less than 2.33 which have v large enough to make K(v-1.0) appreciably less than unity. Taking the $z = \sigma$ as the distance where D(z) is "appreciably less than" D_o would mean taking u = 0 as the value of u above which K(u) is "appreciably less than one" and would therefore lead to the conclusion that virtually all of these stars have

$$\frac{r_{max}}{\sigma} = 10^{v/2} < 10^{1/2} = 3.16 . \qquad [57]$$

Since according to Figure 9a nearly all of the stars with I-K less than 2.33 have spectral types earlier than M0 and according to Table 3

the ratio r_{max}/σ for M0 stars is in the range 0.6 to 1.2, the only surprising aspect of the conclusion that there are no stars in this I-K group with r_{max}/σ greater than about 3.0 is the implication that there may be some with r_{max}/σ that large.

The n(t) distributions for the two other I-K groups shown in Figure 24 become consistent with the $n_o(t)$ curves also shown in the figure at $t \simeq 1.2$ and $t \simeq 1.5$ for $2.33 < I-K < 2.87$ and $2.87 < I-K < 3.38$, respectively. According to the above analysis, these values are suggestive of maximum ratios $r_{max}/\sigma \sim 4$ and $r_{max}/\sigma \sim 6$. However, if one insists on choosing a normalization for $n_o(t)$ such that $\log_{10} n_o(t)$ agrees with the observed n(t) at the largest values of t for which data points are available, then the $\log_{10} n_o(t)$ curves would have to be raised and the value of t at which n(t) becomes consistent with $n_o(t)$ would be increased. Thus, if the $\log_{10} n_o(t)$ curve for the group with $2.33 < I-K < 2.87$ were drawn through the last two data points, the comparison of the observed n(t) with the assumed $n_o(t)$ would lead to the conclusion that some of the stars in the selection must have r_{max}/σ as large as 60 (i.e., $10^{(3.6)/2}$). Making the assumed $n_o(t)$ agree well with the four data points with $t > 3.0$ for the stars with $2.87 < I-K < 3.38$ would result in the conclusion that n(t) does not become consistent with $n_o(t)$ until $t > 3.0$, suggesting r_{max}/σ as large as 30 for some stars in this I-K group. It was pointed out in Section I of Chapter IV that such large values of r_{max}/σ are characteristic of late type supergiants rather than late type giants. By normalizing $n_o(t)$ as done in Figure 24, the observed n(t) data can be

interpreted as due to a giant component giving rise to a distribution which goes as $10^{-t/2}$ for t greater than 1.0 or 2.0 and a supergiant component which causes the observed excess of n(t) over $n_o(t)$ at values of $t > 2.5$.

For the stars with I-K greater than 3.38, the extreme concentration toward the galactic equator which was shown in the latitude distribution presented in the previous chapter takes the form of a distribution function n(t) which deviates from the $10^{-t/2}$ law at even larger values of t. The observed n(t) data for the stars with I-K greater than 3.38 are presented in Figure 25 together with two curves of $\log_{10} n_o(t)$ having different normalization constants. For these very red stars there is no sign of n(t) going as $10^{-t/2}$ until t is greater than 2.0, and, whatever normalization is used for $n_o(t)$, there are significant deviations of n(t) from $n_o(t)$ at values of t greater than 4.0. Thus, the n(t) distribution for the reddest catalog stars points to the conclusion that some of them must be characterized by values of r_{max}/σ on the order of 100. To obtain estimates of the numbers of stars of various luminosities the functions U(v) which satisfy the integral equation (Equation [42]) will be found. The conclusions reached by the somewhat qualitative analysis of the n(t) distributions based on comparing them with the limiting case of a constant space density distribution function $n_o(t)$ can then be put in more quantitative terms.

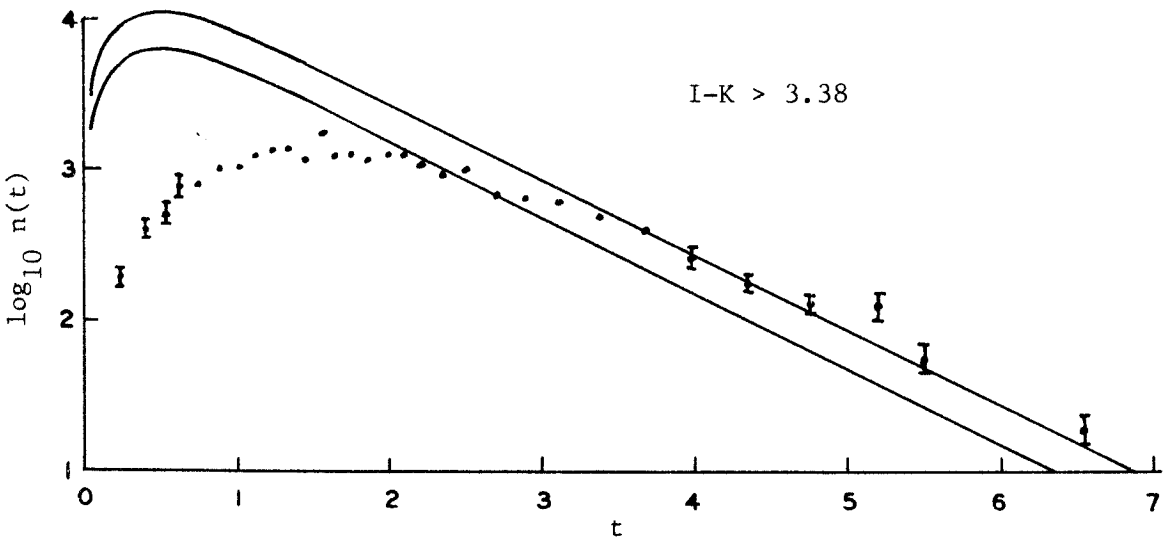

Figure 25.--Observed n(t) for Stars with I-K > 3.38 Compared to $n_o(t)$ on a Logarithmic Scale.

E. Definitions of the Luminosity Function Parameters

Functions U(v) which satisfy the integral equation

$$n(t) = \frac{3(\log_e 10)}{4} \frac{10^t - 1}{10^{3t/2}} \int_{-\infty}^{\infty} K(v-t)U(v)dv \qquad [58]$$

to within the uncertainty in the observed distribution functions n(t) have been found by using a three parameter gaussian representation of U(v) together with the error function form of the kernel K(u), which was derived from Oort's $D(z)/D_o$ curve and given in Equation [48]. The gaussian form of U(v) follows from assuming a gaussian luminosity function $p_v(v)$. To be specific, if it is assumed that the probability of a star having luminosity

$$L = r_{max}^2 = \sigma^2 10^{v'} \qquad [59]$$

such that v' is in the range v to v + dv is given by

$$p_v(v) = \frac{1}{\Delta\sqrt{2\pi}} \exp\left[- \frac{(v-v_o)^2}{2\Delta^2} \right] , \qquad [60]$$

then the function U(v) defined by Equation [41] is

$$U(v) = \frac{4}{3}\pi\sigma^3 D_o 10^{3/2v} \frac{1}{\Delta\sqrt{2\pi}} \exp\left[- \frac{(v-v_o)^2}{2\Delta^2} \right] , \qquad [61]$$

which can be rewritten in gaussian form as

$$U(v) = \frac{A}{\Delta\sqrt{2\pi}} \exp\left[- \frac{(v-v_m)^2}{2\Delta^2} \right] , \qquad [62]$$

where

$$\log_{10}A = \log_{10}(\tfrac{4}{3}\pi\sigma^3 D_c) + \tfrac{3}{2}[v_o + \tfrac{3}{4}(\log_e 10)\Delta^2] \qquad [63]$$

and

$$v_m = v_o + \tfrac{3}{2}(\log_e 10)\Delta^2 \ . \qquad [64]$$

Therefore, the three parameters used in the expression for U(v) are the mean v_m, the standard deviation Δ, and the normalization A. Notice that, as in Equations [51] and [52], A is the area under the function U(v).

If theoretical curves of n(t) calculated from Equation [58] using the three parameter gaussian U(v) are compared with the observed n(t) data on logarithmic plots such as Figures 24 and 25, the shape of the calculated $\log_{10}n(t)$ is a function of v_m and Δ, and its vertical position is determined by the normalization constant A. Such comparisons have been made by eye, and from these comparisons the values of v_m and Δ which appear to fit the data reasonably well have been determined. But the range of v_m and Δ which appear to the eye to fit a particular observed $\log_{10}n(t)$ curve is quite large. Therefore, a quantitative measure of goodness of fit has been adopted.

F. The χ^2 Test for Goodness of Fit

The method adopted here to test the agreement between an observed n(t) distribution, normalized to apply to the whole sky as described in Appendix B, and a theoretical n(t) distribution, calculated from the parameters A, v_m, and Δ using Equations [58] and [62], is essentially the one described by Cramér (46). The range of t from 0 to ∞ is divided into m intervals. The number of stars with a value of t in the range of interval i is ν_i. (More precisely, ν_i is the number of stars weighted according to the procedure described in Appendix B. The actual number of stars in interval i will be referred to below in Equation [67] as N_i, which is typically about three quarters of ν_i.) The number of stars in interval i as predicted by the assumed U(v) is

$$\mu_i = \int_{t_{i-1}}^{t_i} n_c(t)dt \ , \qquad [65]$$

where $n_c(t)$ is the calculated distribution function and t_i is the upper limit of interval i. The normalization parameter A is chosen so that the calculated total number of stars in intervals 1 through k ($k \leq m$) is equal to the observed total number of stars in intervals 1 through k; i.e.,

$$\int_0^{t_k} n_c(t)dt = \sum_{i=1}^{k} \mu_i = \sum_{i=1}^{k} \nu_i \ . \qquad [66]$$

The reason for possibly not normalizing the theoretical distribution to give the same total number as the observed distribution over the whole range of t from 0 to ∞ is that both the latitude distribution and the logarithmic plots of n(t) have shown some evidence that a different population of stars, supergiants, contributes significantly to the sample of stars observed at very low latitudes. The first step in testing for goodness of fit over the range $0 < t < t_k$ consists of calculating the quantity

$$\chi^2 = \sum_{i=1}^{k} \frac{(\nu_i - \mu_i)^2}{\nu_i} \frac{N_i}{\nu_i} . \qquad [67]$$

Here N_i is the actual number of stars with $t_{i-1} < t < t_i$. Then the probability that χ^2 would be this large or larger due only to random sampling errors is obtained by looking in the standard χ^2 table for k-1 degrees of freedom. Cramer indicates that this procedure can be used "for ordinary purposes" if the intervals are chosen large enough to make i > 10.

Table 8 shows the application of this method in comparing the observed n(t) distribution for stars with I-K > 3.38 to that calculated from a U(v) with mean $v_m = 1.80$, standard deviation $\Delta = 0.55$, and A chosen to give agreement on the total number of stars with t < 2.28. Table 8 shows that the total χ^2 after the first 8 groups (i.e., up to t = 2.28) is 3.5. Interpolation using a standard χ^2 distribution for 7 degrees of freedom gives a probability of 0.83 that random errors would give rise to a value of χ^2 greater than 3.5. Therefore, the

TABLE 8

χ^2 TEST APPLIED TO n(t) CALCULATED FROM U(v) WITH $v_m = 1.80$ AND $\Delta = 0.55$

Interval i	Upper limit t_i	Actual number N_i	Weighted number ν_i	Calculated μ_i	$\mu_i - \nu_i$	$\frac{(\mu_i-\nu_i)^2 N_i}{\nu_i} \frac{}{\nu_i}$	Total χ^2 through i
1	0.31	50	61	53.3	-7.7	0.8	0.8
2	0.58	100	123	138.4	15.4	1.6	2.4
3	0.88	200	256	251.6	-4.4	0.1	2.4
4	1.19	250	336	346.8	10.8	0.3	2.7
5	1.45	250	340	332.2	-7.8	0.1	2.8
6	1.70	250	344	331.1	-12.9	0.4	3.2
7	1.98	250	347	358.0	11.0	0.3	3.4
8	2.28	250	349	344.6	-4.4	0.0	3.5
9	2.70	250	351	388.3	37.3	2.8	6.3
10	3.23	250	352	331.9	-20.1	0.8	7.1
11	4.14	250	352	278.9	-73.1	10.8	17.9
12	∞	182	257	154.3	-102.7	29.0	46.9

These data are from stars with I-K greater than 3.38.

The U(v) used was normalized to agree with the total number observed through interval 8, i.e., for $0 < t < 2.28$.

disagreement between the theoretical and the observed distribution over the range $0 < t < 2.28$ would have occurred in five out of six cases due purely to random fluctuations. The theoretical and observed n(t) are in good agreement over this range. In the last 4 groups in Table 8, where t is greater than 2.28, the differences between the calculated and the observed n(t) become so pronounced that by group 12 the total χ^2 has risen to 46.9. Such a large χ^2 is way beyond the limit of a standard χ^2 table for 11 degrees of freedom and has virtually no chance of occurring due to random errors. This failure to agree with the observed n(t) for stars with I-K > 3.38 at large values of t is typical of the calculated n(t)'s which fit well in the range $0 < t < 2.28$. This is shown graphically in Figure 28 below.

Figures 26, 27, and 28 show the observed n(t) distributions for the I-K groups 2.33-2.87, 2.87-3.38, and greater than 3.38 respectively. The observed n(t) distributions in these figures are displayed by showing the values of $\bar{n}_i$, the average of n(t) over the interval $t_{i-1} < t < t_i$ used in the χ^2 test.

$$\bar{n}_i = \frac{\text{number of stars with } t_{i-1} < t < t_i}{t_i - t_{i-1}} . \qquad [68]$$

The curves in each of the figures are distribution functions n(t) calculated using various values of the parameters A, v_m, and Δ. All of the calculated curves shown in Figures 26, 27, and 28 are at least half as probable a fit to the observed n(t) as the most probable fit found. "Probable" here refers to the probability that the χ^2 could be

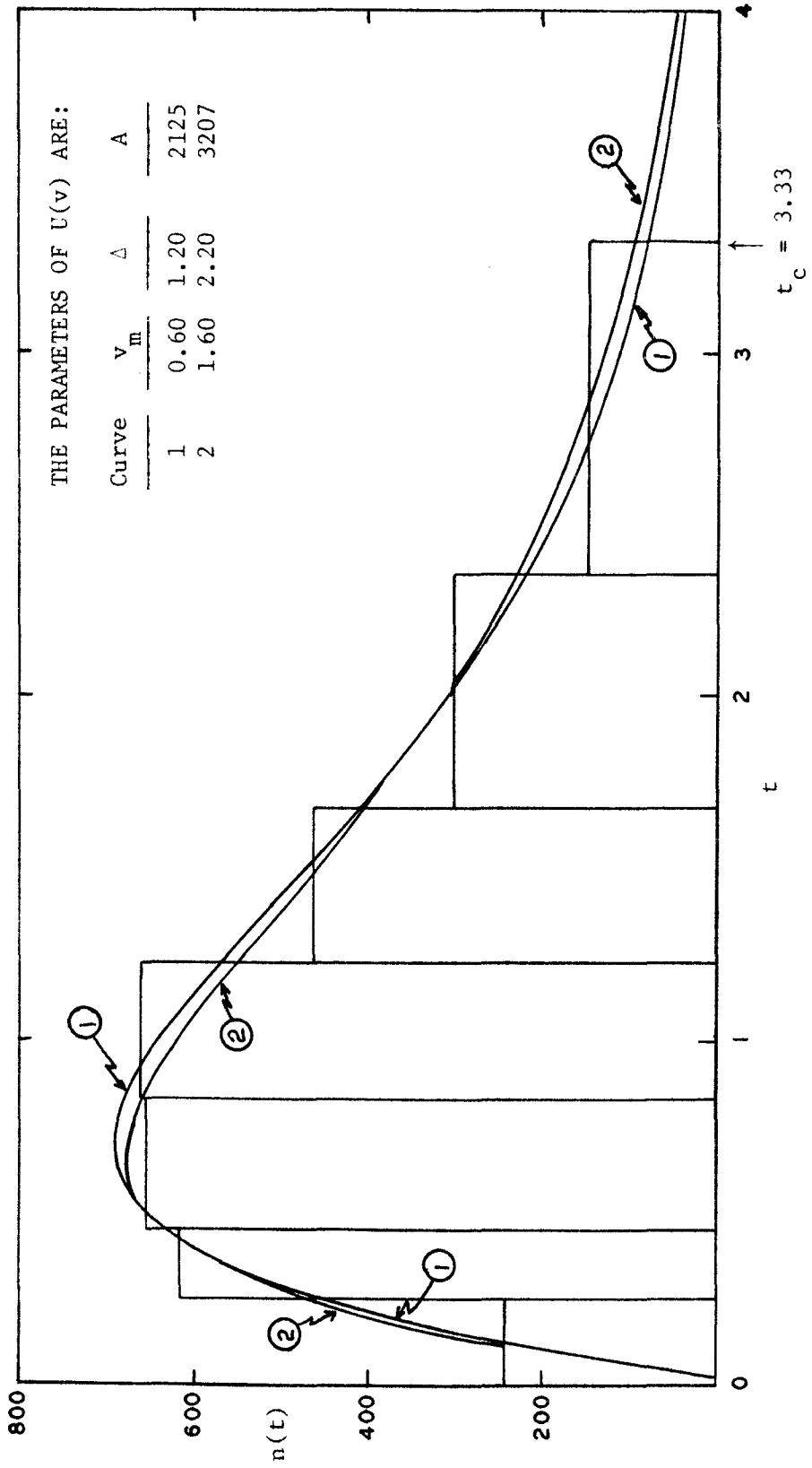

Figure 26. Observed and Theoretical n(t) for Stars with $2.33 < I\text{-}K < 2.87$

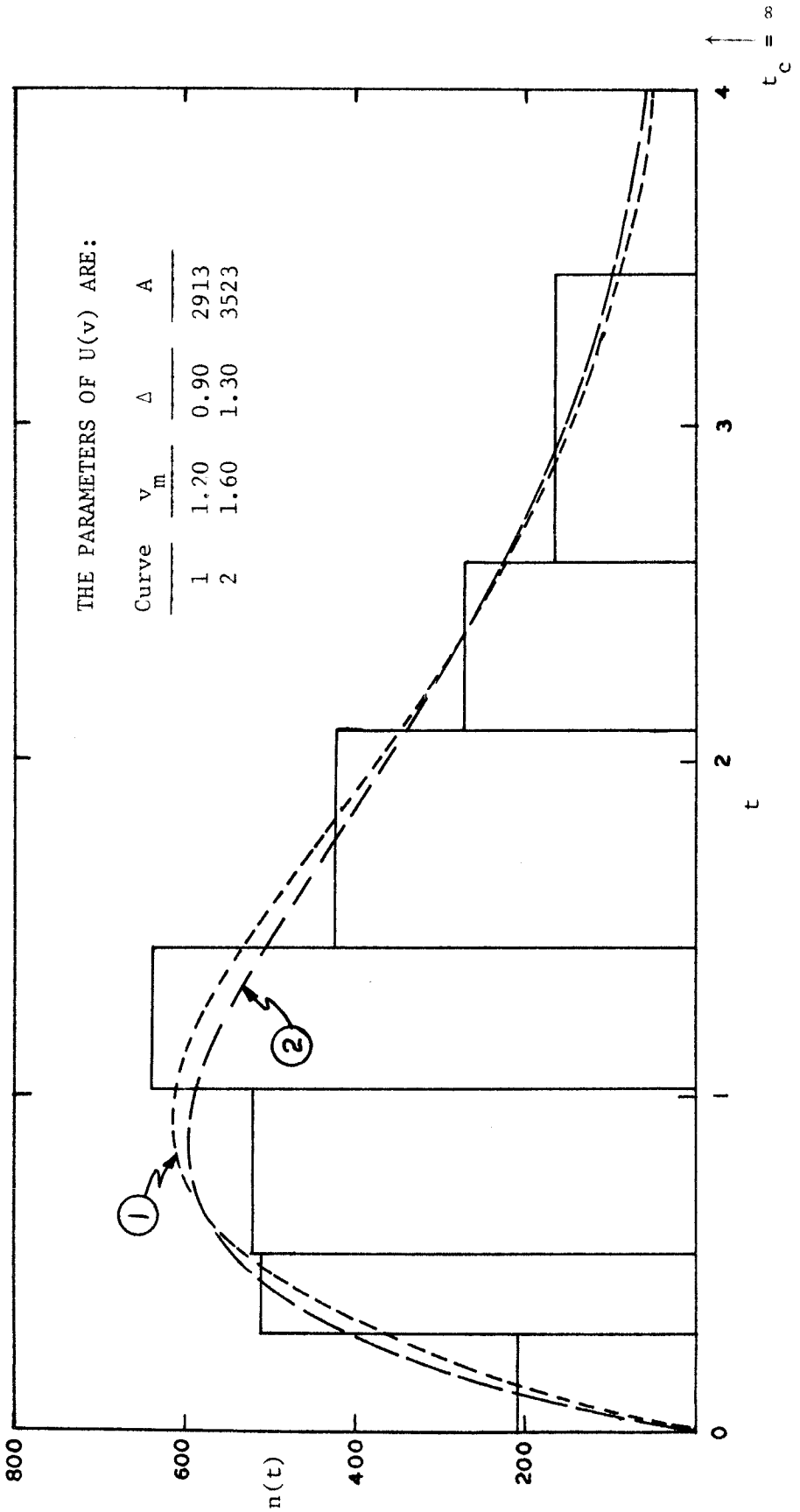

Figure 27. Observed and Theoretical n(t) for Stars with $2.87 < I\text{-}K < 3.38$

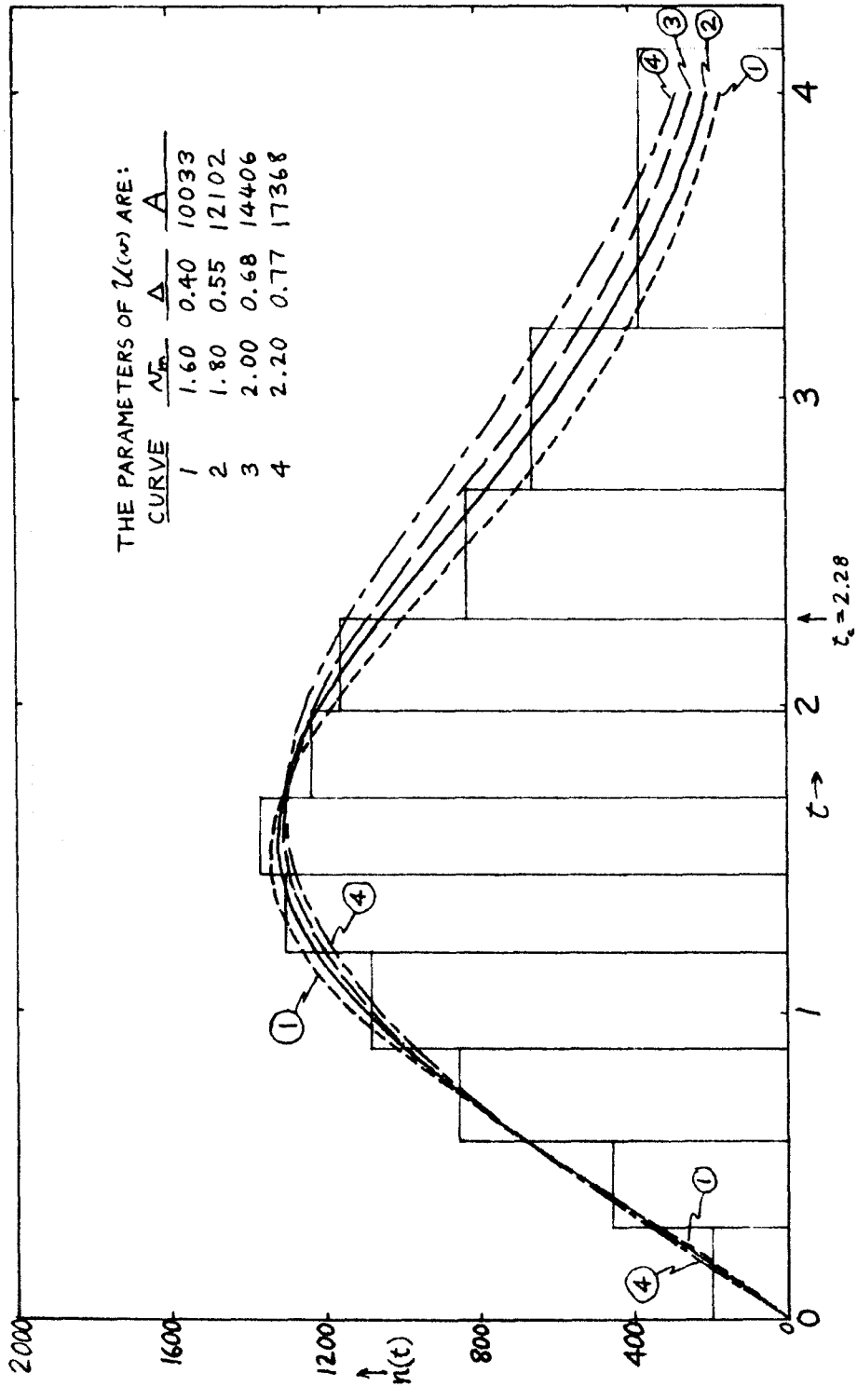

Figure 28. Observed and Theoretical n(t) for Stars with I-K > 3.38

due to random fluctuations. The range of t ($0 < t < t_c$) over which the χ^2 test is applied is very important, as was illustrated by the results given in Table 8, so the upper limit t_c is indicated by an arrow in each figure.

G. I-K < 2.33: No Attempt to Derive Luminosity Function

As shown in Figure 9a in the previous chapter, the stars with I-K less than 2.33 have spectral types ranging from B through K and are, therefore, not at all a homogeneous group. The data in Tables 2 and 3 in the previous chapter make this clear. No attempt has been made to determine a luminosity function for these stars by finding a U(v) which gives the observed n(t).

H. 2.33 < I-K < 2.87: Poorly Determined Luminosity Function

For the next group in order of redness, namely those stars with I-K between 2.33 and 2.87, attempts have been made to find a calculated n(t) which agrees with the observed distribution. Figure 26 shows that parameters A, v_m, and Δ have been found which give a good fit to the observed distribution. However, the parameters which fit the n(t) data for these stars are very poorly determined. The two calculated curves shown in Figure 26 are for quite different functions U(v), one having a mean of 0.60 and a standard deviation of 1.20 while the other has a mean of 1.60 and a standard deviation of 2.20. When these two gaussian U(v) functions are converted into gaussian luminosity functions $p_v(v)$ using the relationships given in Equations [60] through [64], the difference is extreme indeed. U(v) with mean

$v_m = 0.60$ and standard deviation $\Delta = 1.20$ implies $p_v(v)$ with mean $v_o = -4.37$ and the same standard deviation Δ. $U(v)$ with $v_m = 1.60$ and $\Delta = 2.20$ implies $p_v(v)$ with $v_o = -15.12$ and the same Δ. It would be absurd to claim any validity for such results, because it would amount to determining a luminosity function for stars which can be seen only to distances like

$$r_{max} = \sigma 10^{v_o/2} \simeq \sigma 10^{-2.2} , \qquad [69]$$

or even

$$r_{max} = \sigma 10^{v_o/2} \simeq \sigma 10^{-7.6} , \qquad [70]$$

by a method which uses the decrease in space density at a distance σ from the plane as the means of measuring luminosity. The indeterminacy for the stars with I-K between 2.33 and 2.87 may be due to the fact that many of these stars cannot be seen to distances $r_{max} \simeq \sigma$. To see whether or not this is the case the distribution in the luminosity variable v will be calculated for those stars which can be seen.

I. Derivation of N(v), the Luminosity Distribution of Observable Stars

The starting point for calculating the luminosity distribution of those stars which can be seen is the physical interpretation of $U(v)$ given in connection with Equation [43]. There it was pointed out that $U(v)dv$ is the number of stars with luminosity $L = \sigma^2 10^{v'}$ such that v' is in the range v to $v + dv$ which could be seen if the space

density were given by $D_o p_v(v)dv$ throughout the volume of the sphere of radius $r_{max}(v)$. To calculate the distribution in luminosity of the stars actually seen we must take into account the fact that the space density is not constant throughout the volume $\frac{4}{3}\pi r^3_{max}(v)$ but is instead given by

$$D(z)p_v(v)dv = K[u(z)]D_o p_v(v)dv. \qquad [71]$$

Therefore, N(v)dv, defined as the number of stars with luminosity characterized by v to v + dv which are close enough to be seen, is given by

$$N(v)dv = \int_V D_o K[u(z)]p_v(v)dv\, dV\ , \qquad [72]$$

where the volume of integration V is the sphere of radius $r_{max} = \sigma 10^{v/2}$. This differs from U(v)dv by the factor K[u(z)] in the integral, so N(v) can be written as

$$N(v) = U(v)\frac{\int_V K[u(z)]dV}{\int_V dV}$$

$$= U(v)\left[\frac{4}{3}\pi r^3_{max}\right]^{-1} 2\int_o^{r_{max}} K[u(z)]\pi(r^2_{max}-z^2)dz\ . \qquad [73]$$

Changing the variable of integration to $u = 2\log_{10}(z/\sigma)$ this becomes

$$N(v) = U(v)\left[\frac{4}{3}\pi r_{max}^3\right]^{-1} 2\int_{-\infty}^{\log_{10}\frac{r_{max}^2}{\sigma^2}} K(u)\pi(r_{max}^2-\sigma^2 10^u)\frac{(\log_e 10)}{2}10^{u/2}\sigma\, du$$

$$= U(v)\left[\frac{4}{3}\pi\sigma^3 10^{3v/2}\right]^{-1}\pi(\log_e 10)\sigma^3\int_{-\infty}^{v} K(u)[10^v-10^u]10^{u/2}du \ . \quad [74]$$

For the function K(u) adopted here, namely Equation [48],

$$K(u) = \frac{1}{0.7\sqrt{2\pi}}\int_u^\infty \exp\left[-\frac{x^2}{2(0.7)}\right]dx \ , \quad [75]$$

the integration can be carried out by parts. The resulting relationship between N(v) and U(v) is

$$N(v) = U(v)\left[K(v) + \frac{3}{2}10^{c/4}K(c-v)10^{-v/2} - \frac{1}{2}10^{9c/4}K(3c-v)10^{-3v/2}\right], \quad [76]$$

where

$$c = \frac{1}{2}(0.7)^2(\log_e 10) = 0.564 \ . \quad [77]$$

The factor for converting U(v) into N(v), the quantity in brackets in Equation [76], is shown in Figure 29.

J. 2.33 < I-K < 2.87: Luminosity Distribution of Observable Stars, N(v)

Since the spectral types are known for virtually all of the

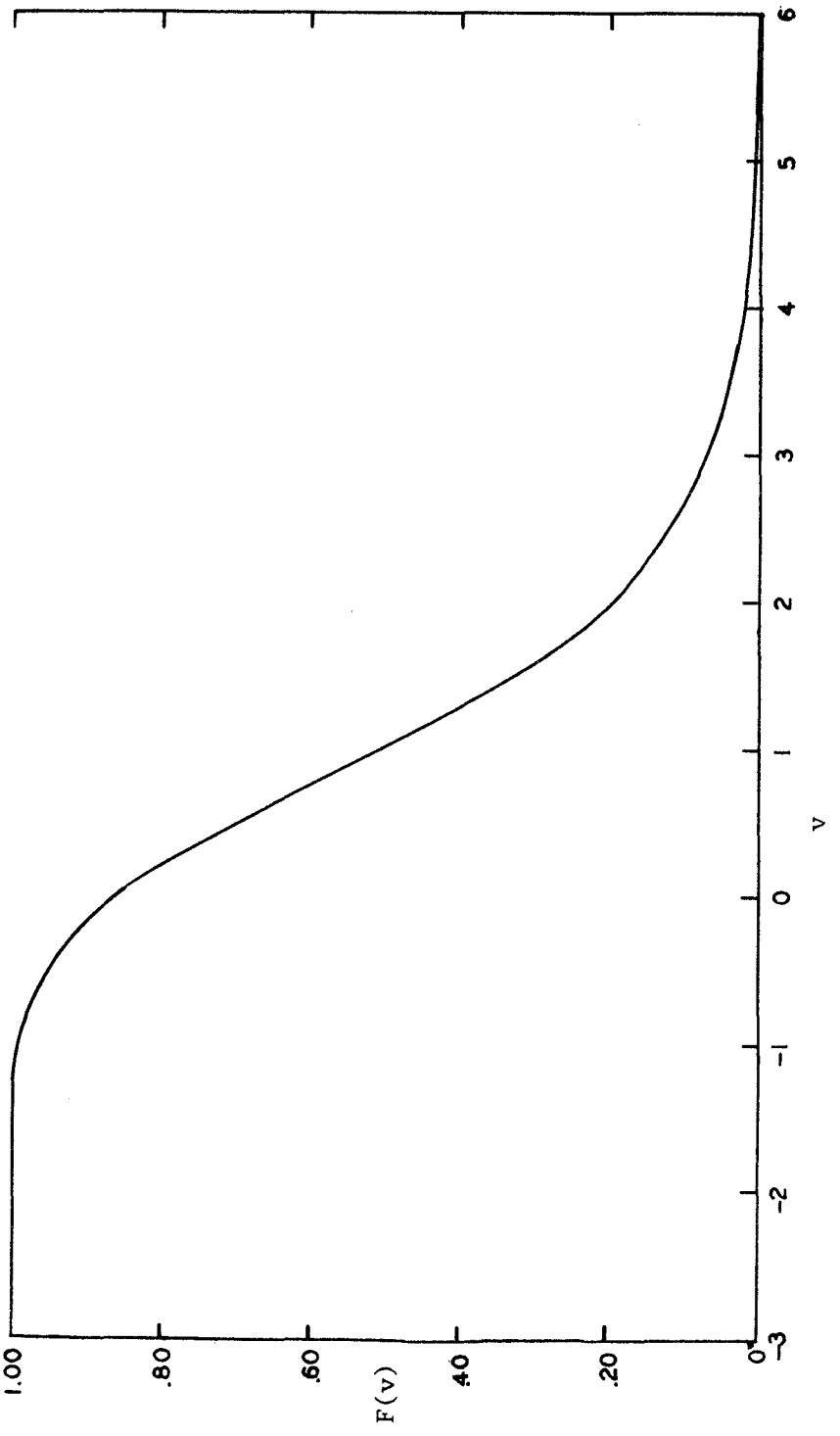

Figure 29. Factor F(v) for Converting U(v) to N(v)

stars in the I-K range 2.33-2.87 (see Figure 9a), the work of other authors summarized in Table 3 can supply information on the luminosities of these stars. Such information can be compared directly with the derived function N(v) for these stars and can therefore help to establish the best choice of a distance scale σ for them. The first step in carrying out this procedure is the obtaining of the functions N(v) from the functions U(v) which were found to give good agreement with the observed n(t) distribution of Figure 26. Figure 30 shows the N(v) curves derived from the two extreme U(v) functions discussed in Section H which fit the data in Figure 26. These two N(v) curves differ in width but are in agreement on the conclusion that the mean luminosity of the stars in this I-K group is that characterized by a value of v somewhere near zero. This would correspond to an average maximum distance $\langle r_{max} \rangle$ approximately equal to the characteristic z distance σ. Figure 9a in the previous chapter shows that the average spectral type for the stars with I-K between 2.33 and 2.87 is about M0 and about 2/3 of these stars have spectral types between K4 and M1. Table 3 puts the average value of r_{max} for K4-M1 giants at between 200 and 300 parsecs. Therefore, the comparison of the N(v) curves in Figure 30 with the data on spectral types and luminosities points to the conclusion that a characteristic width σ of 200 to 300 parsecs is appropriate for the stars in this I-K range. The best estimate of σ for these stars would be to set it equal to the average r_{max} for M0 stars; i.e., σ = 290 parsecs. Table 7 gives values of the characteristic width of the z distribution for K and M giants taken from the

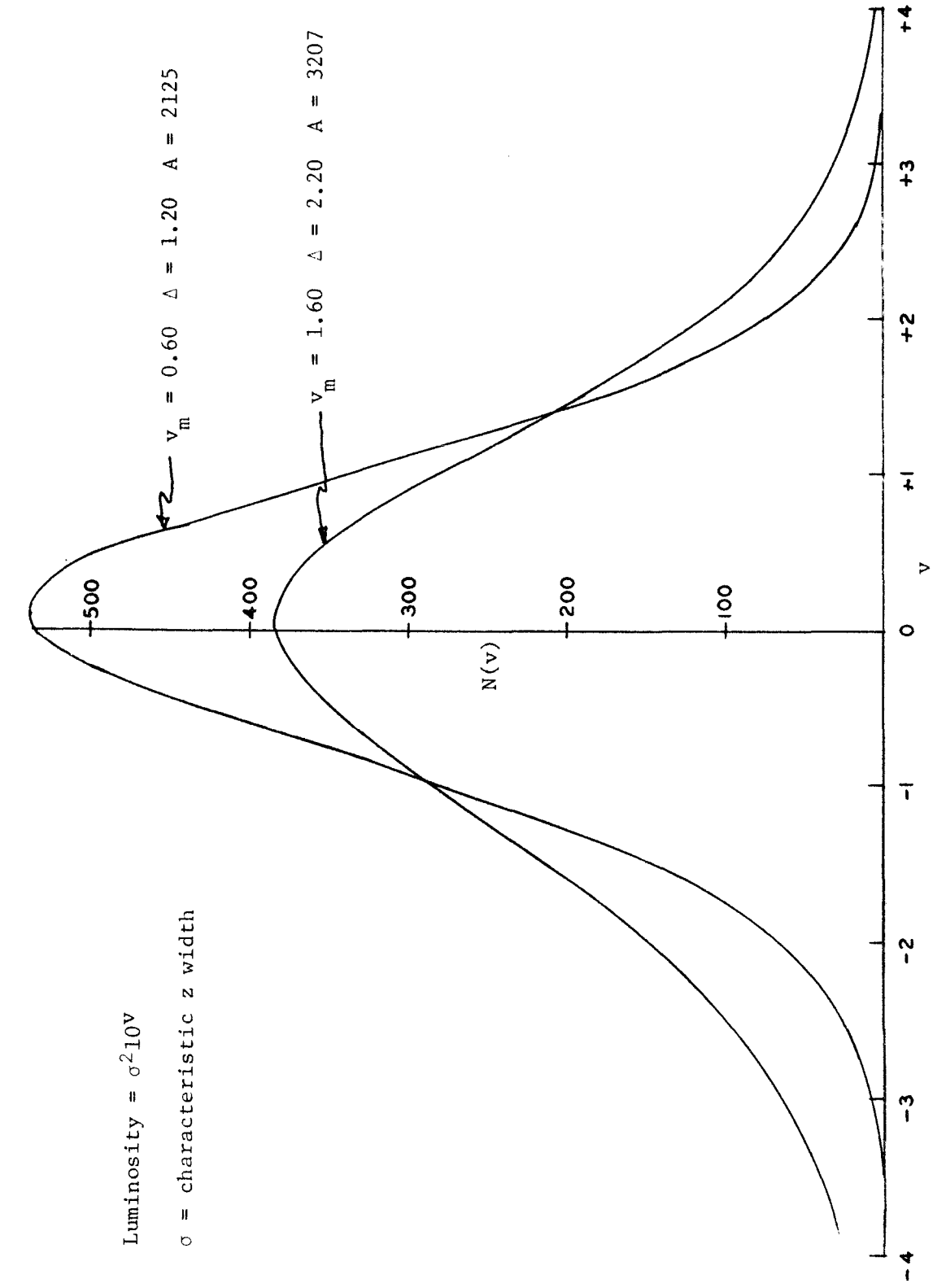

Figure 30.--N(v), The Luminosity Distribution of Observable Stars, for the Stars with 2.33 < I-K < 2.87.

work of various authors. The value given here, namely, σ = 290 parsecs, is consistent with the value one might estimate from Table 7 for M0 giant stars.

The widths of the N(v) functions given in Figure 30 are definitely greater than the width one might estimate from the spread in absolute K magnitudes M_K of K and M giant stars given in Table 3. Over 95 percent of the stars with I-K between 2.33 and 2.87 have spectral types between K0 and M3, and the range in average absolute magnitude M_K for this range in spectral type is from -1.6 to -5.9. The dispersion of absolute magnitudes about the mean for stars of the same spectral type is usually about 0.5 magnitude and certainly less than 1.0 magnitude (7,42,47). From these data one would estimate that over 95 percent of the stars in this I-K group must have M_K between -0.6 and -6.9. This range of about 6 magnitudes corresponds to a range of about 2.4 in v, since v is the $\log_{10}$ of the luminosity and the magnitude scale is such that 5 magnitudes correspond to a factor of 100 in luminosity. Clearly, neither N(v) curve in Figure 30 has 95 percent of its area within a v range of 2.4. The N(v) curve with the smaller width has over 2/3 of its area within a range of 2.4 in v, and is to be preferred over the other because of its closer agreement with the estimates based on the work of other authors.

K. 2.87 < I-K < 3.38: Luminosity Distributions U(v), $p_v(v)$, and N(v)

The n(t) distribution of the stars with I-K between 2.87 and 3.38 was presented in Figure 27 together with two n(t) curves calculated

using the two extreme values of v_m which give a probable fit to the observed data. It is clear from Figure 27 that the theoretical n(t) curves do not match the data as well as the theoretical n(t) curves in Figure 26 matched the data for the stars with I-K between 2.33 and 2.87. Yet the curves in Figure 27 indicate the best fit, according to the χ^2 test, that could be found by varying the mean and standard deviation of U(v). The probability that a χ^2 as large as that calculated from the difference between the best-fit theoretical n(t) and the observed n(t) would be due entirely to random errors is about 0.2. The same kind of probability for the best-fit curves in Figure 26 for the stars with I-K between 2.33 and 2.87 was about 0.8. The most serious discrepancy between the calculated and observed n(t) distributions in Figure 27 is quite obviously over the range $0.53 < t < 1.44$. It appears that the excess of calculated over observed in the interval $0.53 < t < 1.02$ may be balanced by an excess of observed over calculated in the interval $1.02 < t < 1.44$. That this is, in fact, the case can be demonstrated by treating the range $0.53 < t < 1.44$ as a single interval in the χ^2 test. When this is done the probability that the χ^2 is due to random errors increases from about 0.2 to about 0.9. The conclusion to be drawn is that a gaussian form of U(v) does not do a good job of accounting for the rather sharp fluctuation in the observed n(t) near $t = 1.0$ but that it can account for the average of the observed n(t) over the range from $t \simeq 0.5$ to $t \simeq 1.5$.

The parameters of the two extremes of gaussian U(v) which fit the observed n(t) in Figure 27 as well as can be done are $A = 2913$,

$v_m = 1.20$, $\Delta = 0.90$, and $A = 3523$, $v_m = 1.60$, $\Delta = 1.30$. The gaussian luminosity functions $p_v(v)$ which are associated with these two U(v) according to Equations [60]-[64] have the parameters $v_o = -1.60$, $\Delta = 0.90$ and $v_o = -4.24$, $\Delta = 1.30$, respectively. As in the case of the stars with I-K between 2.33 and 2.87, it is not reasonable to claim any validity for luminosity functions such as these which have nearly all of their area contributed by stars too faint to be seen at distances comparable to the characteristic width of their z distribution. But N(v), the luminosity distribution of the stars which can be seen, does have significance and can be obtained from U(v) using Equation [76]. Figure 31 shows the functions N(v) derived from the two extreme U(v) for the stars with I-K between 2.87 and 3.38. Both of these N(v) curves give a mean (and also a median) near v = 0.7. This would say that, on the average, the stars with I-K between 2.87 and 3.38 can be seen to distances

$$\langle r_{max} \rangle \simeq \sigma 10^{0.7/2} = 2.2\sigma \ . \qquad [78]$$

As in the case of the previous I-K group, something is known about the luminosities of the stars in the present I-K group due to their spectral type identifications and the data given in Table 3. Figure 9b shows the spectral type distribution of those stars with I-K between 2.87 and 3.38 which have been identified in the visual star catalogs. Of the 1012 stars in this I-K range 922 have been identified. Assuming that those not identified will tend to be of the later spectral types, the median spectral type for these stars falls between

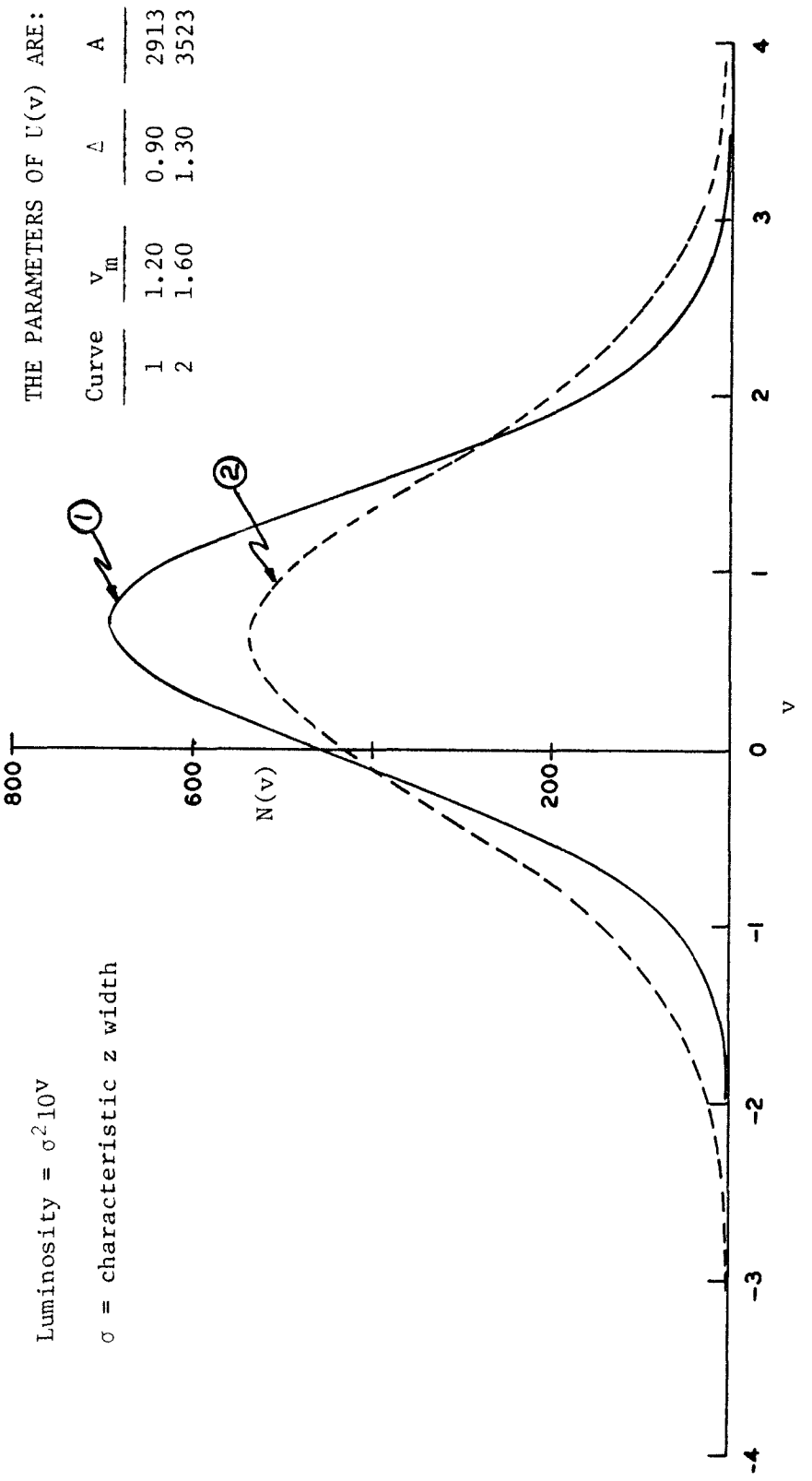

Figure 31.--N(v), The Luminosity Distribution of Observable Stars, for the Stars with 2.87 < I-K < 3.38.

M1 and M2; i.e., 516 of the 1012 are identified as stars of spectral type M1 or earlier. Table 3 gives the mean value of r_{max} for M1 giants as 330 parsecs and that for M2 giants as 420 parsecs. Taking the mean of the N(v) curves for these stars as v = 0.7 and making this consistent with $\langle r_{max} \rangle$ = 330 or 420 parsecs gives σ = 150 or 190 parsecs respectively. These estimates of σ are definitely low compared to other values listed in Table 7 for M giants. In order for σ to be 300 parsecs $\langle r_{max} \rangle$ would have to be 660 parsecs which would mean that the M1 and M2 giants in this I-K group are about one magnitude brighter than the average absolute magnitudes given in Table 3.

The widths of the N(v) curves in Figure 31 can be compared with the range of absolute magnitudes M_K which would be predicted from the spectral type distribution in Figure 9b with the aid of Table 3. Nearly 800 of the stars with I-K between 2.87 and 3.38 were identified as having spectral types between K4 and M3. Recalling that about 10 percent of the 1012 stars were not identified with any spectral type, it is safe to say that over 80 percent of the stars in this I-K group have spectral types from K4 through M3. According to Table 3 the range in average absolute magnitude M_K for this range in spectral type is from -3.3 to -5.9. Allowing for a dispersion of somewhat less than ±1.0 magnitude for the M_K values of giant stars of the same spectral type, one would estimate that over 80 percent of these stars have M_K values within a range of about 4.5 magnitudes, which would correspond to a range of 1.8 in v. The narrower of the two N(v) curves given in Figure 31 has about 80 percent of its area in a range of about 2.8 in v. Therefore, as in the case of the previous I-K group, the range of luminosities

predicted on the basis of identified types and their expected absolute magnitudes is smaller than the width of the theoretical N(v) curves and would suggest the narrower N(v) curve as the one to adopt.

L. I-K > 3.38: Finding a Probable and Reasonable U(v)

The observed n(t) distribution for the reddest 45 percent of the stars in the infrared catalog was presented in Figure 28, together with four theoretical n(t) curves. The χ^2 test for goodness of fit and the normalization of the U(v) were carried out using the first 8 intervals of t shown in the figure, i.e., for $t < 2.28$. The four theoretical n(t) curves shown in Figure 28 are the best fits for $0.00 < t < 2.28$ which could be obtained with 4 different values of the mean of U(v), namely, v_m = 1.6, 1.8, 2.0, and 2.2 for curves Nos. 1, 2, 3, and 4 respectively. For values of v_m equal to 1.4 and smaller or 2.4 and larger, no value of Δ could be found which gave a fit over the range $o < t < 2.28$ which was half as probable as the best fit shown in Figure 28. Table 9 gives the χ^2 and the probability of χ^2 being that large due to random errors for the curves shown in Figure 28. No gaussian U(v) can give a reasonable fit to the observed n(t) over all 12 intervals.

For $t > 2.28$ the four curves in Figure 28 become quite different. One way to choose among them would be to require that the calculated n(t) be less than the observed n(t) at large values of t. This criterion would be in keeping with the conclusion drawn from the latitude distribution that some of the stars observed at very low latitudes

TABLE 9

SOME DATA ON THE CURVES IN FIGURE 28

Curve	U(v) parameters			Mean of $p_v(v)$	χ^2 test over the range $0 \leq t < t_c$					
					$t_c = 2.28$		$t_c = 3.23$		$t_c = \infty$	
	v_m	Δ	A	v_o	χ^2	Prob.	χ^2	Prob.	χ^2	Prob.
1	1.60	0.40	10033	1.05	4.6	.70	12.1	.21	85.4	.00
2	1.80	0.55	12102	0.76	3.5	.83	7.1	.62	46.9	.00
3	2.00	0.68	14406	0.40	4.2	.75	11.5	.24	28.4	.00
4	2.20	0.77	17368	0.15	5.0	.66	24.4	.00	29.1	.00

(high values of t) must be from a population which has a value of r_{max}/σ characteristic of supergiants rather than giants. Thus the excess of observed stars with large values of t could be attributed to the supergiant contribution while the n(t) calculated from U(v) would be due to late type M giants. This interpretation would favor curve No. 1 over the other three.

Table 9 also gives the mean of the gaussian luminosity function $p_v(v)$ associated with each of the four U(v) functions which gave the n(t) curves in Figure 28. The standard deviation of $p_v(v)$ is the same as that of the U(v). Unlike the $p_v(v)$ derived for the previous I-K groups, a significant fraction (over half) of the area of these luminosity functions is in the range $v > o$, where it is possible to measure luminosity by making use of the decrease in space density in the z direction. But because the differences among the four $p_v(v)$ functions are very great, it is desirable to have a criterion for preferring one of them over the others.

Before comparing the results derived from the n(t) distribution of the reddest stars with what little data is available on late M giants, a "most probable" luminosity distribution U(v) will be obtained and its consequences discussed for various assumed values of the characteristic distance σ. The "most probable" U(v) is to be taken as the gaussian function

$$U(v) = \frac{A}{\Delta\sqrt{2\pi}} \exp\left[-\frac{(v-v_m)^2}{2\Delta^2}\right] \qquad [79]$$

which gives the best fit to the observed n(t) distribution. Goodness of fit is measured by the probability that the χ^2 calculated from the differences between the theoretical and the observed numbers of stars within the various t intervals could have arisen purely from random fluctuations. This χ^2 procedure was described in Section F, and Table 8 was given as an example. For the stars with I-K greater than 3.38 the range of t over which the χ^2 test is applied is critical in determining the parameters of U(v) which give the best fit. In keeping with the idea that the excessively high concentration of red stars at very low latitudes can be attributed to supergiants rather than giants the following criteria have been used to select the number of intervals over which the χ^2 test is to be applied:

1. Groups 1 through 8 ($0 < t < 2.28$) must be included in the χ^2 test. For the faintest stars in the catalog ($K = 3.00$), $t = 2.28$ corresponds to a latitude b given by

$$|b| = \sin^{-1}10^{-2.28/2} = 4\overset{\circ}{.}2 \ , \qquad [80]$$

   according to Equation [9]. This allows for the exclusion of all stars within 4.2 degrees of the equator and of all but the faintest at somewhat higher latitudes.

2. All groups not included in the χ^2 test (i.e., groups k + 1 through 12 when the test is applied to groups 1 through k) must have a calculated number less than the observed number.

The division into groups of stars on the basis of t intervals is given in Table 8 and in Figure 28. The χ^2 test for the data presented in

Table 8 could not be applied over intervals 1-8 only, because criterion No. 2 is not met. The assumed U(v) would result in 37.3 more stars in group 9 than are observed in that range of t. Therefore, the probability that a U(v) with $v_m = 1.80$ and $\Delta = 0.55$ accounts for the observed n(t) must be measured by a χ^2 test which includes groups 1-9 rather than only 1-8. When this is done the probability of these parameters accounting for the distribution of t is .68 as opposed to the .83 which resulted from the χ^2 test applied to groups 1-8. Thus the application of criterion No. 2 has reduced the probability that this U(v) accounts for the observed n(t) distribution. The probabilities associated with curves No. 3 and No. 4 in Figure 28 are markedly lowered by the requirement that the χ^2 test be applied up to the group where the calculated number permanently falls below the observed number.

The probability derived according to the procedure described above is shown as a function of the parameters v_m and Δ in Figure 32. This figure shows that the most probable combination of v_m and Δ is close to $v_m = 1.70$, $\Delta = 0.48$. The range of values of v_m and Δ which give reasonably good fits to the observed data can be determined from Figure 32. For instance, v_m can be taken to be as small as 1.50 or as large as 1.90 and still result in a fit which is over two thirds as probable as the one with maximum probability. For $v_m = 1.70$ the standard deviation Δ can range from 0.42 to 0.53 without the probability falling below two thirds of the maximum probability. A knowledge of the range of v_m and Δ over which a reasonable fit to the data can be obtained is needed to estimate the uncertainty in any quantities derived

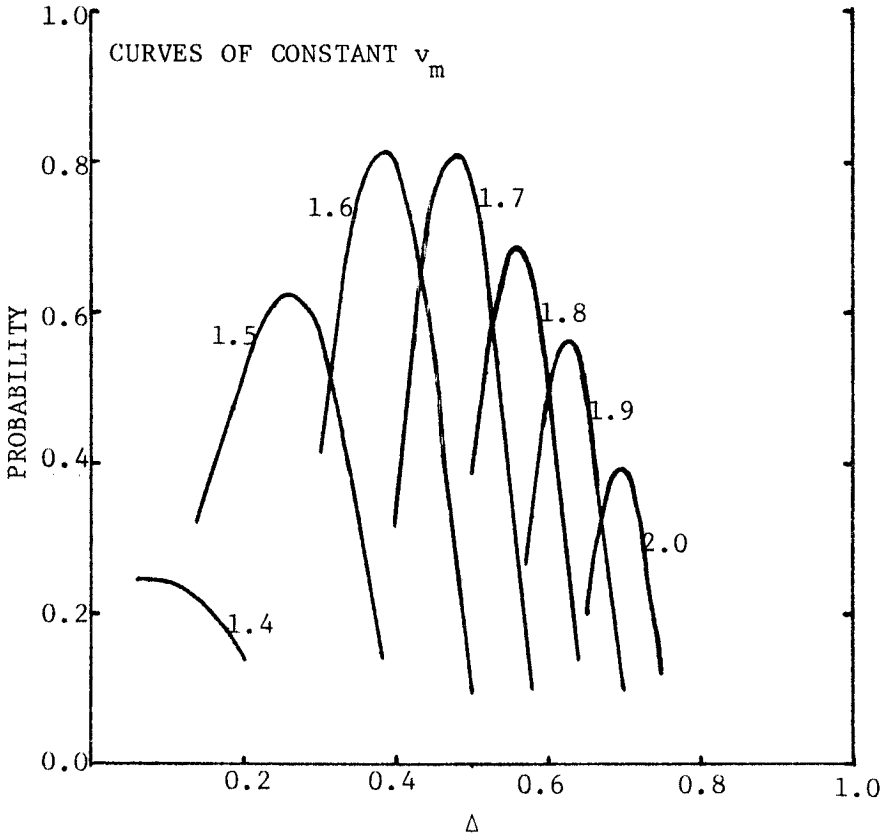

Figure 32.--The Probability of the Luminosity Distribution U(v) as a Function of Its Parameters v_m and Δ .

from them. Figure 33 shows the observed n(t) compared to n(t) curves calculated from the most probable U(v) and from some other U(v)'s which are from two thirds to three fourths as probable.

M. I-K > 3.38: The Space Density and the Luminosity Function

An important quantity which can be derived from the parameters of a gaussian U(v) is D_o, the number of stars per unit volume in the galactic plane. Equations [60] through [64] give the relationships between a gaussian U(v) and the gaussian luminosity function $p_v(v)$ which would be associated with it. The space density D_o of these stars, counting all luminosities, is given by

$$N_\sigma \equiv D_o\sigma^3 = \frac{3}{4\pi}A10^{-3[v_m-3(\log_e 10)\Delta^2/4]/2} \quad . \qquad [81]$$

This follows from Equation [63] when Equation [64] is used for v_o. Therefore, the parameters A, v_m, and Δ of the gaussian U(v) can be used to give the number of stars of all luminosities in a cube of edge σ if the space density were a constant D_o throughout the volume. The range of values of N_σ which are consistent with the observed data can be estimated by calculating this number for the extreme values of the parameters. Table 10 gives some extreme values of the parameters v_m, Δ, and A which result in fits to the observed n(t) which are from 1/2 to 3/4 as probable as the best fit, which is also included in the table. The range of N_σ associated with the range in parameters shown in Table 10 is from 20 to 50 with the most probable value being 29. The actual space density D_o depends on the distance scale assumed, i.e., on the

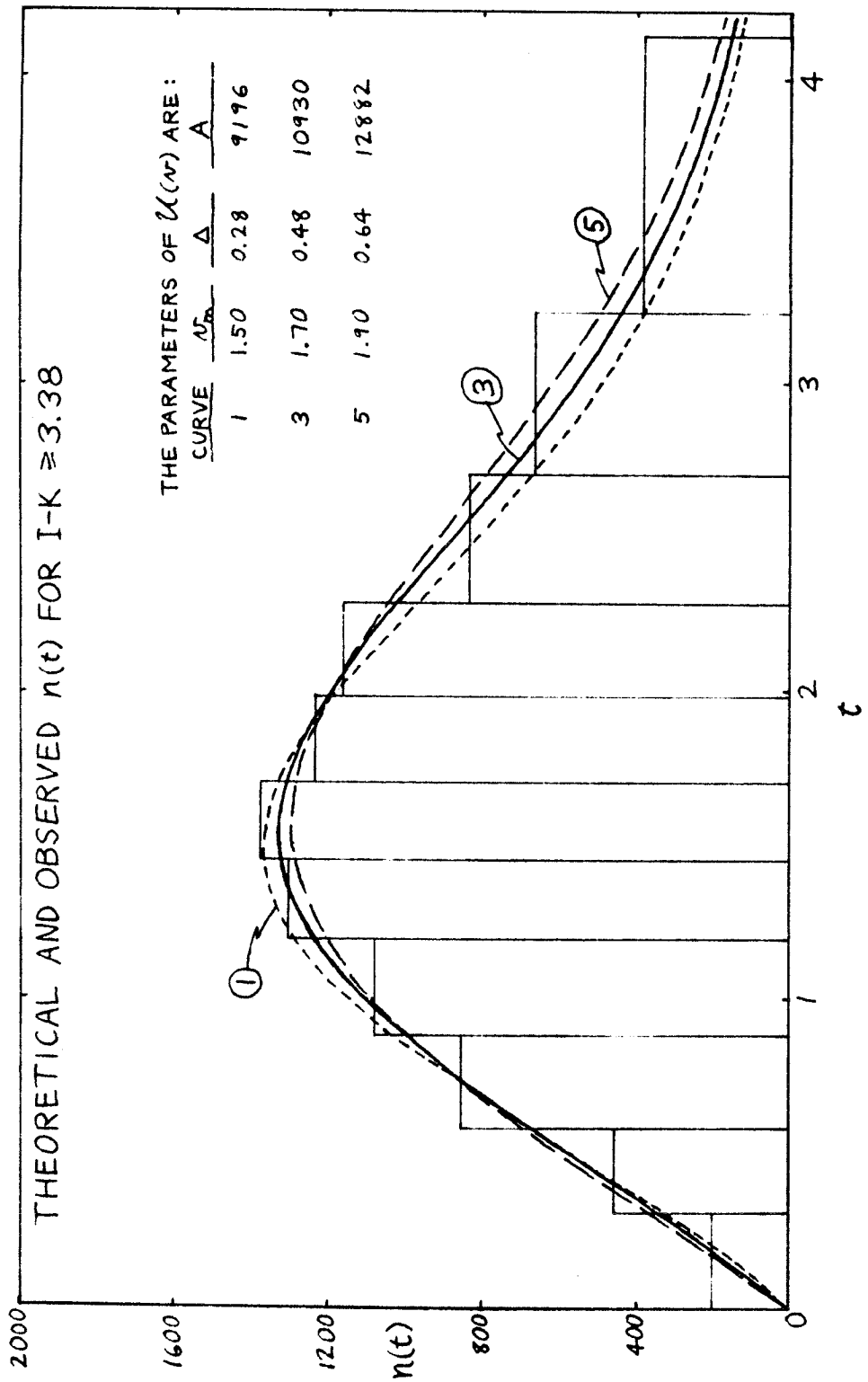

Figure 33.--Observed and Theoretical n(t) for Stars with I-K > 3.38.

TABLE 10

POSSIBLE LUMINOSITY FUNCTIONS FOR I-K $\geq$ 3.38

	U(v) parameters				Mean of the lum.funct.	
	mean v_m	std.dev. Δ	norm. A	Probability	v_o	$N_\sigma = D_o\sigma^3$
1	1.50	0.28	9196	.61	1.23	20
2	1.70	0.42	11167	.51	1.09	21
3	1.70	0.48	10930	.81	0.90	29
4	1.70	0.54	10686	.46	0.69	41
5	1.90	0.64	12882	.54	0.49	50

value of σ. Figure 34 shows D_o in units of stars per 10^6 cubic parsecs as a function of σ in units of parsecs for the most probable fit ($D_o\sigma^3 = 29$) and for the two extreme values of N_σ given in Table 10. If the stars with I-K greater than 3.38 are taken to be giants of spectral type M5 or later, Table 3 would predict a space density on the order of unity. According to Figure 34, a space density $D_o \simeq 1$ star per 10^6 pc^3 would require a characteristic distance $\sigma \simeq 310$ parsecs.

Table 10 also gives the value of v_o, the mean of a gaussian luminosity function $p_v(v)$ which would be associated with the gaussian function U(v), for each of the combinations of v_m and Δ given there. The choice of U(v), a solution to the integral equation, together with a choice of σ, the characteristic distance in the z direction, amounts to taking the number of stars per unit volume in the galactic plane with luminosity given by $\sigma^2 10^{v'}$ where v' is in the range v to v + dv as equal to

$$D_o p_v(v)dv = \frac{N_\sigma}{\sigma^3} \frac{1}{\Delta\sqrt{2\pi}} \exp\left[-\frac{(v-v_o)^2}{2\Delta^2}\right]dv \ . \qquad [82]$$

This luminosity function in terms of v can be converted to one in terms of absolute K magnitude M_K by making use of the fact that M_K is defined as the magnitude of the star as it would appear at the standard distance of 10 parsecs. Since the limiting K magnitude is 3.00, the relationship between v and M_K is

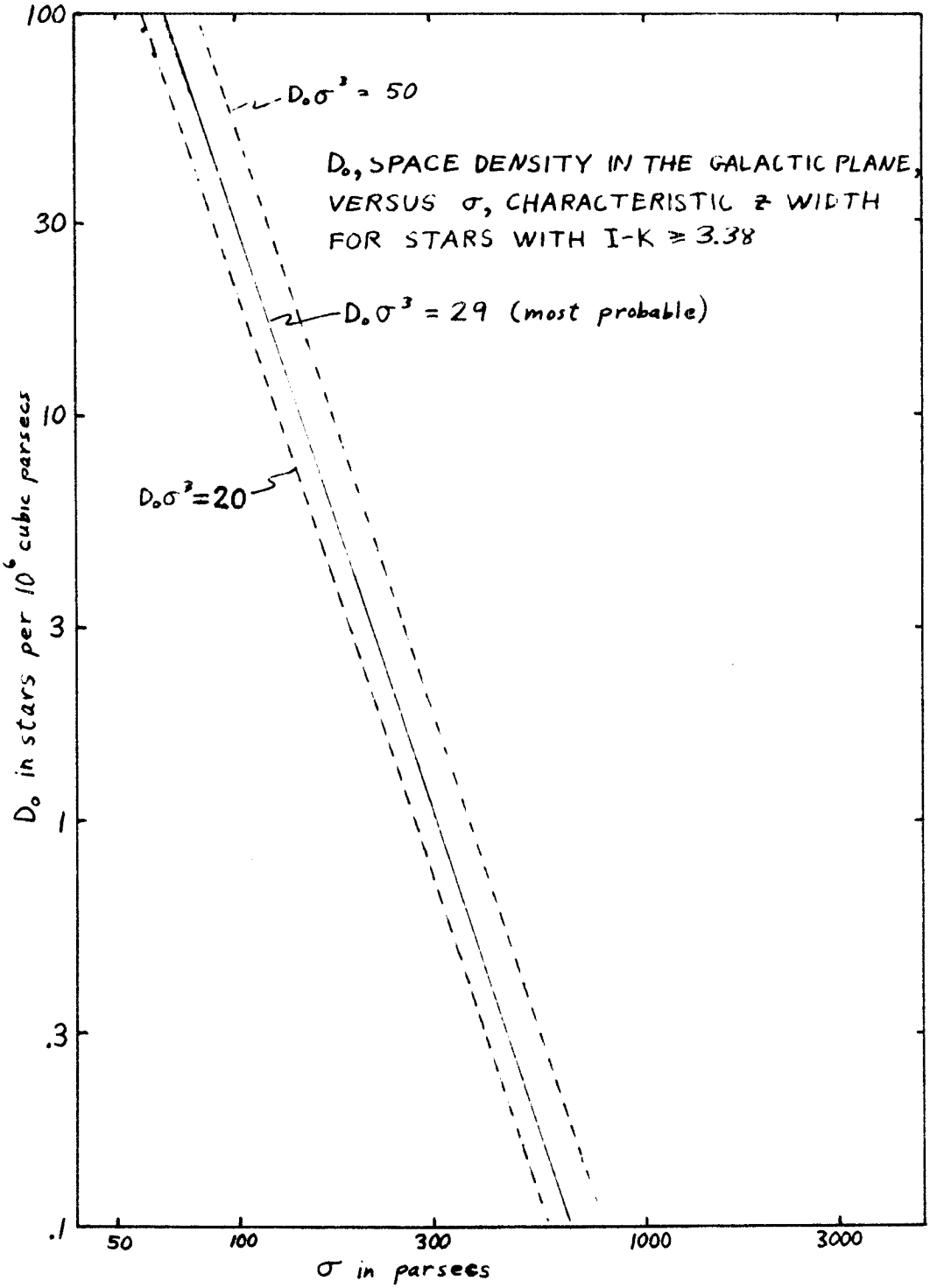

Figure 34.--D_o versus σ Derived from the Possible U(v) Given in Table 10.

$$\sigma^2 10^v = r_{max}^2 = \left[10 \cdot 10^{0.2(3.00-M_K)}\right]^2 , \qquad [83]$$

which gives

$$v = 2 + 0.4(3.00) - 0.4M_K - 2 \log_{10}\sigma$$

$$= -0.8 - 0.4M_K - 2 \log_{10}(\sigma/100) , \qquad [84]$$

where σ is in parsecs. Therefore, the luminosity function in terms of M_K is

$$p(M_K) = p_v(v)\left|\frac{dv}{dM_K}\right|$$

$$= \frac{1}{2.5\Delta\sqrt{2\pi}} \exp\left[-\frac{1}{2\Delta^2}\{-0.8 - 0.4M_K - 2 \log_{10}(\sigma/100) - v_o\}^2\right]. \qquad [85]$$

This is a normal distribution with mean

$$M_o = -2 - 5 \log_{10}(\sigma/100) - 2.5v_o \quad (\sigma \text{ in parsecs}) \qquad [86]$$

and standard deviation

$$\Delta_M = 2.5\Delta . \qquad [87]$$

Table 11 summarizes the space density and luminosity function data which result from the application of the above analysis to three of the U(v) functions presented in Table 10. The three are: the most probable ($v_m = 1.70$, $\Delta = 0.48$, $A = 10930$) and the two extremes ($v_m =$

TABLE 11

POSSIBLE LUMINOSITY FUNCTIONS FOR STARS WITH I-K ≥ 3.38
EXPRESSED IN TERMS OF ABSOLUTE K MAGNITUDE, M_K

Parameters of gaussian $p(M_K)$ for various values of σ in parsecs		Extreme 1 $v_m = 1.50$ $\Delta = 0.28$ $A = 9196$	Most Probable $v_m = 1.70$ $\Delta = 0.48$ $A = 10930$	Extreme 2 $v_m = 1.90$ $\Delta = 0.64$ $A = 12882$
	D_o	2.5	3.6	6.3
$\sigma = 200$	M_o	-6.6	-5.8	-5.0
	Δ_M	0.70	1.20	1.60
	D_o	.73	1.1	1.9
$\sigma = 300$	M_o	-7.5	-6.6	-5.9
	Δ_M	.70	1.2	1.6
	D_o	.22	.32	.55
$\sigma = 450$	M_o	-8.4	-7.5	-6.7
	Δ_M	.70	1.2	1.6

Luminosity function $p(M_K) = \frac{1}{\Delta_M\sqrt{2\pi}} e^{\frac{-(M_K-M_o)^2}{2\Delta_M^2}}$ per unit M_K .

To get number of stars per unit volume multiply by D_o which is in units of number of stars per 10^6 cubic parsecs.

1.50, Δ = 0.28, A = 9196, and v_m = 1.90, Δ = 0.64, A = 12882). For each of the three U(v), Table 11 gives the values of D_o and M_o which result from setting σ = 200, 300, and 450 parsecs.

N. I-K > 3.38: N(v) and Some Conclusions Regarding Late M Giants

Table 11 summarizes the conclusions which can be drawn regarding the distribution of luminosities per unit volume of space. The distribution of luminosities of the stars which are observable is given by the function N(v) which was derived in Section I. The distributions N(v) derived from the U(v) functions being considered here are shown in Figure 35. In addition to the v scale on the abscissa in Figure 35 three M_K scales are indicated. These additional scales correspond to the three choices of σ used in Table 11.

As in the cases of the less red I-K groups already considered, the different N(v) distributions in Figure 35 have about the same mean, in this case somewhere between v = 1.35 and v = 1.55. This mean value of v corresponds to a value of r_{max} 5 or 6 times σ. The procedure used for the other I-K groups, that of finding the average spectral type of the stars in the group and then looking up the average r_{max} for that type in Table 3, cannot be applied here because about 3/4 of these stars have not been identified in the visual catalogs. The spectral type distribution of those stars which have been identified was presented in Figure 9b and discussed briefly at the end of Section G in Chapter IV. The conclusion reached there was that the majority of stars with I-K greater than 3.38 must be of spectral type later than M2. When the M_K values in Figure 35 are compared with the average

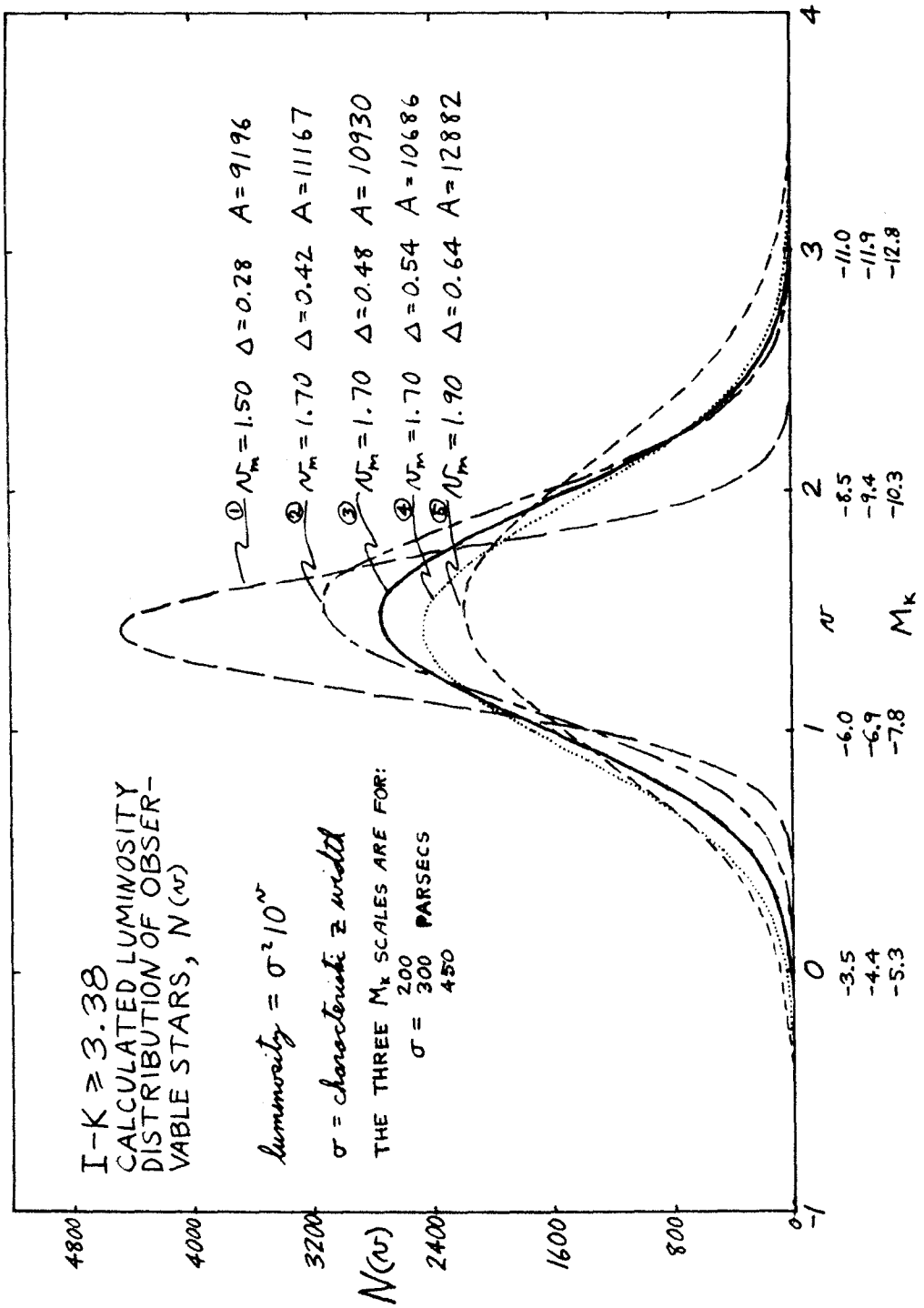

Figure 35.--N(v), The Luminosity Distribution of Observable Stars, for the Stars with I-K > 3.38.

values of M_K given in Table 3, it appears that even for a σ of 200 parsecs the average spectral type must be later than M4. If the average r_{max} for M4 giants (760 parsecs) were taken as the average maximum distance $\langle r_{max} \rangle$ for this I-K group, Figure 35 would imply the surprising result that the σ for these stars is only 125 (i.e., 750/5) parsecs.

Table 11 and Figure 35 pretty well summarize what the n(t) distribution of the stars with I-K greater than 3.38 reveal about the space density and luminosity of these stars. It is possible to adopt values of the parameters v_m, Δ, A, and σ which result in conclusions which are consistent with the data given in Table 3 for late M giants. For instance, the most probable U(v) taken together with a characteristic half-width σ = 300 parsecs leads to the conclusion that the luminosity function for these stars has a mean absolute magnitude M_K of about -6.6 and a standard deviation of 1.2 magnitudes. The integral over all luminosities would give a space density in the galactic plane of D_o = 1.1 stars per 10^6 cubic parsecs. These numbers are in fair agreement with the data of Table 3 for M3-M5 giant stars, if it is assumed that an appreciable fraction of the M3 giants in the infrared catalog have I-K less than 3.38 and are therefore not contributing to this sample. The σ assumed here, 300 parsecs, is a possible value for late M giants according to Table 7.

O. <u>I-K > 3.38: The Supergiant Component</u>

Some stars with I-K greater than 3.38 were not accounted for by the U(v) functions considered to be probable. These are of course the

stars which caused the excess of observed n(t) over calculated n(t) at large values of t and which were deliberately excluded from the χ^2 test used to find probable U(v) functions. In accordance with the interpretation adopted in Section L for setting up the χ^2 testing procedure, these excess stars will be called the supergiant component of the stars with I-K greater than 3.38. In this interpretation the number of supergiants would be equal to the excess of observed over calculated in the n(t) distribution beyond t_c, the upper limit of the χ^2 test. Since the normalization of the U(v) function has been chosen to make the calculated number with t less than t_c agree with the observed number with t less than t_c, the excess of observed over calculated for the whole range of t is equal to the excess for $t > t_c$. Table 12 gives the excess of the observed number of stars over the number of stars calculated from each of the five U(v) functions which have been presented previously in this discussion. From Table 12 the number of supergiants can be estimated as 250 ± 100. The numbers given in Table 12 were taken from n(t) distributions weighted so as to apply to the whole sky as explained in Appendix B. The weight assigned to stars very close to the galactic equator was about 1.4, so the 250 supergiants estimated from Table 12 would correspond to about 180 supergiants in the region of sky covered by the infrared catalog.

Table 13 shows how the excess stars are distributed among the last three t intervals. The fraction of stars not accounted for by the luminosity function associated with U(v) (i.e., the fraction considered to be supergiants) increases with t. This is shown in Table 13 for

TABLE 12

THE NUMBER OF OBSERVED STARS NOT ACCOUNTED FOR BY THE n(t) CURVES CALCULATED FROM THE PROBABLE U(v) FUNCTIONS FOR I-K > 3.38

Curve	U(v) parameters v_m	U(v) parameters Δ	Probability	Excess of observed over calculated
1	1.50	0.28	.61	354
2	1.70	0.42	.51	239
3	1.70	0.48	.81	258
4	1.70	0.54	.46	277
5	1.90	0.64	.54	153

TABLE 13

FRACTION OF THE STARS WITH I-K > 3.38 NOT ACCOUNTED FOR BY THE VARIOUS U(v) FUNCTIONS

Interval	t range	Actual number in range	Fraction not accounted for by curve No.: 1	2	3	4	5
10	2.70-3.23	250	.22	.09	.12	.15	--
11	3.23-4.14	250	.38	.26	.28	.30	.17
12	>4.14	182	.55	.45	.46	.47	.36

each of the U(v). Assuming the luminosity function associated with the most probable U(v) (i.e., curve No. 3 in Tables 12 and 13), the prediction of Table 13 is that 84 (46 percent) of the 182 stars with $I-K > 3.38$ and $t > 4.14$ are supergiants.

CHAPTER VI

CONCLUSIONS

Conclusions regarding the properties of the stars included in the infrared catalog are presented in Table 14. The results presented in Table 14 have been taken from the data and the analyses of Chapters IV and V. The stars with I-K less than 2.33 have spectral types ranging from O through K and were not analyzed for luminosity distribution because they form such a heterogeneous group and because very few of them could be detected at distances greater than the characteristic half-width of their z distribution. Only for the reddest group (I-K > 3.38) has it been reasonable to draw conclusions regarding the luminosity function itself, i.e., regarding the number of stars per unit luminosity per unit volume of space. These conclusions were presented in Table 11, which shows values for the space density in the galactic plane ranging from .2 to 6 stars per 10^6 cubic parsecs and values for the mean absolute K magnitude ranging from -5.0 to -8.4. Such large ranges are due to the uncertainty in the value of the characteristic half-width σ and the rather wide range of luminosity function parameters which fit the observed n(t) distribution.

In this chapter these conclusions regarding the properties of the infrared catalog stars will be compared with the work of other authors. In particular, the longitude distribution of the reddest stars (I-K > 3.38) will be compared with the longitude distribution of the stars found on the survey at Case referred to in Chapter I, and

TABLE 14

SUMMARY OF PROPERTIES OF OBSERVED STARS

Property	I-K Range 2.33-2.87	2.87-3.38	>3.38
Luminosity class	III	III	III*
Spectral type	K4-M1	M0-M3	M4≤
Characteristic half-width σ	300 pc	300 pc	300 pc
Mean r_{max} of observable stars	300 pc	700 pc	1700 pc
Mean absolute magnitude $\langle M_K \rangle$	-4.4	-6.2	-8.1
Standard deviation of M_K	2.5	2.0	1.0

To scale these values for $\sigma \neq 300$ use the fact that r_{max} is proportional to σ and the absolute K magnitude is given by

$$M_K = 3.0 - 5 \log_{10}(r_{max}/10 \text{ pc}) .$$

*Section 0 of Chapter V indicates that about 4 percent of these stars are probably supergiants.

the longitude distribution of suspected supergiants found on the two surveys will be compared. Finally, an estimate of the space density gradient in the galactic plane will be made for late M giants.

A. Stars with 2.33 < I-K < 3.38: The Luminosity Distribution and the Characteristic Distance from the Galactic Plane

The luminosity distributions of observable stars derived from the catalog stars with I-K less than 3.38 and shown in Figures 30 and 31 indicate that a significant fraction of these stars are not luminous enough to be included in the catalog if they were at distances greater than the characteristic half-width σ of their z distributions. As a consequence of this fact, a meaningful determination of the luminosity functions of the stellar populations from which these stars are drawn is not possible using the n(t) analysis described in Chapter V, because that analysis makes use of the decrease in the space density of stars in the z direction to measure the maximum distances at which the stars could be detected. Therefore, in the case of stars with I-K between 2.33 and 3.87, the determination of luminosities must rest with the derived functions N(v) shown in Figures 30 and 31, i.e., with the luminosity distribution of the stars actually included in the infrared catalog. In Chapter V it was indicated that the narrower functions in Figures 30 and 31 were to be preferred because they were in better agreement with the data given in Table 3. It was also indicated in Chapter V that the means of the functions N(v) shown in Figure 30 (2.33 < I-K < 2.87) were consistent with the luminosities given in

Table 3 for giant stars of spectral type K4-M1 with a characteristic half-width σ of 200-300 parsecs, but that the means of the functions N(v) in Figure 31 ($2.87 < I-K < 3.38$) were not consistent with the luminosities given in Table 3 for giant stars of spectral type M0-M3 with a characteristic half-width σ of 200-300 parsecs. The specifics of these two cases will now be considered.

The average star with I-K between 2.33 and 2.87 can be seen to a distance

$$\langle r_{max} \rangle \simeq \sigma 10^{0.0/2} = \sigma, \qquad [88]$$

where $\langle r_{max} \rangle$ is the distance associated with the mean of the N(v) curves in Figure 30. The average star in this I-K group has a spectral type M0 according to Figure 9a. The average absolute K magnitude of M0 giant stars is $M_K = -4.3$ according to Table 3. The maximum distance at which a star of this M_K would have an apparent K magnitude less than 3.0 and therefore be included in the infrared catalog is

$$r_{max} = 10 \cdot 10^{-0.2(M_K - 3.0)} = 2.9 \cdot 10^2 \text{ parsecs}, \qquad [89]$$

as is also given in Table 3. A characteristic half-width σ of 290 parsecs would be within the rather wide range of estimates of the characteristic half-width given in Tables 3 and 7 for K and M giant stars.

The average star with I-K between 2.87 and 3.38 can be seen to a distance

$$\langle r_{max} \rangle \simeq \sigma 10^{0.7/2} = 2.25\sigma , \qquad [90]$$

according to the means of the N(v) functions in Figure 31, and has a spectral type M1.5 according to Figure 9b. Table 3 gives the average M_K and r_{max} for this spectral type as about -4.8 magnitudes and 3.6 x 10^2 parsecs respectively. But applying Equation [90] to stars with a characteristic half width σ = 280 parsecs, a value which agrees with Tables 3 and 7 for M giants, gives r_{max} = 630 parsecs and M_K = -6.0 mag. Therefore, either the average luminosity at 2.2μ of the early M giants in the infrared catalog is about one magnitude brighter than the results of other authors summarized in Table 3 would indicate, or the characteristic half-width of the distribution of these stars perpendicular to the plane of the galaxy is considerably less than other studies have suggested; i.e., 360/2.25 = 160 parsecs, as opposed to 280 parsecs.

To conclude that the characteristic half-width is smaller for the stars with I-K between 2.87 and 3.38 than it is for the stars with I-K between 2.33 and 2.87 would be qualitatively consistent with the values of σ given in Table 3 for the K3-K5 giants as compared with the M giants. The result given in Table 3 that the space density of giant stars of type K3-K5 falls to one half its value in the galactic plane at a distance of 500 parsecs from the plane is from the work of Upgren (42) and is based on about 90 stars in a 400 square degree area near the north galactic pole. The characteristic half-width of 250 parsecs for M giants is from a space density function D(z) derived by Blanco (7) from a list by Upgren (48) of 50 giant M stars in the same 400 square degree area. Blanco says the result applies to stars M2 and later. Upgren estimated that his survey in the north galactic pole area was

complete to a photographic magnitude of 13.0. The method used in Chapter V to derive the relationship between the luminosities of the red giant stars and their characteristic width in the z direction is obviously very different from that of Upgren and Blanco and gives results which represent some kind of average over many directions in addition to that of the north galactic pole.

There is also some justification for drawing the other conclusion mentioned above, namely that early M giants in the infrared catalog have an average M_K of -6.0 rather than the value of -4.8 obtained from Table 3. The values of M_K given in Table 3 for giant M stars were obtained by subtracting the intrinsic colors $(V-K)_o$ given by Johnson (25) from the absolute visual magnitudes M_V given by Blanco (7). (An additional 0.2 mag. was subtracted to account for an average difference between Johnson's V magnitude and the old visual magnitude.) Now, Johnson's intrinsic colors $(V-K)_o$ were determined from measurements of stars in the *Yale Catalogue of Bright Stars* (17), which contains stars selected on the basis of brightness in V magnitude, while the stars included in the infrared catalog are selected on the basis of brightness in K magnitude. This difference in selection criteria would account for the stars in the infrared catalog having a larger $(V-K)_o$ and therefore a smaller M_K. It is even possible that a difference in average M_K on the order of a magnitude could be attributed to this selection effect. Evidence that this is possible comes from a comparison of the average color index V-K obtained from infrared catalog stars identified in the Walker-D'Agati selection from the SAO with

the average intrinsic color index $(V-K)_o$ given by Johnson (25) for M giant stars. For each spectral type M0 through M3 the average V-K based on the SAO and the infrared survey is more than 1.2 magnitudes greater than Johnson's $(V-K)_o$.

Before leaving the matter of the conclusions to be drawn from the luminosity distributions derived for the catalog stars with I-K between 2.33 and 3.38, it should be pointed out that an explanation of the inconsistencies described here is not to be found in the difference between a mean absolute magnitude determined from a sample of stars within a volume of space and that determined from a sample of stars brighter than some apparent magnitude. This difference is discussed by Blaauw (24) in the article which is the source of the absolute visual magnitudes M_V given in Table 3 for the stars earlier than M0. Blaauw places the M_V values which have been used in Table 3 in a group of those which "generally refer to stars selected according to apparent magnitude." The M_V values for the M stars in Table 3 are taken from a review article by Blanco (7) and are described by him as generally derived from stars brighter than apparent visual magnitude 6.0. Thus, both the mean absolute visual magnitudes given in Table 3 and the mean absolute K magnitudes derived from the infrared catalog are based on stars selected according to apparent magnitude.

B. Stars with I-K > 3.38: The Luminosity Distribution and the Characteristic Distance from the Galactic Plane

The luminosity distribution of observable stars derived from the catalog stars with I-K greater than 3.38 was presented in Figure 35,

which shows a N(v) distribution with a mean near v = 1.5 and a standard deviation of about 0.5. This indicates that virtually all of these stars are luminous enough to be included in the infrared catalog even when at distances greater than the characteristic half-width of their z distribution. For this reason it is possible to attach some significance to a luminosity function per unit volume of space derived from the n(t) analysis described in Chapter V. The parameters of possible luminosity functions of the stellar population from which these stars are drawn were presented in Table 11, and it was pointed out in Section N of Chapter V that the most probable luminosity function, the one in the center of the matrix in Table 11, could be interpreted as consistent with data presented in Table 3 for a population of giant stars generally later than M3. This luminosity function assumes that σ is 300 parsecs and gives the number of stars per unit M_K per 10^6 cubic parsecs as

$$D_o p(M_K) = \frac{1.1}{1.2\sqrt{2\pi}} \exp\left[-\frac{(M_K+6.6)^2}{2(1.2)^2}\right]. \qquad [91]$$

Since neither $\langle M_K \rangle$, the average absolute K magnitude, nor σ, the characteristic half-width of the z distribution, are very well established by previous work on the late M giants (spectral type > M4), there is little basis for a decision to adopt a value of either $\langle M_K \rangle$ or σ and then to calculate the other from the fact that the average luminosity of the observed stars with I-K > 3.38 corresponds to v ≈ 1.5; i.e.,

$$\langle M_K \rangle \simeq -2 - 5 \log_{10}\left(\frac{\sigma}{100 \text{ pc}}\right) - \frac{5}{2}(1.5) \ . \qquad [92]$$

The space density function D(z) presented by Blanco (7), which was the source of the σ = 250 parsecs value given in Table 3, was not considered by Blanco to be significantly different from Oort's D(z) function for K giants (44), which was adopted in Section C of Chapter V as the empirical standard for the shape of the function K(u) used in the n(t) analysis. However, according to Figure 22 and Table 7, Blanco's curve implies a σ of 282 parsecs and Oort's curve fits the standard form with a σ of 212 parsecs. The study by Hidajat and Blanco (45), which was the basis of the large value σ = 450 parsecs in Table 7, is a space density analysis for the M giant stars brighter than an infrared (I) magnitude 13.0 in three fields of area 5 square degrees each. In such a small area of sky there are not enough bright stars to obtain an estimate of the space density in the solar vicinity, and the D(z) values derived apply to regions of the galaxy from 1 to 8 kiloparsecs away from the sun (45). The absolute magnitudes of the giants later than M4 are considered uncertain by Blanco (7), as is indicated by the colon (:) in Table 3. For the spectral types later than M7 Blanco expects that the mean absolute visual magnitude is +0.3 or fainter. If this expectation is correct, extrapolation of the intrinsic color indices $(V-K)_o$ given in Table 3 would suggest that the mean absolute K magnitude is about -9 or -10 for the latest M giants. Given these uncertainties, Table 11 and Figure 35 must remain the summary of what

can be concluded from the n(t) analysis of the catalog stars with I-K greater than 3.38.

C. Comparison of the Longitude Distribution of the Reddest Stars (I-K > 3.38) with that of M5-M10 Giants from the Case Survey

Some confirmation of the conclusion drawn in Chapter V that the stars in the reddest I-K group are generally of spectral type later than M4 can be obtained by comparing the longitude distribution of these stars with that of M5-M10 giant stars found on the Case photographic infrared survey mentioned in Chapter I (5,6,7). Figure 36 shows the distribution in longitude ℓ^{II} of the stars with I-K greater than 3.38 which are within 2.5 degrees of the galactic equator compared with a similar distribution of the M5-M10 stars found on the Case survey (5). The results of the Case survey were reported in terms of the old galactic coordinates b^{I} and ℓ^{I} defined by Ohlsson (49), in which the pole is placed 1.5 degrees from the pole of the new coordinates b^{II} and ℓ^{II}. Figure 36 presents the distribution in new longitude ℓ^{II} of the Case stars within 2.0 degrees of the old galactic equator. The surface density is 6 or 8 times greater on the Case survey, but the relative numbers of stars in different longitude intervals are about the same in the two surveys. As was mentioned in Chapter I, identifications of individual infrared catalog stars with the brighter stars from the Case survey reveal that there is an appreciable number of stars common to both surveys.

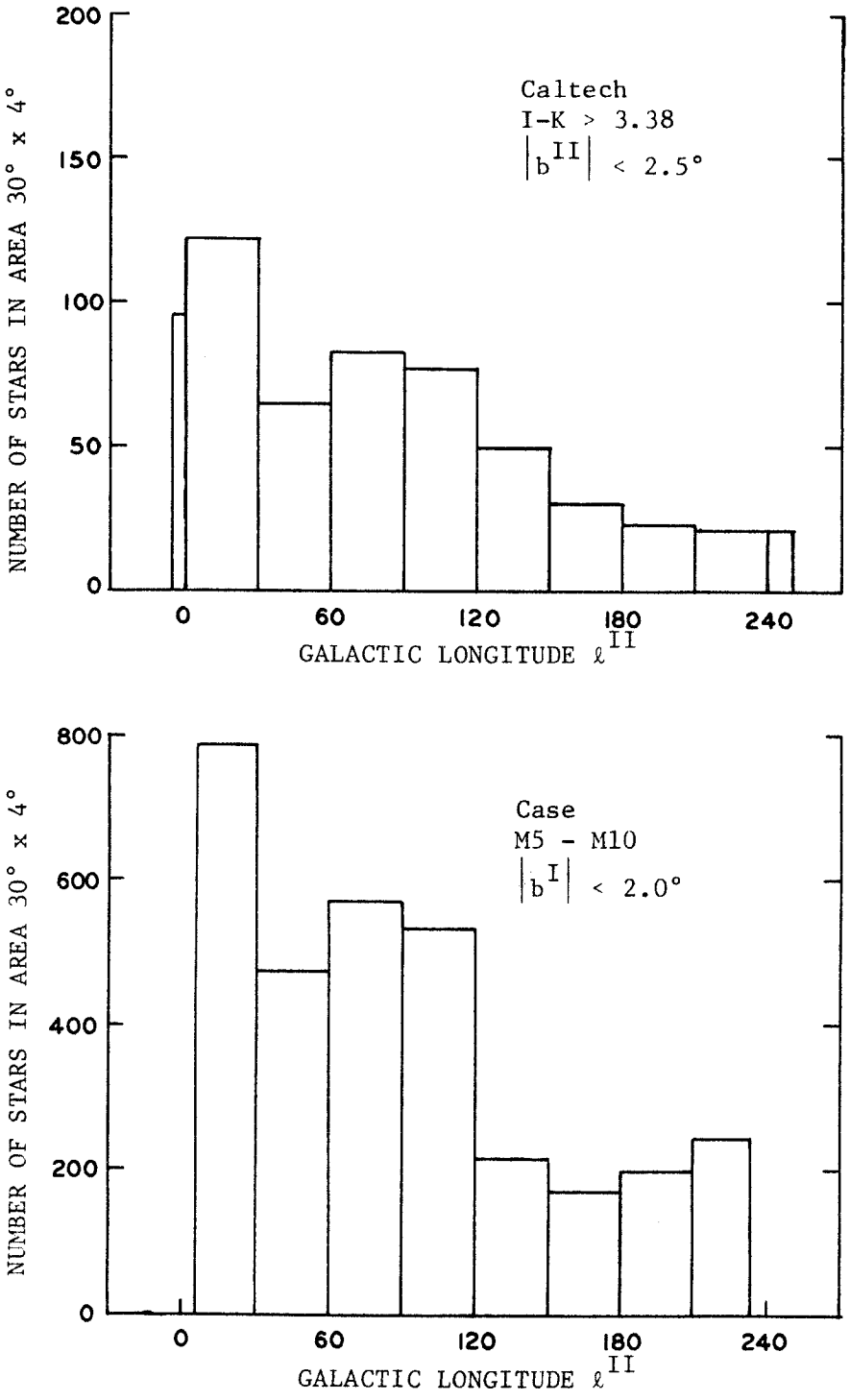

Figure 36.--Longitude Distribution of Stars with I-K > 3.38 Compared to Longitude Distribution from Case Survey.

D. The Longitude Distribution of Possible Supergiants

The longitude distribution in Figure 36 for the stars with I-K greater than 3.38 would show less concentration toward $\ell^{II} < 120°$ if the stars called supergiants in Section O of Chapter V were removed from the distribution. This cannot be done on an individual basis because the supergiant component is revealed and defined only in a statistical sense, i.e., in the excess of stars at low latitudes and large values of t. According to Table 13 the most probable luminosity function for the stars with I-K greater than 3.38 does not account for 46 percent of those with t greater than 4.14. Therefore, nearly half of the stars in a longitude distribution of those with t greater than 4.14 and I-K greater than 3.38 would be supergiants in the sense of Chapter V. Such a longitude distribution is given in Figure 37. Clearly the removal of about half of the stars in this distribution from the one shown in Figure 36 would decrease, but not remove entirely, the concentration toward $\ell^{II} < 120°$. For purposes of comparison, Figure 37 also presents the longitude distribution for reddened M0-M4 stars which were found on the Case survey within 6 degrees of the old galactic equator ($|b^{I}| < 6°$). Lists of these reddened stars were published by Nassau, Blanco, and Morgan (12) and by Blanco and Nassau (50). Like the infrared catalog stars with t greater than 4.14, these early M stars which show highly reddened spectra on the Case survey plates should constitute a sample rich in supergiants, because a large amount of reddening may be due to a star's being at a great distance. In fact, Sharpless (38) used the above lists of reddened early M stars to

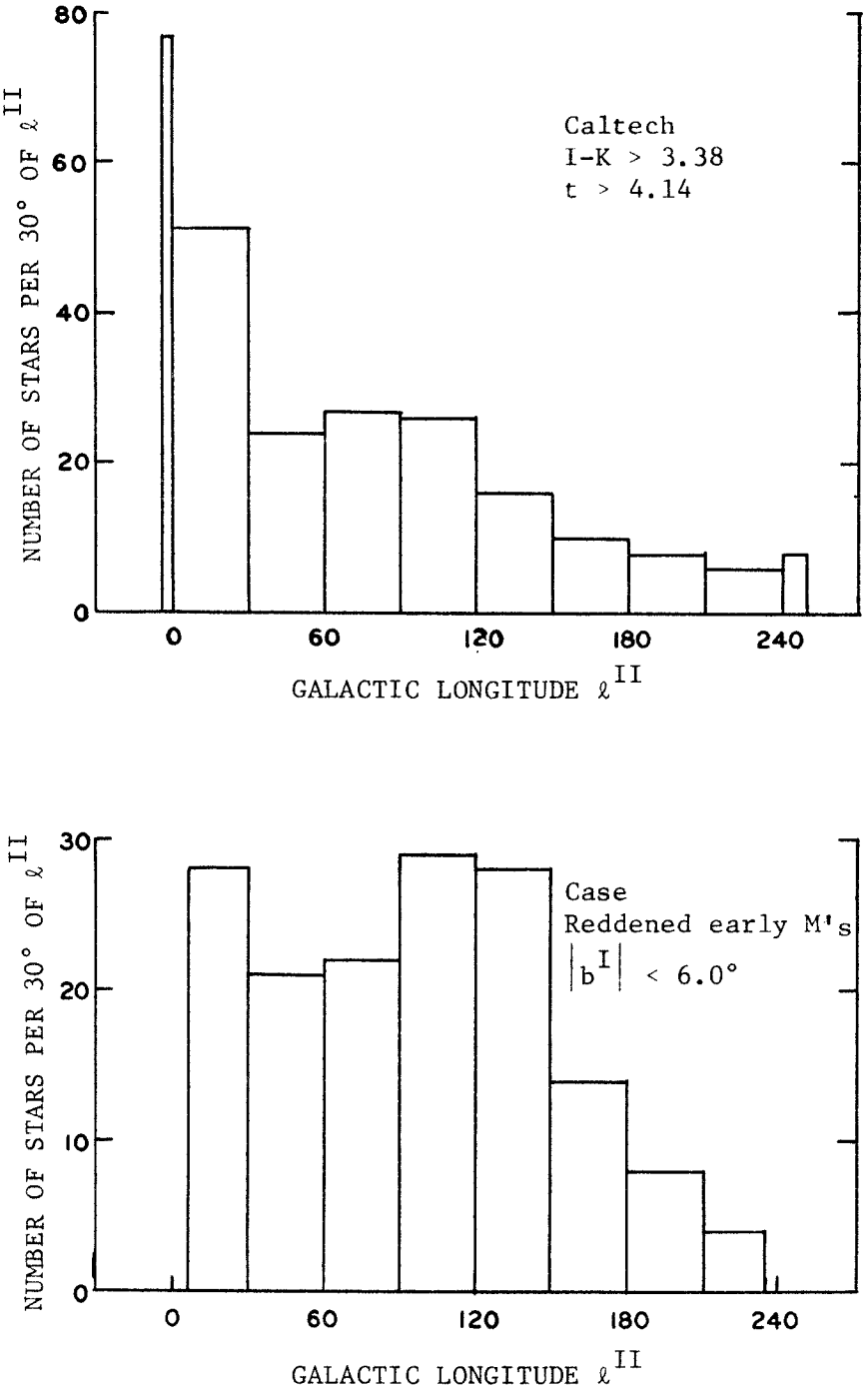

Figure 37.--Longitude Distributions of Possible Supergiants from the Two Micron Survey and the Case Survey.

associate 8 more M supergiants with the double cluster h and χ Persei. The principal difference between the two distributions in Figure 37 is the greater concentration of the reddened early M stars in the $120° < \ell^{II} < 150°$ range. This is the longitude range which includes the h and χ Persei stars. In Section O of Chapter IV it was pointed out that, as shown in Table 6, the M supergiants associated with h and χ Persei are not distributed symmetrically about the new galactic equator but are between $b^{II} = -1°$ and $b^{II} = -4°$. Since nearly all stars with $t > 4.14$ are of necessity well within a degree of the equator, the h and χ Persei M supergiants would tend to be excluded from Figure 37 by the statistical definition used here. The most striking feature of the longitude distribution of the catalog stars with I-K greater than 3.38 and t greater than 4.14 is the high concentration in the range $-5° < \ell^{II} < 30°$. Unfortunately, the Case survey did not extend quite far enough south to provide a comparison within 5 degrees of the longitude of the galactic center.

The very high concentration of possible supergiants shown in Figure 37 for the longitude range $-5° < \ell^{II} < 0°$ is due to there being 10 stars within half a degree of the galactic equator in the 5 degrees of longitude which were surveyed south of the galactic center direction. There is no corresponding concentration in the longitude range $0° < \ell^{II} < 5°$. The overall high concentration of possible supergiants between $\ell^{II} = -5°$ and $\ell^{II} = 30°$ can be taken as an indication of spiral arms in the galaxy between the sun and the galactic center. Such spiral arms are shown in various studies of galactic spiral structure; e.g.,

work by Sharpless (31) and Becker (51). Bidelman (52) has studied the space distribution of supergiants of spectral type later than A4 and finds evidence of three spiral arms between the sun and the galactic center. He places the innermost of these arms about one third of the distance from the center of the sun. The sun is generally taken to be 10 kiloparsecs from the galactic center (53).

E. An Estimate of the Space Density Gradient in the Galactic Plane for the Stars with I-K > 3.38

The higher concentration of the stars with I-K greater than 3.38 at longitudes toward the galactic center as compared to longitudes toward the anti-center suggests that the space density of these stars decreases with distance from the galactic center. This asymmetry of the longitude distribution is evident in the galactic coordinate map (Figure 13) and in the longitude histogram of stars within 2.5 degrees of the equator (Figure 36). Using the luminosity distribution of observable stars N(v) derived in Section N of Chapter V to obtain the average distance to which stars with I-K greater than 3.38 can be seen, the distance scale for changes in space density in the galactic plane can be related to the distance scale for changes in space density normal to the plane.

As indicated in Chapter V in connection with the N(v) functions shown in Figure 35 the average star with I-K greater than 3.38 can be seen to a distance 5 or 6 times σ the characteristic half-width of the z distribution of these stars. Thus the number of stars in a particular longitude range at all latitudes is indicative of the number of

stars at those longitudes at an average distance $\langle r_{max} \rangle$ of 5 or 6 times σ. By taking the ratios of the numbers of stars in different longitude ranges one obtains an estimate of the relative space densities in the different directions but at about the same average distance $\langle r_{max} \rangle$. Table 15 presents the relevant data for making such an estimate of relative space densities. The "weighted total" of stars in each of the longitude ranges (Column 4) refers to the total number of stars which would be seen if the whole celestial sphere were like that particular longitude range. The general procedure for weighting the observed stars in order to extrapolate their numbers to the parts of the sky not covered is described in Appendix B. The actual number of stars counted in each longitude range is given in Column 3 of Table 15. In order to remove the contribution of the stars interpreted as being supergiants rather than late M giants, stars with a value t greater than 4.2 were not counted in making up Table 15. The relative weighted totals given in Column 5 have been normalized to unity near $\ell^{II} = 90°$.

For stars which are in the galactic plane at longitude ℓ^{II} and at an average distance $\langle r_{max} \rangle$ from the sun, the average projection along the line from the sun to the galactic center is $\langle r_{max} \rangle \cos \ell^{II}$. To first order in $\langle r_{max} \rangle / R_o$, where R_o is the distance from the sun to the galactic center ($\sim$10 kiloparsecs), the distance from the galactic center to a point in the plane $\langle r_{max} \rangle$ from the sun at longitude ℓ^{II} is given by

$$R \simeq R_o - \langle r_{max} \rangle \cos \ell^{II} . \qquad [93]$$

TABLE 15

DATA FOR GRADIENT ESTIMATE

ℓ^{II} range	cos ℓ^{II} at mid-range	Actual number of stars	Weighted total of stars	Relative weighted total	$\log_{10}$ of relative weighted total
0°-30°	+0.965	402	5056	1.410	.150
30°-60°	+0.707	318	3816	1.065	.028
60°-90°	+0.259	306	3672	1.024	.010
90°-120°	-0.259	286	3491	.974	-.012
120°-150°	-0.707	231	2857	.796	-.099
150°-210°	-1.000	413	2478	.692	-.160
210°-240°	-0.707	162	1993	.556	-.255
120°-150° 210°-240°	-0.707	393	2498	.697	-.156

In the limit where this is true, a plot of the number of stars at distance $\langle r_{max} \rangle$ as a function of cos ℓ^{II} is a plot of the number of stars at a distance $R_o - r$ from the galactic center as a function of r where r is measured in units of $\langle r_{max} \rangle$. Figure 38, which is based on the data given in Table 15, shows both the relative numbers of stars and the logarithms of those numbers plotted versus cos ℓ^{II}. The error bars on the points indicate the standard deviation associated with the actual number of stars which went into determining the point, i.e., a fractional standard deviation of $1/\sqrt{N}$ where N is given in Column 3 of Table 15. The straight lines drawn in Figure 38 were determined by applying a χ^2 test to lines of various slope and intercept and adopting the ones with smallest χ^2. For purposes of the χ^2 testing the two inconsistent points at cos $\ell^{II} = -0.707$ were averaged together as in the last line of Table 15. Neither line is a good fit, but some estimate of the space density gradient can be obtained from Figure 38.

The straight line in the linear plot in Figure 38 gives the relationship

$$D/D_o = 0.95 + 0.30 \cos \ell^{II} , \qquad [94]$$

where D/D_o is the space density at distance $R_o - \langle r_{max} \rangle \cos \ell^{II}$ from the galactic center relative to that a distance just under R_o from the galactic center. Equation [94] says that the relative space density decreases linearly from 1.25 to 0.65 as one goes from a distance $\langle r_{max} \rangle$ toward the galactic center to the same distance directly away from the

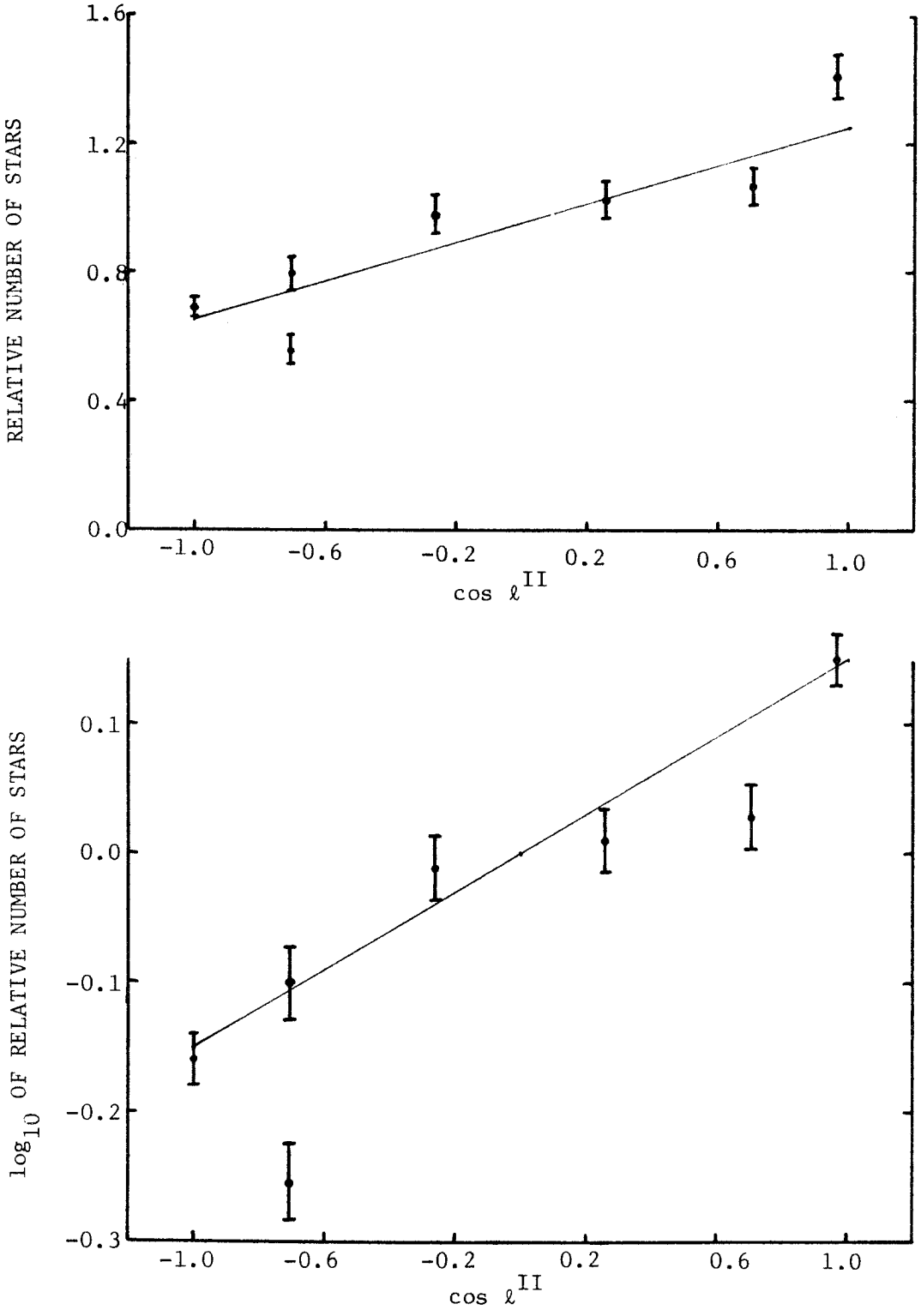

Figure 38. Relative Number of Stars versus cos ℓ^{II}

center. The straight line in the logarithmic plot in Figure 38 gives the relationship

$$D/D_o = 10^{0.15 \cos \ell^{II}} , \qquad [95]$$

which gives about the same linear approximation as Equation [94]. Therefore, the gradient estimate obtained from Figure 38 is a factor of $10^{0.15}$ ($\simeq 1.4$) per $\langle r_{max} \rangle$, where $\langle r_{max} \rangle$ is 5 or 6 times the characteristic half-width σ.

In a review of the literature on galactic structure Scheffler and Elsässer (54) cite some results for the radial gradient near the sun of the space density of various stellar objects. The only result given there for giant M stars is one from a paper by Sanduleak (55) in which the space density in the galactic plane of giants M7 or later is estimated from star counts in 25 selected areas of one square degree each. Sanduleak gives this space density as

$$D(R) = 150 \times 10^{-0.23\ R} \text{ stars}/10^6 \text{ pc}^3 , \qquad [96]$$

where R, the distance from the galactic center in kiloparsecs, is in the range 4 kpc < R < 12 kpc. (Sanduleak apparently used about 8 kiloparsecs as the distance from the sun to the galactic center.) Thus, Sanduleak's estimate of the logarithmic radial gradient of density near the sun, defined as

$$\alpha \equiv \left[\frac{\partial [\log_{10} \frac{D(R)}{D_o}]}{\partial R} \right]_{R_o} , \qquad [97]$$

is -0.23 per kiloparsec. The average value of this quantity α for other objects which Scheffler and Elsasser group together with red giants as "disk-population" objects is given by them as -0.3 per kpc, i.e., a factor of 2 per kiloparsec.

To compare the gradient derived here with the other results just cited it is necessary to assume a value of the characteristic half-width σ and then to take the logarithmic gradient as being

$$\alpha = \frac{-0.15}{\langle r_{max} \rangle} = -\frac{0.15}{5\sigma} . \qquad [98]$$

For the three values of σ used in Chapter V as indicative of the range of possible values, namely σ = 200, 300, or 450 parsecs, the logarithmic radial gradient near the sun would be α = -0.15, -0.10, or -0.07 per kiloparsec respectively. All of these values of α indicate a smaller gradient that the other results cited. This fact could be used as a reason for preferring the smallest of the suggested values of σ, i.e., 200 parsecs. Some reconciliation of the difference in the gradient estimates may be found by taking into account the fact that $\langle r_{max} \rangle$ is the average distance to which the stars could be seen rather than the average distance at which they actually are. Assuming the average K magnitude of the stars to be 2.5 would mean that the stars are closer than their maximum distance by a factor of

$$r/r_{max} = \sqrt{s_{min}/s} = 10^{-0.2(3.0-2.5)} = 0.8 . \qquad [99]$$

(See Equations [14], [15], and [16].) This modification makes the

gradient estimate larger by a factor of 1.25, but it is still smaller than Sanduleak's value, even if σ is taken as 200 parsecs. For the assumption σ = 300 parsecs, which was used in Table 14, the present estimate of the logarithmic radial gradient of space density for late M giants in the solar vicinity is

$$\alpha \simeq -1.25 \frac{0.15}{5(0.300)} = -0.125 \text{ per kiloparsec.} \qquad [100]$$

APPENDIX A

INTERSTELLAR REDDENING AND ABSORPTION

Interstellar extinction can affect the analysis given in this thesis in two ways. One is by causing a star's observed color index I-K to be greater (i.e., redder) than the intrinsic color index $(I-K)_o$. Since I-K has been used to separate the stars in the infrared catalog into four groups which were analyzed separately, interstellar reddening could cause a star to be put into an I-K group which is not representative of its intrinsic color $(I-K)_o$. The other effect of interstellar extinction would be to make a star's apparent brightness at 2.2μ less than it would be if there were no interstellar extinction at 2.2μ. Thus the signal s from a star of luminosity L at distance r would not be given by

$$s = \frac{L}{r^2} \quad \text{no interstellar extinction} \qquad [101]$$

as assumed in Equation [14], but would be smaller than L/r^2 by a factor which depends on the amount of interstellar extinction between the earth and the star.

H. L. Johnson (56) has summarized much of the work related to the determination of the wavelength dependence of interstellar extinction. The data in Table 16 have been taken from this article by Johnson. Table 16 gives the reddening in three different color indices relative to the reddening in the color index B-V. Reddening in a color index, B-V for example, is denoted by E(B-V) because the wavelength dependence

TABLE 16

COLOR EXCESS AND ABSORPTION RATIOS

Description	$\frac{E(V-R)}{E(B-V)}$	$\frac{E(V-I)}{E(B-V)}$	$\frac{E(V-K)}{E(B-V)}$	$\frac{A_V}{E(B-V)}$
van de Hulst curve #15	0.80	1.62	2.78	3.0
Whitford	0.88	1.54	2.84	3.0
Perseus (21 stars)	0.84	1.60	2.62	3.0
Cygnus (6 stars)	0.87	1.63	2.81	3.6(3)
Cepheus (6 stars)	0.82	1.58	2.50	4.8(2)
NGC 6611 (5 stars)	0.95	1.78	3.20(1)	3.5(1)
NGC 2244 (5 stars)	0.81	1.65	3.14(3)	5.6(3)
Scorpius (5 stars)	0.67	1.55	3.35	3.6
Ophiuchus (4 stars)	0.89	1.69	2.78	
NGC 6530 (4 stars)	1.23(3)	2.13(3)	3.38(2)	
Orion sword (4 stars)	1.25	2.55	5.00	5.0
Aquila (2 stars)	0.84	1.59	2.72	3.5
Taurus-Orion (2 stars)	0.89	1.69	2.78	
Orion belt (2 stars)	1.08	2.15	4.26(1)	4.8
Capricornus (1 star)	0.87	1.53	3.00	
Auriga (1 star)	0.57	1.57	2.52	6.3
Average of 1st 3:	0.84	1.59	2.75	3.0
Average of Johnson's:	0.89	1.72	2.96	3.3

Explanation:

These data are taken from the article by Johnson (56). Johnson reproduces the results of Whitford (57) and van de Hulst (58), and presents the other results based on his own data. When one of the ratios given by Johnson is based on fewer stars than indicated in the left hand column, the actual number is given in parentheses following the ratio in question. The values for the ratio $R = A_V/E(B-V)$, which are based on Johnson's work, are taken from his extrapolations of the relative absorption versus reciprocal wavelength ($1/\lambda$) to $1/\lambda = 0$. He presents such extrapolations only for those regions where there are results available from another method of determining R.

The average of Johnson's data presented in the last line of the table was taken giving each ratio a weight equal to the number of stars used to obtain it.

of the interstellar extinction causes the blue (B) light to be reduced by a greater factor than the visual (V) thus causing the observed difference in magnitudes B-V to be in *excess* of the actual color index $(B-V)_o$ at the surface of the star. The defining relationship is

$$E(B-V) \equiv (B-V)_{observed} - (B-V)_{intrinsic} \equiv (B-V) - (B-V)_o. \quad [102]$$

The response as a function of wavelength for each color band is that given by Johnson (22) and the effective wavelengths of the bands are (59):

Johnson's Band	Effective wavelength (microns)
B	0.44
V	0.55
R	0.70
I	0.90
K	2.2

As given in Section A of Chapter III, the I magnitude used in the Caltech infrared survey has an effective wavelength of 0.80μ, and is therefore about midway between the R and I bands defined by Johnson. To estimate the ratio of the reddening in the color index I-K used on the infrared survey E(I-K), to the reddening in the color index B-V defined by Johnson, E(B-V), the following formula is used:

$$\frac{E(I-K)_{survey}}{E(B-V)} = \frac{E(V-K)}{E(B-V)} - \frac{1}{2}\left[\frac{E(V-R)}{E(B-V)} + \frac{E(V-I)_{Johnson}}{E(B-V)}\right]. \quad [103]$$

The result, taken from the average values at the bottom of Table 16, is

$$\frac{E(I-K)_{survey}}{E(B-V)} \equiv \frac{E(I-K)}{E(B-V)} = 2.75 - \frac{1}{2}[0.84 + 1.59] = 1.54 \ , \quad [104]$$

or

$$\frac{E(I-K)_{survey}}{E(B-V)} \equiv \frac{E(I-K)}{E(B-V)} = 2.96 - \frac{1}{2}[0.89 + 1.72] = 1.66 \ , \quad [105]$$

depending on which set of averages is used. This means that if a star is reddened by m magnitudes in B-V the average interstellar reddening law predicts that it is reddened by about 1.6 m magnitudes in I-K. In terms of signal strength s this means that if the ratio of observed signal at 0.44μ to observed signal at 0.55μ is

$$\frac{s(0.44)}{s(0.55)} = \left[\frac{s(0.44)}{s(0.55)}\right]_o 10^{-0.4m} \quad [106]$$

then the ratio of observed signals at 0.8μ and 2.2μ is

$$\frac{s(0.8)}{s(2.2)} = \left[\frac{s(0.8)}{s(2.2)}\right]_o 10^{-0.4(1.6)m} \ . \quad [107]$$

In Equations [106] and [107] the brackets with subscript zero refer to intrinsic brightnesses.

Equations [104] and [105] are useful for estimating the amount of reddening in I-K because the amount of reddening in B-V has been measured in different regions of the sky by various observers. Some values for $E_o(B-V)$, the total reddening in magnitudes of the color

index B-V toward the galactic pole, are:

$E_o(B-V)$	Author
.060 ± .007	van den Bergh (60)
.055 ± .003	Kron and Mayall (61)
.067 ± .003	Kron and Mayall (61)
.028 ± .036	Peterson (62)

These values for $E_o(B-V)$ are derived by measuring the color excess E(B-V) for distant objects at various galactic latitudes b and fitting the data with a function of the form

$$E(B-V) = \text{constant} + E_o(B-V)\csc|b| \ . \qquad [108]$$

This assumes that the objects measured are beyond the absorbing layer of interstellar dust. The half-width of the dust layer is between 20 and 100 parsecs (63,64). Actually, the color excess E(B-V) in many directions in the sky cannot be accounted for by a single absorbing layer (60,63,65), and Equation [108] should be taken as expressing some kind of an average value of E(B-V) for objects which are more than about 200 parsecs from the galactic plane.

At low galactic latitudes, say $|b| < 5°$, the amount of interstellar absorption and reddening varies a great deal from one region of the sky to another. This has been demonstrated by T. Neckel (63) who used photometric B and V magnitudes for about 4700 stars of known spectral-luminosity class to derive the color excess E(B-V) as a function of distance in 207 regions covering the entire celestrial sphere.

In the zone $\left|b^{II}\right| < 7°$ Neckel finds 3 regions, with a combined area of about 50 square degrees, where E(B-V) is greater than 1.3 magnitudes within one kiloparsec of the sun, and 7 regions, with a combined area of about 300 square degrees, where E(B-V) within a kiloparsec is less than 0.2 magnitude. Regions of the sky where E(B-V) is somewhere between these two extremes are mixed together all along the galactic equator. Neckel's analysis of the data yields an average B-V reddening in the galactic plane of about 0.8 magnitude per kiloparsec, with most of the absorbing matter concentrated within 20 parsecs of the galactic plane. Fernie (66) also used B and V magnitudes together with spectral-luminosity classes to derive values for the reddening per kiloparsec near the galactic equator. His results show a range in E(B-V) from about 0.2 mag/kpc to about 1.0 mag/kpc with an average of about 0.6 mag/kpc. Allen (64) gives values for A_V, the total absorption in V, near the galactic plane obtained by three different selection criteria. The values of A_V can be converted to E(B-V) using the relationship $A_V = 3.0\ E(B-V)$ which is also given by Allen. The E(B-V) obtained with various selection criteria are:

0.7 mag/kpc from stars selected by true distance,

0.3 mag/kpc from stars selected by visibility,

0.1 mag/kpc from stars selected by avoiding clouds.

All of these results confirm the rather spotty nature of interstellar reddening and absorption in the galactic plane. The three average values of E(B-V) given here are in good agreement, but an average value should not be used without being aware of the fact that large deviations from

it are to be expected in many areas. The average E(B-V) near the galactic plane suggested by the above results is about 0.7 mag/kpc.

From the above results the following conclusions may be drawn concerning the amount of interstellar reddening to be expected in I-K. For stars not in the galactic plane, say about 200 parsecs or more from it, the reddening in I-K (in magnitudes) goes as

$$E(I-K) \simeq 0.08 \csc|b| \ . \qquad [109]$$

In the galactic plane the average reddening in I-K is about 1.1 mag/kpc, but the variation from one direction to another may be very large, ranging from 0.2 mag/kpc in clear areas to 2.0 mag/kpc in areas of heavy obscuration.

The amount of reddening per kiloparsec required to make a giant star of a particular spectral type have an apparent I-K greater than 3.38, i.e., have I-K large enough to be in the reddest I-K group, is estimated in Table 17. For each spectral type in Table 17 the intrinsic color $(I-K)_o$ is taken to be the mean I-K given in Figure 5 and the maximum distance at which that type star will be bright enough to be in the infrared catalog is taken to be the r_{max} given in Table 3. The reddening in magnitudes per kiloparsec required to make a star with intrinsic color $(I-K)_o$ at distance r_{max} have an apparent I-K equal to 3.38 is given. The required reddening in I-K estimated in Table 17 becomes comparable to 1.1 mag/kpc, the above estimate of the average reddening in the galactic plane, for spectral types later than M2. Therefore, it is likely that some of the stars with I-K greater than

TABLE 17

SOME REDDENING ESTIMATES

Spectral type	Intrinsic color $(I-K)_o$	r_{max}(kpc)	Reddening (mag/kpc) in I-K needed to make I-K > 3.38
K0	1.87	.083	18.2
K3	2.10	.145	8.8
K5	2.37	.275	3.7
M0	2.49	.290	3.1
M1	2.60	.33	2.4
M2	2.59	.42	1.9
M3	2.73	.60	1.1
M4	2.94	.76	0.6

3.38 are intrinsically more like the stars in the group with I-K between 2.87 and 3.38 but are included with the reddest group due to interstellar reddening.

In order correctly to interpret the latitude and n(t) distributions of the stars in the reddest I-K group one must know to what extent the high concentration toward the galactic equator as compared with the galactic poles is due to interstellar reddening. If a significant number of the stars near the galactic equator are intrinsically more like stars with I-K less than 3.38 than like the other stars with I-K greater than 3.38, the fact that the counterparts of these stars at higher latitudes, where the reddening is not as great, are not included in the latitude distribution will result in a greater concentration toward the equator than would result from a grouping based on intrinsic properties. One method of testing whether or not this effect has played a significant role in determining the observed latitude distribution is to see how many low latitude stars may be missing from the group with I-K less than 3.38 and therefore, presumably, reddened into the group with I-K greater than 3.38. Figure 39 shows the two latitude distributions which must be compared to make this test. This figure shows the number of stars per 100 square degrees in various latitude zones. The dashed lines are for stars with I-K greater than 3.38 and the solid lines for I-K less than 3.38. There is no evidence in Figure 39 that stars which are reddened out of the group with I-K less than 3.38 are contributing significantly to the large increase in the surface density of the redder stars observed at low latitudes. In

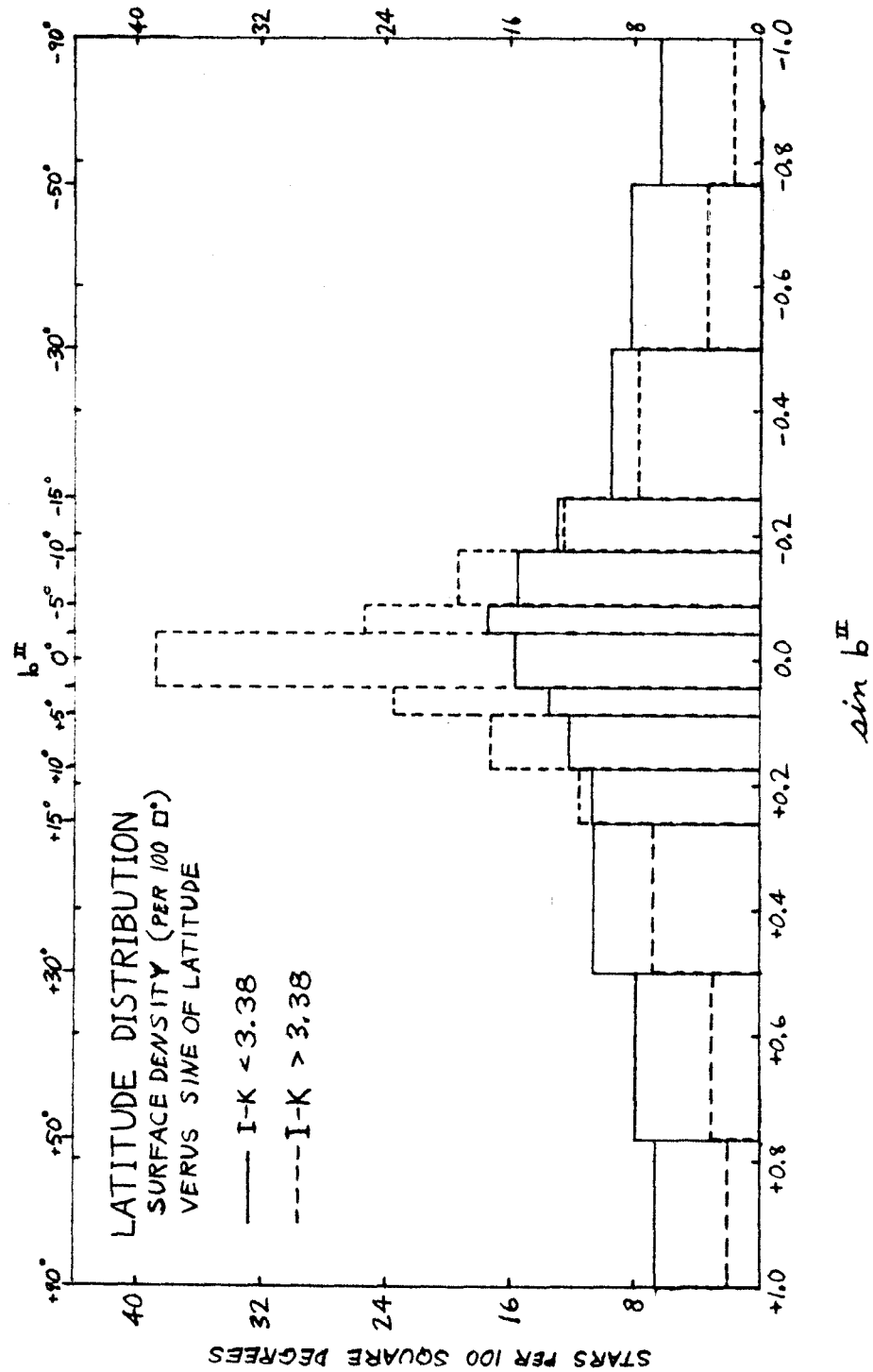

Figure 39.--Latitude Distributions for Stars with I-K < 3.38 and for Stars with I-K > 3.38.

fact, since the surface density of the stars with I-K less than 3.38 is either constant or increasing (within the statistical accuracy) as the equator is approached, any low latitude stars which are transferred from the redder group to the less red group would still be contributing to an excess of stars at low latitudes rather than accounting for a deficiency. The actual numbers of stars in the various latitude zones used in Figure 39 are given in Table 18, and from these numbers the statistical uncertainties in the calculated surface densities can be estimated.

The possibility that interstellar dust is affecting the data through its extinction (absorption) of 2.2μ radiation must also be considered. There is less agreement on the ratio of A_K, total absorption in the K band, to E(B-V), the color excess in B-V, than there is on the ratio E(I-K)/E(B-V), which was calculated from the data in Table 16. Table 16 gives some values of the ratio of total to selective absorption, usually called R and defined by

$$R \equiv \frac{A_V}{E(B-V)} \, . \qquad [110]$$

Johnson (56) cites values of R determined by various observers for various regions of the sky, and these values range from 2.6 to 6.5. Converting absorption in V into absorption in K by

$$A_K = A_V - E(V-K) \qquad [111]$$

results in the conclusion that such a large range in R would imply

TABLE 18

LATITUDE DISTRIBUTION DATA USED IN FIGURE 39

Range of latitude b^{II} (degrees)	Area covered by survey in this b^{II} range (sq. deg.)	Number of stars in this area with I-K:		Number per 100 sq. deg. with I-K:	
		<3.38	>3.38	<3.38	>3.38
+90 to +50	4822	319	96	6.6	2.0
+50 to +30	5407	427	164	7.9	3.0
+30 to +15	4056	430	278	10.6	6.8
+15 to +10	1346	145	156	10.8	11.6
+10 to + 5	1322	161	228	12.2	17.3
+5.0 to +2.5	651	88	153	13.5	23.5
+2.5 to -2.5	1277	200	496	15.7	38.8
-2.5 to -5.0	626	109	159	17.4	25.4
- 5 to -10	1220	190	237	15.6	19.4
-10 to -15	1178	153	148	13.0	12.6
-15 to -30	3225	308	250	9.6	7.8
-30 to -50	3406	281	113	8.2	3.3
-50 to -90	3432	219	56	6.4	1.6
All latitudes	31968	3030	2534	9.5	7.9

that the absorption in K ranges from less than a tenth to about a half of that in V. If the old standard reddening curve, which is essentially that of Whitford (57), is adopted, the absorption in K would be less than one tenth the absorption in V and about one third the reddening in B-V. In this case the average absorption A_K near the galactic equator would be about 0.2 mag/kpc.

One effect of absorption at 2.2μ would be to decrease the number of stars observed in regions of large absorption. This would result in the observed star density being lower near the galactic equator than it would be if there were no absorption. There is certainly no evidence of this effect in the latitude distribution of the infrared stars shown in Figure 39, but it cannot be ruled out, because the comparison is with a hypothetical "no absorption" case.

Another effect of absorption of 2.2μ would be to change the apparent K magnitudes measured. Since, according to Equations [21] and [32],

$$t = 0.4(3.0-K) + 2 \log_{10}\left|\csc b^{II}\right| , \qquad [112]$$

an absorption in K of about 0.2 magnitude per kiloparsec would mean a change in t given by

$$\Delta t \simeq 0.1 \text{ per kiloparsec} . \qquad [113]$$

The effect of absorption is to make t smaller than it would be otherwise. For stars within 5 degrees of the equator t must be greater than 2.1. The intervals used in Figures 26, 27, 28, and 33 for

presenting the observed n(t) distributions are considerably larger than the changes in t which would result from the rate given in Equation [113] applied in a dust layer with a characteristic half-width of 100 parsecs or less. For instance, a star 100 parsecs from the plane and 2000 parsecs from the sun would have t greater than 2.6 and Δt about 0.2. The width of the intervals used in the observed n(t) distributions are about 0.5 or greater for t above 2.6.

APPENDIX B

THE CONSTRUCTION OF THE DISTRIBUTION FUNCTIONS

The general method used to present the distribution of some observed quantity, say y, in this thesis has been to count the number of stars which have a value of y in a particular range, to divide the number by the range to get the average density $\overline{n}$ over the range, and to take $\overline{n}$ as applying to the value of y which is the median of the values of y observed in the range. The fractional standard deviation of each value of $\overline{n}$ calculated this way has been taken to be $1/\sqrt{N}$, where N is the number of stars with y in the particular range. In constructing the latitude distributions the ranges, or intervals, of the galactic latitude b were specified and the number in each range was then counted. For the I-K distribution (Figure 6) and for the many n(t) distributions the range of each interval was determined by a choice of the number of stars to be in the interval.

The fact that not all of the sky was covered by the infrared survey is reflected in the procedure used to construct the latitude distributions and the n(t) distributions. The procedure used to construct the latitude distributions will be explained first. Figure 40 shows the northern and southern survey limits as a function of the galactic longitude ℓ^{II} and latitude b^{II} plotted on a linear scale. This figure has been used to construct Table 19 which gives, for each of the longitude-latitude zones, the area (in square degrees) actually covered by the infrared survey. The dashed lines in Table 19 are used

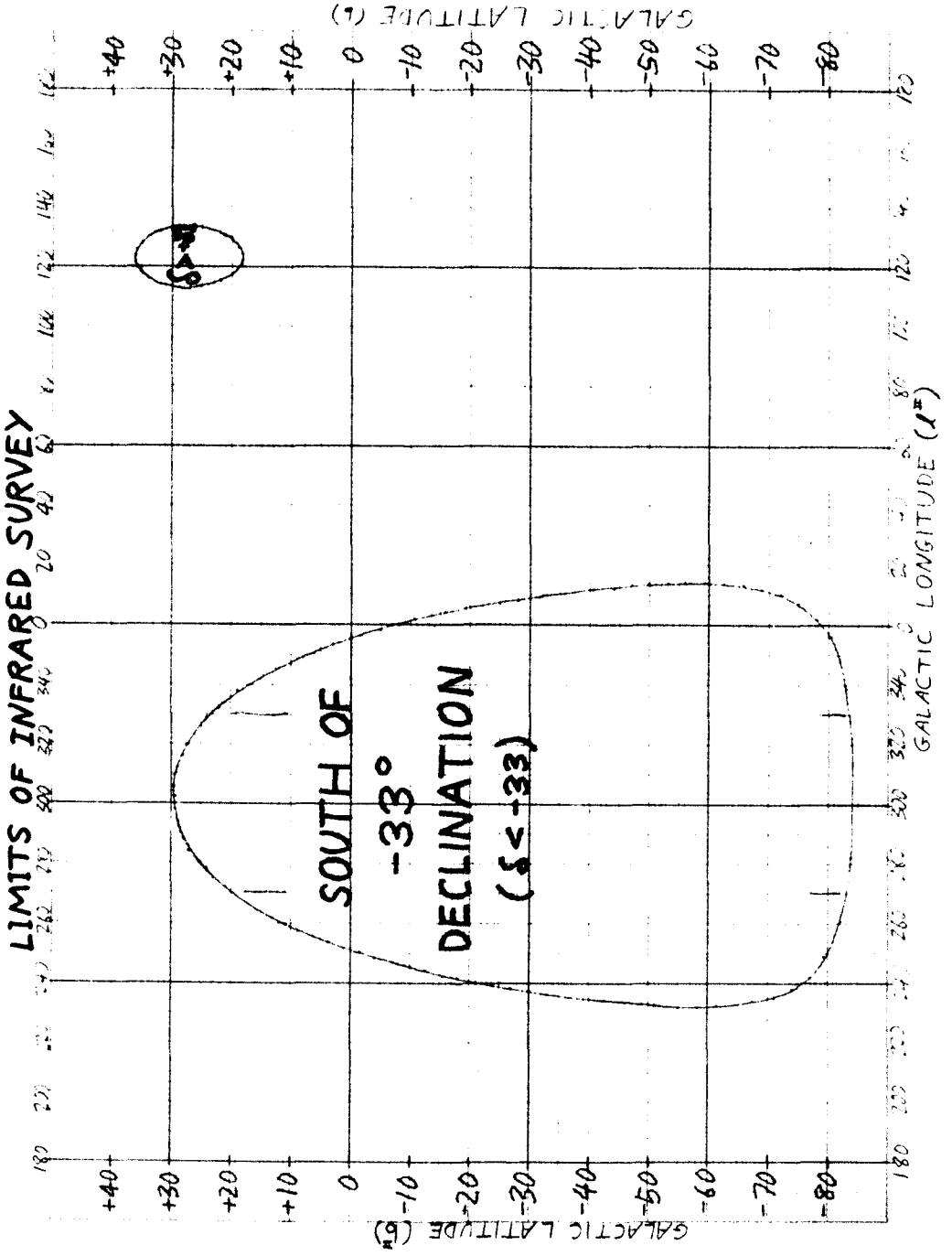

Figure 40.--The Galactic Longitude and Latitude of the Limits of the Infrared Survey.

TABLE 19

AREA SURVEYED IN EACH LONGITUDE-LATITUDE ZONE

Latitude range b^{II} (degrees)	Area (sq. deg.) surveyed in longitude range ℓ^{II} (degrees)											
	0-30	30-60	60-90	90-120	120-150	150-180	180-210	210-240	240-270	270-300	300-330	330-360
+90 to +50	401.8	401.8	401.8	401.8	401.8	401.8	401.8	401.8	401.8	401.8	401.8	401.8
+50 to +30	456.9	456.9	456.9	434.6 (95%)	403.4 (88%)	456.9	456.9	456.9	456.9	456.9	456.9	456.9
+30 to +15	414.2	414.2	414.2	356.3 (86%)	291.4 (70%)	414.2	414.2	414.2	399.5 (96%)	102.3 (25%)	59.1 (14%)	362.1 (88%)
+15 to +10	146.3	146.3	146.3	146.3	146.3	146.3	146.3	146.3	102.5 (70%)	0	0	73.5 (50%)
+10 to + 5	148.5	148.5	148.5	148.5	148.5	148.5	148.5	148.5	81.7 (55%)	0	0	52.1 (35%)
+5.0 to +2.5	74.8	74.8	74.8	74.8	74.8	74.8	74.8	74.8	34.0 (45%)	0	0	19.0 (25%)
+2.5 to +1.5	29.9	29.9	29.9	29.9	29.9	29.9	29.9	29.9	12.5 (42%)	0	0	6.0 (20%)
+1.5 to +0.5	30.0	30.0	30.0	30.0	30.0	30.0	30.0	30.0	11.5 (38%)	0	0	5.5 (18%)

[continued on next page]

TABLE 19--Continued

Latitude range b^{II} (degrees)	Area (sq. deg.) surveyed in longitude range ℓ^{II} (degrees)											
	0-30	30-60	60-90	90-120	120-150	150-180	180-210	210-240	240-270	270-300	300-330	330-360
+0.5 to -0.5	30.0	30.0	30.0	30.0	30.0	30.0	30.0	30.0	11.0 (37%)	0	0	5.0 (17%)
-0.5 to -1.5	30.0	30.0	30.0	30.0	30.0	30.0	30.0	30.0	10.5 (35%)	0	0	4.0 (13%)
-1.5 to -2.5	29.9	29.9	29.9	29.9	29.9	29.9	29.9	29.9	9.5 (32%)	0	0	3.0 (10%)
-2.5 to -5.0	74.8	74.8	74.8	74.8	74.8	74.8	74.8	74.8	21.7 (29%)	0	0	6.0 (08%)
-5 to -10	147.1 (99%)	148.5	148.5	148.5	148.5	148.5	148.5	148.5	32.8 (22%)	0	0	1.0 (01%)
-10 to -15	134.2 (92%)	146.3	146.3	146.3	146.3	146.3	146.3	146.3	19.5 (13%)	0	0	0
-15 to -30	327.3 (79%)	414.2	414.2	414.2	414.2	414.2	414.2	403.5 (97%)	9.0 (02%)	0	0	0
-30 to -50	286.4 (62%)	456.9	456.9	456.9	456.9	456.9	456.9	378.1 (83%)	0	0	0	0
-50 to -90	253.4 (63%)	401.8	401.8	401.8	401.8	401.8	401.8	322.1 (80%)	24.2 (06%)	10.2 (02%)	9.6 (02%)	401.8

to set off the longitude-latitude zones which are not completely covered by the survey. To construct the latitude distributions in Figures 14, 15, 17, and 39 the number of stars N in each particular zone was divided by the area surveyed in that zone. As mentioned above, the standard deviation for the surface density S so computed was taken to be $\pm S/\sqrt{N}$.

The n(t) distributions which are presented in Figures 24, 25, 26, 27, 28, and 33 are extrapolations to the whole sky of the distribution of t for the stars actually included in the infrared catalog. In order to carry out this extrapolation the entire sky was divided into 30 zones each covering 6 degrees of galactic latitude, a 3 degree range of b^{II} in the northern hemisphere together with the corresponding 3 degree range of b^{II} in the southern hemisphere. The fraction f of the sky surveyed in each zone was calculated using Figure 40. Then the n(t) distribution was constructed after giving each star a weight

$$w = 1/f \qquad [114]$$

determined by which of the 30 latitude zones it happened to be in. Table 20 gives the latitude zones and weighting factors used. To illustrate the use of Table 20 consider the following example: Each star with latitude b^{II} between +30° and +33° or between -30° and -33° is counted as 1.27 stars because out of the 720 degrees of longitude (360 degrees in each hemisphere) only 569 are covered by the survey thus giving the weighting factor

$$w = \frac{720}{569} = 1.27 \ . \qquad [115]$$

TABLE 20

WEIGHTING FACTORS FOR n(t) DISTRIBUTIONS

Zone	Range of $\lvert b^{II} \rvert$	Number of deg. of ℓ^{II} surveyed	Weight given to each star in zone
1	0°- 3°	512	1.41
2	3°- 6°	512	1.41
3	6°- 9°	514	1.40
4	9°-12°	516	1.40
5	12°-15°	520	1.38
6	15°-18°	522	1.38
7	18°-21°	517	1.39
8	21°-24°	522	1.38
9	24°-27°	518	1.39
10	27°-30°	548	1.31
11	30°-33°	569	1.27
12	33°-36°	574	1.25
13	36°-39°	583	1.23
14	39°-42°	583	1.23
15	42°-45°	582	1.24
16	45°-48°	581	1.24
17	48°-51°	580	1.24
18	51°-54°	579	1.24
19	54°-57°	578	1.25
20	57°-60°	578	1.25
21	60°-63°	579	1.24
22	63°-66°	580	1.24
23	66°-69°	582	1.24
24	69°-72°	584	1.23
25	72°-75°	591	1.22
26	75°-78°	597	1.21
27	78°-81°	610	1.18
28	81°-84°	640	1.13
29	84°-87°	720	1.00
30	87°-90°	720	1.00

Obviously, this procedure makes the assumption that the stars in the longitude range covered by the infrared survey are representative of the stars in the longitude range not covered. The value of $\overline{n}$ for a particular range of t is the quotient of the weighted sum divided by the range of t. The standard deviation of this value is calculated from the actual (not weighted) number of stars in the particular range of t.

REFERENCES

1. Neugebauer, G., Martz, D. E., and Leighton, R. B., *Ap. J.*, 142, 399 (1965).

2. Ulrich, B. T., Neugebauer, G., McCammon, D., Leighton, R. B., Hughes, E. E., and Becklin, E., *Ap. J.*, 146, 288 (1966).

3. Neugebauer, G., and Leighton, R. B., *Two Micron Sky Survey, A Preliminary Catalog* (Washington: National Aeronautics and Space Administration, 1969).

4. Johnson, H. L., *Comm. Lunar and Planet. Lab.*, 3, No. 53 (1965).

5. Nassau, J. J., and Blanco, V. M., *Ap. J.*, 120, 464 (1954).

6. Nassau, J. J., Blanco, V. M., and Cameron, D. M., *Ap. J.*, 124, 522 (1956).

7. Blanco, V. M., *Stars and Stellar Systems*, Vol. V: *Galactic Structure*, ed. A. Blaauw and M. Schmidt (Chicago: The University of Chicago Press, 1965), chap. 12.

8. Kron, G. E., Gascoigne, S. C. B., and White, H. S., *A. J.*, 62, 205 (1957).

9. Blanco, V. M., *A. J.*, 69, 730 (1964).

10. Nassau, J. J., and Blanco, V. M., *Ap. J.*, 120, 118 (1954).

11. Nassau, J. J., and Blanco, V. M., *Ap. J.*, 120, 129 (1954).

12. Nassau, J. J., Blanco, V. M., and Morgan, W. W., *Ap. J.*, 120, 478 (1954).

13. Hetzler, C., *Ap. J.*, 86, 509 (1937).

14. Johnson, H. L., Mendoza V., E. E., and Wisniewski, W. Z., *Ap. J.*, 142, 1249 (1965).

15. Johnson, H. L., *Science*, 157, 635 (1967).

16. *Smithsonian Astrophysical Observatory Star Catalog* (Washington: Smithsonian Institution, 1966).

17. Hoffleit, D., *Yale Catalogue of Bright Stars*. 3d edition. (New Haven: Yale University Observatory, 1964).

18. Boss, B., *General Catalogue of 33342 Stars for the Epoch 1950* (Carnegie Institution of Washington, Washington, D.C.), 1937.

19. Kukarkin, B. V., Parenago, P. P., Efremov, Y. U. I., and Gol'opov, P. N., *General Catalogue of Variable Stars* (Moscow: Acad. Sci. U.S.S.R.), 1958.

20. Johnson, H. L., *Ap. J.*, 135, 69 (1962).

21. Kron, G. E., White, H. S., and Gascoigne, S. C. B., *Ap. J.*, 118, 502 (1953).

22. Johnson, H. L., *Ap. J.*, 141, 923 (1965).

23. Johnson, H. L., *Bol. Tonantzintla y Tacubaya Obs.*, 3, 305 (1964).

24. Blaauw, A., *Stars and Stellar Systems*, Vol. III: *Basic Astronomical Data*, ed. K. Aa. Strand (Chicago: The University of Chicago Press, 1963), chap. 20.

25. Johnson, H. L., *Ann. Rev. of Astronomy and Astrophysics*, 4, 193 (1966).

26. Gliese, W., *Z. Astrophysik*, 39, 1 (1956).

27. Fourth Fundamental Catalogue (FK4), *Veröff. Astr. Rechen Inst. Heidelberg*, No. 10 (1963).

28. Allen, C. W., *Astrophysical Quantities*. 2d edition. (London: The Athlone Press, 1963), p. 241.

29. Johnson, H. L., Mitchell, R. I., Iriarte, B., and Wisniewski, W. Z., *Comm. Lunar and Planet. Lab.*, 4, No. 63 (1966).

30. Allen, C. W., *Astrophysical Quantities*. 2d edition. (London: The Athlone Press, 1963), p. 228.

31. Sharpless, S., *Stars and Stellar Systems*, Vol. V: *Galactic Structure*, ed. A. Blaauw and M. Schmidt (Chicago: The University of Chicago Press, 1965), chap. 7.

32. Trumpler, R. J., and Weaver, H. F., *Statistical Astronomy* (Berkeley: University of California Press, 1953), p. 452.

33. Allen, C. W., *Astrophysical Quantities*. 2d edition. (London: The Athlone Press, 1963), p. 251.

34. Trumpler, R. J., and Weaver, H. F., *Statistical Astronomy* Berkeley: University of California Press, 1953), p. 257.

35. Blaauw, A., Gum, C. S., Pawsey, J. L., and Westerhout, G., *M. N.*, 121, 123 (1960).

36. Johnson, H. L., *Ap. J.*, 149, 345 (1967).

37. Wildey, R. L., *Ap. J. Supp. Series*, 8, 439 (1964).

38. Sharpless, S., *Pub. A. S. P.*, 70, 392 (1958).

39. Gum, C. S., Kerr, F. J., and Westerhout, G., *M. N.*, 121, 132 (1960).

40. Blaauw, A., *M.N.*, 121, 164 (1960).

41. Elvius, T., *Stars and Stellar Systems*, Vol. V: *Galactic Structure*, ed. A. Blaauw and M. Schmidt (Chicago: The University of Chicago Press, 1965), chap. 3.

42. Upgren, A. R., *A. J.*, 67, 37 (1962).

43. Rhijn, P. J. van, *Pub. Kapteyn Astr. Lab. Groningen*, No. 59 (1956).

44. Oort, J. H., *B.A.N.*, 15, 45 (1960).

45. Hidajat, B., and Blanco, V. M., *A. J.*, 73, 712 (1968).

46. Cramér, H., *Mathematical Methods of Statistics* (Princeton: Princeton University Press, 1946), p. 416.

47. Westerlund, B. E., *M.N.*, 130, 45 (1965).

48. Upgren, A. R., *A. J.*, 65, 644 (1960).

49. Ohlsson, J., *Ann. Lund. Obs.*, 3 (1932).

50. Blanco, V. M., and Nassau, J. J., *Ap. J.*, 125, 408 (1957).

51. Becker, W., *Z. Astrophysik*, 58, 202 (1964).

52. Bidelman, W. P., *I. A. U. Symposium*, No. 5: *The Large Scale Structure of the Galactic System*, ed. N. G. Roman (Cambridge: Cambridge University Press, 1958), p. 54.

53. Schmidt, M., *Stars and Stellar Systems*, Vol. V: *Galactic Structure*, ed. A. Blaauw and M. Schmidt (Chicago: University of Chicago Press, 1965), p. 526.

54. Scheffler, H., and Elsässer, H., *Landolt-Börnstein New Series*, Group VI, Vol. I: *Astronomy and Astrophysics*, ed. H. H. Voigt (Berlin: Springer-Verlag, 1965), p. 619.

55. Sanduleak, N., *A. J.*, 62, 150 (1957).

56. Johnson, H. L., *Stars and Stellar Systems*, Vol. VII: *Nebulae and Interstellar Matter*, ed. B. M. Middlehurst and L. H. Aller (Chicago: University of Chicago Press, 1968), chap. 5.

57. Whitford, A. E., *A. J.*, 63, 201 (1958).

58. Hulst, H. C. van de, *Rech. Astr. Obs. Utrecht*, 11, Part 1, 1 (1949).

59. Johnson, H. L., *Comm. Lunar and Planet. Lab.* 3, No. 53 (1965).

60. Bergh, S. van den, *A. J.*, 72, 70 (1967).

61. Kron, G. E., and Mayall, N. V., *A. J.*, 65, 581 (1960).

62. Peterson, B., Thesis: California Institute of Technology (1968).

63. Neckel, T., *Z. Astrophysik*, 63, 221 (1966).

64. Allen, C. W., *Astrophysical Quantities*. 2d edition. (London: The Athlone Press, 1963), p. 242.

65. Mihalas, D., *Galactic Astronomy* (San Francisco: W. H. Freeman and Co., 1968), p. 70.

66. Fernie, S. D., *A. J.*, 67, 224 (1962).